



**HAL**  
open science

# Charging station for electric vehicle using hybrid sources

Fouad Eltoumi

► **To cite this version:**

Fouad Eltoumi. Charging station for electric vehicle using hybrid sources. Other. Université Bourgogne Franche-Comté, 2020. English. NNT : 2020UBFCA009 . tel-03145375

**HAL Id: tel-03145375**

**<https://theses.hal.science/tel-03145375v1>**

Submitted on 18 Feb 2021

**HAL** is a multi-disciplinary open access archive for the deposit and dissemination of scientific research documents, whether they are published or not. The documents may come from teaching and research institutions in France or abroad, or from public or private research centers.

L'archive ouverte pluridisciplinaire **HAL**, est destinée au dépôt et à la diffusion de documents scientifiques de niveau recherche, publiés ou non, émanant des établissements d'enseignement et de recherche français ou étrangers, des laboratoires publics ou privés.



**THESE DE DOCTORAT DE L'ETABLISSEMENT UNIVERSITE BOURGOGNE  
FRANCHE-COMTE  
PREPAREE A FEMTO-ST Franche Comté Electronique Mécanique Thermique et  
Optique - Sciences et Technologies UMR CNRS 6174**

Ecole doctorale n°37  
SPIM - Sciences Physiques pour l'Ingénieur et Microtechniques

Doctorat de Génie électrique

Par  
ELTOUMI Fouad

**Charging Station for Electric Vehicles Using Hybrid Sources**

Thèse présentée et soutenue à UTBM, Rue Thierry Mieg, F-90010 Belfort Cedex, Salle I102,  
le Mardi 28 Mai 2020 à 13H00.

Composition du Jury :

Prof. HILAIRET Mickael	Université de Technologie de Belfort-Montbéliard	Président du Jury
Prof. BETHOUX Olivier	Sorbonne Université	Rapporteur
Dr. EBRAHIM Mohamed	Université de Benha, Cairo Égypte	Rapporteur
Prof. BACHA Seddik	Université Grenoble Alpes	Examineur
Prof. DJEMAI Mohamed	Université Polytechnique Hauts-de-France	Examineur
Dr. BECHERIF Mohamed	Université de Technologie de Belfort-Montbéliard	Directeur de Thèse
Dr. RAMADAN Hiatham	Université de Technologie de Belfort-Montbéliard	Codirecteur de Thèse

# Abstract

Higher penetration of electric vehicles (EVs) and plug-in hybrid electric vehicles requires efficient design of charging stations to supply appropriate charging rates. This would trigger stress on conventional grid, thus increasing the cost of charging. Therefore, the use of on-site renewable sources such as photo-voltaic (PV) energy alongside to the conventional grid can increase the performance of charging station. In this thesis, PV source is used in conjunction with grid to supply EV load. However, the PV is known for its intermittent nature that is highly dependent on geographical and weather conditions. To compensate the intermittency of PV, a battery storage system (BSS) is combined with the PV in a grid-tied system for providing a stable operation of hybrid PV based charging station. Generally, hybrid sources-based charging station should be cost effective, efficient, and reliability to supplement the variable needs of EVs load in different scenarios. In this thesis, efficient hierarchical energy management strategy is proposed and applied to maximize on-site PV energy, to meet the variable load of EVs considering the fast response of BSS and putting less stress on grid. This strategy improves the overall performance, the reliable and cost. An efficient bidirectional power conversion stage is introduced for BSS in the form of interleaved buck-boost converter to ensure the safe operation of BSS and reduce losses during conversion stage. This topology enables reducing the current ripples and therefore, increasing the power quality. To extract the maximum power from PV system under intermittent weather conditions, MPPT is used alongside with interleaved boost converter to ensure the continuity of power from PV source. Similarly, for vehicles charger stage, to meet the dynamic power demands of EVs; while, keeping the balance between available generation amounts, interleave converter is proposed combined to sub-management strategy. The proposed conversion stage and management address the low depending on grid sources for the charging purposes when, peak load is present at the grid side. Hence, the proposed charging strategy greatly decreases the stress on grid especially at peak hours. To operate the system under desirable conditions, a rule-based management strategy (REMS) is proposed. This interactive strategy with limits in response time strategy, initializing from maximized utilization of PV source, then using BSS to supplement power and utilizing grid during intermittent conditions affecting PVs. The management strategy ensures reliable operation of system, while maximizing the PV utilization, meeting the EVs demand and maximizing the life the BSS. In this thesis, a hybrid charging system based on PV, BSS and conventional grid is proposed to support the needs of EVs load. Efficient energy conversion stage is proposed using interleaved buck-boost converters to improve the quality of power. State of charge estimation (SoC) of lithium-ion battery using an extend Kalman filter (EKF) is proposed. On-line management strategy is developed to maximize the renewable energy utilization, to insert lesser stress on grid and to improve the utilization of BSS.

**Key words:** Electric vehicle charging station, power conversion stages, battery modelling energy management system.

## Résumé

Une plus grande utilisation des véhicules électriques (VE) et hybrides rechargeables exige une conception efficace des stations de recharge pour fournir des taux de charge appropriés. Le raccordement d'une station sur le réseau électrique conventionnel provoquerait des perturbations, ce qui augmenterait le coût de la recharge. Par conséquent, dans ce scénario, l'utilisation de sources renouvelables sur site telles que l'énergie photovoltaïque (PV) en appui au réseau conventionnel peut augmenter les performances de la station de recharge. Dans cette thèse, une source PV est utilisée conjointement avec le réseau pour compléter la charge des VE. Cependant, le PV est connu pour sa nature intermittente qui dépend fortement des conditions géographiques et météorologiques. Ainsi, pour compenser l'intermittence du PV, un système de stockage à batterie (BSS) est combiné avec le PV dans un système raccordé au réseau, fournissant un fonctionnement stable de la station de recharge PV hybride. En général, les stations de recharge hybrides devraient être rentables, efficaces et fiables pour répondre aux besoins variables de la charge des VE dans différents scénarios. Dans cette thèse, une stratégie efficace de gestion hiérarchique de l'énergie est proposée et appliquée pour maximiser l'énergie photovoltaïque sur site, pour répondre à la charge variable des VE en utilisant une réponse rapide du BSS et en réduisant la sollicitation de réseau. Cette stratégie globale améliore la performance ainsi que la fiabilité et la rentabilité. Un étage de conversion de puissance bidirectionnel efficace est introduit pour le BSS sous la forme d'un convertisseur buck-boost entrelacé pour assurer le fonctionnement du BSS et réduire les pertes pendant la phase de conversion. Cette topologie a des caractéristiques qui permettent d'améliorer les ondulations du courant et par conséquent, d'augmenter considérablement la qualité de l'énergie. De même, pour extraire la puissance maximale du système PV dans des conditions météorologiques intermittentes, une MPPT est utilisée en même temps que le convertisseur élévateur entrelacé pour assurer la continuité de la puissance de la source PV. De même, pour l'étage de charge des véhicules, afin de répondre aux demandes dynamiques de puissance des VE; tout en maintenant l'équilibre entre les quantités de production disponibles, un convertisseur d'entrelacement est proposé en complément de la stratégie de sous-gestion. En particulier, cette étape de conversion et de gestion porte sur la faible utilisation du réseau notamment lors de pointes de puissance. Ceci diminue considérablement la perturbation sur le réseau, surtout aux heures de pointe, et améliore donc la performance du système dans son ensemble. Pour exploiter l'ensemble du système dans des conditions souhaitables, une stratégie de gestion de l'énergie en ligne est proposée. Cette stratégie en temps réel fonctionne de manière hiérarchique, en s'initialisant à partir d'une utilisation maximale de la source PV, puis en utilisant le BSS pour compléter l'alimentation et en utilisant le réseau en cas de conditions intermittentes ou lorsque la quantité de PV est faible. La stratégie de gestion assure un fonctionnement fiable du système, tout en maximisant l'utilisation du PV, en répondant à la demande des VE et en maximisant la durée de vie du BSS. Dans cette thèse, un système de charge hybride basé sur le PV, le BSS et le réseau conventionnel est proposé pour répondre aux besoins de charge des VE. Une étape

efficace de conversion de l'énergie a été proposée en utilisant des convertisseurs entrelacés de type buck-boost pour améliorer la qualité de l'énergie et, en fin de compte, une stratégie de gestion en ligne est développée pour maximiser l'utilisation de l'énergie renouvelable, en insérant moins de stress sur le réseau et en améliorant l'utilisation du BSS.

**Mots clés :** station de charge de véhicule électrique, étages de conversion de puissance, modélisation de la batterie, système de gestion de l'énergie.

# Table of Contents

<b>Acronyms</b>	<b>6</b>
<b>List of Figures</b>	<b>7</b>
<b>List of Tables</b>	<b>8</b>
<b>Chapter 1: Introduction</b>	<b>9</b>
1.1 Thesis motivation	<b>10</b>
1.2 Thesis objectives and contribution	<b>12</b>
1.3 Charging structure design	<b>13</b>
1.4 Thesis outline	<b>17</b>
<b>Chapter 2: EV charging system and RES integration: An Overview</b>	<b>19</b>
2.1 Introduction	<b>20</b>
2.2 EV charging framework and standards	<b>21</b>
2.3 Hybrid sources-based charging system architecture: Literature review	<b>25</b>
2.4 A comparison of charging systems architectures	<b>35</b>
2.5 Hierarchical Control for EVs Charging System	<b>37</b>
2.6 Conclusion	<b>45</b>
<b>Chapter 3: EV charging system modelling and control</b>	<b>47</b>
3.1 Introduction	<b>48</b>
3.2 PV system modelling and MPPT control	<b>49</b>
3.3 BSS /EV battery and their power conversion step	<b>60</b>
3.4 AC/DC interlinking converter for the EVs charging station	<b>65</b>
3.5 Conclusion	<b>69</b>
<b>Chapter 4: Lithium-ion Battery modelling and SoC estimation</b>	<b>70</b>
4.1 Introduction	<b>72</b>
4.2 Lithium-ion Battery modelling	<b>72</b>
4.3 SoC estimation method for lithium-ion battery	<b>77</b>
4.4 Simulation results and discussion	<b>81</b>
4.5 Conclusion	<b>83</b>
<b>Chapter 5: Energy Management of proposed EVs charging model</b>	<b>84</b>
5.1 Introduction	<b>85</b>
5.2 General operating modes of charging station	<b>86</b>
5.3 Rule- based Energy management system (REMS) algorithm	<b>88</b>
5.4 Results and discussion	<b>96</b>
5.5 A Comparison of the PV BSS grid-based REMS with grid charging	<b>103</b>
<b>Chapter 6: Conclusion and Discussion</b>	<b>106</b>
<b>Reference</b>	<b>112</b>

## Acronyms

BMS	Battery Management System
BSS	Battery Storage System
CPs	Charging Points
CC	Constant Current
CV	Constant Voltage
DER	Distributed Energy Sources
DG	Distributed Generation
EMS	Energy Management System
EV	Electric Vehicles
EKF	Extend Kalman Filter
ESS	Energy Storage System
EVCS	EV Charging Station
FC	Fuel Cell
FL	Fuzzy Logic
G2V	Grid to Vehicle
GHG	Green House Gas
KF	Kalman Filter
LP	Linear Programming
MILP	Mixed Integer linear Programming
MPPT	Maximum Power Point Tracking
IBC	Interleaved Boost Converter
IBDC	Interleaved Bi-Directional Converter
ICEV	Internal Combustion Engine Vehicles
ILC	Inter-Linking Converter
IMC	Internal Model Control
PV	Photovoltaic
REMS	Rule based Energy Management
RES	Renewable Energy System
SoC	State of Charge
SOH	State of Health
TOU	Time of Use
V2G	Vehicle to Grid
VOC	Voltage open circuit
WT	Wind Turbine

## List of Figures

Fig 1. 1: On-board and off-board of EV chargers.	14
Fig 1. 2: Charging station configurations based on a common bus system.	15
Fig 1. 2: Hierarchical control of EV charging station	17
Fig 2. 1: AC micro-grid structure with EVs chargers.	31
Fig 2. 2: PV panels, BSS and EVs connected to the common DC bus with grid connection.	32
Fig 2. 3: Topology of AC-DC hybrid micro-grid structure.	33
Fig 2. 4: Hierarchical control of EV charging stations.	38
Fig 2. 5: EMS structure for EV charging station.	40
Fig 2. 6: Centralized control architecture.	43
Fig 2. 7: Decentralized control architecture	44
Fig 3. 1: EV charging station module based on DC micro-grid.	49
Fig 3. 2: Equivalent circuit model PV panel.	50
Fig 3. 3: Flow chart for the MPPT control.	51
Fig 3. 4: Interleaved (DC/DC) Converter.	52
Fig 3. 5: Switches conduction timeline, case 1.	53
Fig 3. 6: Behavior of interleaved converter in each small interval case 1.	54
Fig 3. 7: Waveforms of different signals, case 1.	55
Fig 3. 8: Switches conduction timeline, case 2.	56
Fig 3. 9: Behavior of interleaved converter in each small interval case 2.	56
Fig 3. 10: Waveforms of different signals, case 2.	57
Fig 3. 11: Switches conduction timeline, case 3.	57
Fig 3.12: Behavior of interleaved converter in each small interval for case 3.	58
Fig 3. 13: Switches conduction timeline, case 3.	59
Fig 3. 14: bidirectional interleaved converters for BSS and charger side.	61
Fig 3. 15: Block diagram of bidirectional interleaved converters.	62
Fig 3. 3a: Control scheme of IBDC.	63
Fig 3. 16b: Controller scheme of IBDC.	63
Fig 3.17: buck DC/DC converter	64
Fig3.18: PI controller scheme of EV c charger	65
Fig.3.19: Voltage and current waveforms of the charging battery.	65
Fig 3. 4: AC/DC micro-grid with DC charging station.	66
Fig 3.21: AC side of the micro-grid.	66
Fig 3. 22: Block diagram of voltage and current double closed-loop control for PWM rectifier.	68
Fig 3.23: Voltage and current waveforms of phase a on the grid side during rectification.	69
Fig.3. 24: The grid side current during load fluctuation.	69
Fig 4.1: Schematic diagram for the DP model.	73
Fig 4.2: Battery test bench.	74
Fig 4.3: Battery voltage during charging and discharging.	74
Fig 4.5: Experimental current and voltage profiles of charge/discharge.	76
Fig 4.6: Nonlinear relationship between the OCV and SoC	76
Fig 4.7: The first order Thevenin equivalent model.	77
Fig 4.8: Simulink model of ECM and EKF.	81
Fig 4.9: The real voltage load and the estimated voltage under UDDS.	82
Fig 4.10: battery input current.	82

Fig 4.11: EKF SoC estimation 90-20% and SoC estimation Error.	<b>83</b>
Fig 5. 1: General system structure and EMS of the EV charging station	<b>86</b>
Fig 5. 2: Generic power flow scenarios of charging stations.	<b>87</b>
Fig 5.3: Operation at overload situation.	<b>94</b>
Fig 5.4: Operation at underload situation.	<b>95</b>
Fig5.6: Electricity grid price and EV charging price.	<b>96</b>
Fig 5.7 A: Power flow of charging system components and BSS SoC at 50 %.	<b>98</b>
Fig 4.7 B: Power flow of charging system components and BSS SoC 85 % on clear day.	<b>99</b>
Fig. 5.7C: Power flow of charging system components and BSS SoC 25 % on clear day.	<b>100</b>
Fig5.8: PV energy to grid in case of SoC high and low EVs load.	<b>100</b>
Fig. 5.9 A: power flow and BSS SoC 85 % on cloudy day.	<b>101</b>
Fig 5.9 B: power flow and BSS SoC 50 % on cloudy day.	<b>102</b>
Fig 5.9 C: power flow and BSS SoC 25 % on cloudy day.	<b>103</b>
Fig 5.10: Different charging scenarios considering different grid electricity price.	<b>104</b>

## List of Tables

Table 1. 1: Global sales of EV.	<b>10</b>
Table 2. 1: Comparison between EV charging levels and international standards.	<b>22</b>
Table 2. 2: Charging station architectures presented in literature	<b>34</b>
Table 2. 3: A qualitative comparison of AC and DC based charging system architectures.	<b>37</b>
Table 2. 4: Centralized/decentralized characteristics.	<b>45</b>
Table 3. 1 charging system component parameters.	<b>48</b>
Table 3.2: Parameter of PI controller for the EV charger	<b>65</b>
Table 4.1: The battery parameters values at charging and discharging.	<b>75</b>
Table 5. 1: General charging station operating modes.	<b>86</b>
Table 5.2: parameter used in the energy management strategy.	<b>89</b>
Table 5.3: Price comparison of REMS-based PV BSS grid charging and the grid charging.	<b>105</b>

# **Chapter 1: Introduction**

## 1.1 Thesis motivation

Nowadays, vehicles are considered vital elements in everyday life for personal mobility and transport of goods as reflected by the continuous demand for petroleum. Along with such a demand, the rise in fuel costs and increasing global concerns over the environment because of air pollution and climate change have elicited apprehensions. Consequently, certain governments have encouraged car manufacturers to create environmentally friendly and low-emission transportation alternatives [1]. In this context, Electric Vehicles (EVs) have been developed and utilized to minimize dependency on fossil fuels; this has resulted in the reduction of emissions of greenhouse gases and other pollutant [2]. Furthermore, vehicle emission standards have been imposed to avert environmental damage caused by conventional vehicles [3]; several countries, such as the United States, the United Kingdom, Japan, and Europe, have adopted standards on transportation systems to reduce vehicle emissions. In this context, the net percentage of “atmospheric aerosol particles” produced by vehicles exhaust have been significantly reduced by 99 %, since the Euro 5 emission standards. Besides, carbon dioxide and nitrogen dioxide have been significantly reduced since Euro 1 emission standard onwards. However, vehicle emissions are targeted to be reduced by 35 mg/km of nitrogen dioxide and 95 g/km of carbon dioxide by 2020 in Europe [4].

Table 1. 2: Global sales of EV.

	<b>Sales (k)</b>	<b>Δ 2018 vs 2019</b>
<b>China</b>	430.7	+ 111%
<b>USA</b>	116.2	+ 87 %
<b>Norway</b>	36.3	+ 74 %
<b>Germany</b>	33	+ 72 %
<b>France</b>	24.3	+ 38 %
<b>Netherlands</b>	17.8	+ 118 %
<b>Korea</b>	17.7	+ 63 %
<b>Canada</b>	13.1	+ 37 %
<b>UK</b>	12.7	+ 62 %

Under such a paradigm shift, EVs are becoming more competitive in terms of cost compared with Internal Combustion Engine Vehicles (ICEVs). Aware of the performance of EVs, several countries, among them the USA, UK, China, and European countries, have formulated a number of resolutions and extended important funding to encourage the extensive adoption of EVs [5]. Table 1.1 depicts the mass integration of EVs in several countries. Based on future planning scenarios, by 2050, all EV fleets will be supplied by Renewable Energy Sources (RES) [3], [6]. In fact, the increasing adoption and use of EVs are the outcome of the advance in battery technology and the expansion of battery charging facilities in an attempt to satisfy their energy requisites. Thus, the general infrastructure of the charging system is essential for the promotion

of EVs. However, the main weakness of EV charging infrastructures is that their use is not environmentally friendly as they depend only on the grid as power source. Indeed, renewable represent a distributable and time-bounded energy source, whereas the charging of EVs can be controlled; evidently, it logically relies on the combination of RES and EVs.

Accordingly, it is necessary to balance electricity production and EV charging to guarantee and preserve secure constant grid operation. The irregular nature of RES production is considered as one of the main problems that must be resolved for the future operation of the electricity grid. Conventionally, load fluctuation control is generally not effective to balance the grid and execute operational strategy as well as power control under various load operating states. Generally, a potential solution is load scheduling by controlling the progress of the RES production; this has been proposed because further electricity production scheduling is crucial during power system functioning. Moreover, EVs have proven their ability to support the main grid in preserving certain equilibrium between demand and supply; this increases the potential for the RES penetration. In fact, numerous published research articles as those in [7] discussed this subject. Furthermore, PV production may lead to the further penetration of EVs because the energy requirement of these vehicles do not result in a considerable rise in the total load [8]. However, the integration of EVs and PVs into the grid, either separately or in combination, necessitates adequate planning; otherwise, system consistency can be compromised. As far as power grid operators are concerned, time uncertainty is the most crucial aspect in PV production [9]. The problem with EVs is that they can disturb the demand side and cause grid overload; this condition can result in a decrease in both power quality and grid stability. The authors in [10], concluded that the integration of EV and PV into the grid has to be planned and controlled; for example, through the employment of a scheduled load approach, the number of PVs and EVs penetrating into the grid can increase.

Evidently, the employment of renewable in the EV charging system is beneficial in the sense that it: (i) minimizes the loading effect of EVs on the grid; (ii) resolves the voltage regulation problems associated with the electricity grid; (iii) reduces utility supply costs; (iv) expands the energy storage by increasing renewable production; (v) improves the effectiveness of both Vehicle-to-Grid (V2G) and Vehicle-to-Home (V2H) strategies; (vi) decreases fuel cost and (vii) prevents CO<sub>2</sub> emissions. RES such as Photovoltaic (PV), Wind Turbine (WT), Fuel Cell (FC), hydroelectricity, biogas and other RES are ideal potential sources to charge and power EVs. These systems together with the energy storage systems (ESS) and the related electrical equipment's, combined by appropriate connection methods provide the charging requirements of EV's. The use of the local power sources, including the RES, allows feeding EVs with more employment of RES.

Currently, RES are able to scale up electricity production in power grid including mainly PV, WT and biomass energy. Generally, they are easily employed to charge EVs due to their high energy density, their

low cost of construction as well as their simple implementation and the increased efficiency of electricity production [11, 12]. Solar energy becomes widely used due to the high magnitude of solar energy on the Earth surface and its non-polluting and noiseless nature. The PV system in the stand-alone mode is generally unreliable as PV electricity production is influenced by the weather and environmental conditions. However, the PV modules are characterized by their simple structure, small size, lightweight and their stability in transport and installation. Moreover, the PV system takes short construction period and can be easily installed with other power sources and simply used at homes and/or public spaces. An energy storage device at the charging station can significantly mitigate the variability in PVs power output [13, 14]. PV solar panels to charge EVs are employed for several reasons:

1. The cost of solar PV has declined steadily in the recent decades to reach less than 1 € /Wp [6].
2. PV panels can be installed on rooftops and in parking spaces near EV parking lots.
3. The peak demand of EVs charging is reduced at grid side since the charging power is partially generated from PV panels.
4. PV charging systems use a BSS to store the energy produced by PV panels, which helps managing daytime and seasonal climate variations affecting solar production.
5. The recharging of EVs by solar energy is cheaper than that by system based on the grid.

Considering today's power grid structure and the rapid growth of EVs load where the adjustment of the primary energy structure of the grid side greatly increases the cost of power grid transformation, the charging of EVs from PV panels has the potential of making EVs more environmentally and economically feasible by decreasing the overall charging facility costs. In this thesis, the solar-based EV charging station together with the conventional Alternating Current (AC) grid and ESS where energy storage is installed to store any PV power excess or to provide energy to charge EVs if PV production is not available, especially during peak hours. Thus, the EVs can be charged easily even in insufficient energy to satisfy the total demand.

## **1.2 Thesis objectives and contribution**

In this thesis, the design and development of a high-performance charging system for EVs in worksite, which uses solar energy, grid connection and storage system, is accomplished to increase the availability and reliability of the charging station. This PhD work aims at developing hybrid sources-based charging platform to efficiently charge the EVs, enhancing the utilization of integrated renewable sources such as PV while charging the EVs, and showing the effect of employing energy storage devices on performance of the charging station.

To achieve these objectives, this thesis focuses on four aspects:

1. Designing unidirectional and bidirectional power conversion topologies for the different power sources.
2. Modeling charging system using a hybrid power source to charge EVs considering the inter-relationship between EVs load needs, PV production, local storage energy levels and grid.
3. Designing a coordinated control to enhance the system stability.
4. Formulating EVs charging energy management based on the solar forecast, grid load curve, BSS energy level.

This work deals with the charging of EVs from hybrid power sources in the public area, such as office buildings and work-places, depending on: (i) large public area where PV panels and other components, such as ESS and EV chargers, can be installed; (ii) the working day which largely corresponds to the hours of daylight where the solar energy is available for longer time to charge the EVs batteries; and (iii) the charging power levels used for charging EV battery which may be low since the vehicles are being parked at the workplace for many hours, which minimizes the cost and complexity of the EV charging and charger devices. The integration of PVs and EVs into the grid as well as energy storage, either separately or in combination, necessitate coordinated control and optimal load scheduling. Otherwise, power grid consistency can be compromised. Time uncertainty is the most crucial aspect in PV energy productions. In fact, EVs load may disturb the demand side and cause grid overload. Therefore, the storage system capacity of the charging system and the limits of the electricity grid are considered in the design the EV coordinated charging system.

The main contributions can be summarized as:

1. Determining power EVs charging topology in terms of power density, efficiency, and control.
2. Developing reliable and stable (voltage and frequency) electrical charging system for EVs.
3. Establishing coordinated control between several power sources.
4. Ensuring the necessary power management between the hybrid sources and EVs.

### **1.3 Charging structure design**

The objective of studying and analyzing the EV charging system design is developing a reliable and efficient charging station to meet the increasing power demand of EVs at the selected site and to supply power back into electricity grid or consume it by conventional load at the same site. However, an important issue that should be considered in this context, is that RES energy production depends on the location of installation, the seasonal variations, the daily weather change, the power grid stability issues (e.g. power quality and voltage variation) and the storage system capacity. Consequently, in this thesis, an integrated system design for a hybrid PV/grid/ storage system for EVs charging is implemented.

The difference between energy demand and supply and its impact on the charging system design are considered. Moreover, a comprehensive modeling of meteorological data, such as solar irradiation and temperature, is essential together with an analysis of the daily traveling habits of EV users. In designing the EV charging system, the power conversion steps required for the charging system, considering the nominal power of the PV/grid/BSS, should be determined. Simultaneously, the ESS can regulate the variations in solar energy production or the electricity grid and store energy during the periods of overproduction to supply the charging system at low production levels. In the modern charging systems, smart charging methods are employed to make the EV charging process follow the variables of power sources production [15, 16].

In this thesis, the charging station is designed considering the hierarchical control. The first level control and on-line energy management to maximize the PV power utilization rate, enhance the charging system capacities, reduce the cost of electricity purchase from the grid and minimize the grid stress resulting from simultaneous recharging of the large number of EVs is illustrated. By combining the electricity grid with the use of PV and ESS beside the implementation of the relevant control and energy management system (EMS), a positive impact of this combination on the charging process of EVs can be introduced.

### 1.3.1 EV charging power conversion: topologies

The EV chargers can be off-board or on-board as shown in Fig 1.1. Typically, the use of off-board chargers may reduce the total cost and the size of the vehicle. More recently, AC grids has been utilized to power EVs with embedded chargers [17].

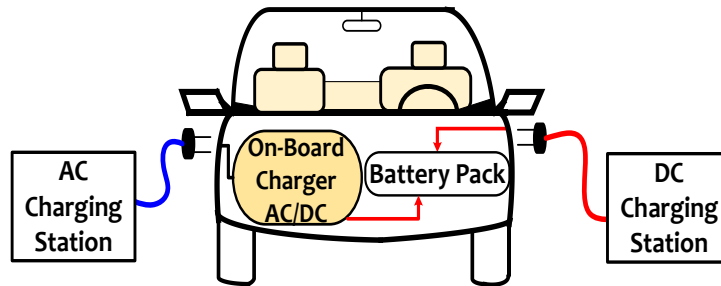
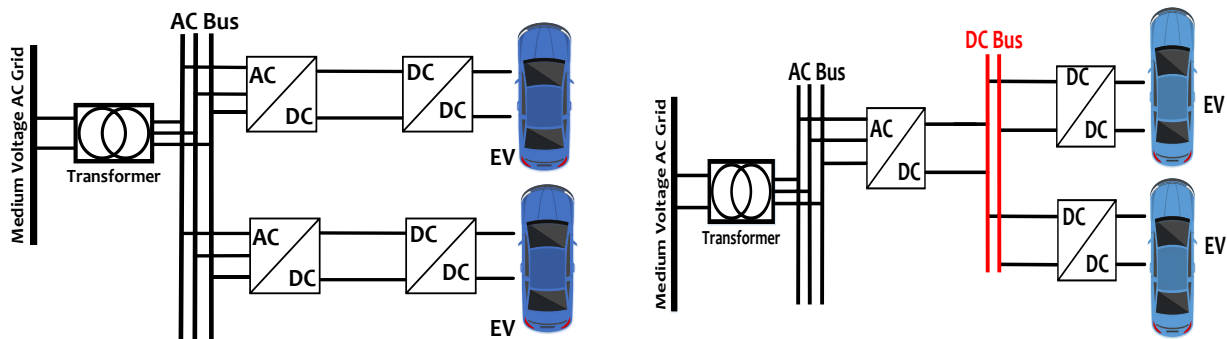


Fig. 1. 3: On-board and off-board of EV chargers.

The fast charger as an on-board option for an EV is hampered by the cost of the electronic components required for energy conversion, which increases the overall cost of EVs. However, on-board chargers cannot provide fast EV charging because of the power electronics high costs associated with the EV and the necessity to increase the capacity of the charger in the vehicle. To ensure fast EV charging, off-board chargers providing high DC power are used [2, 18]. It is noteworthy that, for off-board chargers, every AC/DC power conversion is performed through an independent inverter. Therefore, it is essential to raise the power of the converters to guarantee the vehicle fast charging. The findings obtained by numerous

published studies have been implemented on EV charging stations to design and develop efficient and reliable EV charging systems. Accordingly, it is relevant to study the concept of a public facility installed with high-power off-board chargers functioning as a charging station. Such a station can provide EVs with the same functionality as a fuel station by supplying the EV batteries with direct current and allow rapid recharging [19, 20]. As for the charging station architecture relying on grid connection, only two options (AC and DC) can be considered. In the first architecture, the secondary side of the step-down transformer is used as a common AC bus where each load is connected to the bus via independent AC/DC stages. In the second architecture, a single AC/DC stage is configured to provide a common DC bus service for the system load [21, 22].

The common AC bus is one of the options suggested to design a charging station, as demonstrated in Fig. 1.2(a b). In this structure, each charging unit has a separate stage rectifier linked to a common AC coupling point on the secondary side of the transformer. In Fig 1.2a, a number of charging units have independent rectifiers; a low operating power factor can generate undesirable harmonic impacts on the power grid [23]. It is important to note that the use of renewable systems (such as PV or ESS), which produce direct current electricity, also requires a DC/AC level; this increases the use of conversion levels in the grid. A single AC/DC stage with high power levels is employed as a second option architecture for EV charging, as illustrated in Fig. 1.2b. The DC bus powers several charging units and provides a more flexible structure with the ability to integrate RES and energy storage devices; actually, these systems are mainly DC sources. The charging station based on the DC bus requires fewer energy conversion steps compared to a charging system based on the AC bus.



(a) EVs charging unit based Common AC bus.

(b) EVs charging units based Common DC bus.

Fig. 1. 4: Charging station configurations based on a common bus system.

Separate inverters and rectifiers are used in PV system and EV chargers to convert DC/AC/DC power. The AC grid is utilized as a mean of energy exchange between energy sources and EVs. However, the AC-based charging system is inefficient and inflexible because of:

1. EV and PVs systems are basically DC-based. Therefore, power exchange into AC requires more power

conversion stages to reduce the overall system efficiency than the corresponding exchange into DC. In AC charging systems, high-power converters typically have two power conversion steps, a DC/AC step and an AC/DC step.

2. The extra power conversion steps for the EV charger and PV source in the AC charging system increase the complexity of system control and rise the overall charging system cost.
3. Both PV panel inverter and EV charger rectifier operate as independent systems without using any common control unit, which further complicates the implementation of practical charging mechanisms to control EV charging based on PV production.
4. EV charging units and PV panels have independent rectifiers that may generate undesirable harmonic distortions.
5. The V2G requires a bi-directional charge/discharge EV charger. The batteries of EVs are generally recharged from the grid and energy is re-injected into the grid. In this case, EVs can operate as a controllable distributed source connected to the grid. Currently, in the AC-based charging, the bi-directional EV chargers are inefficient and cannot support V2G option.

The DC system is beneficial in the sense that it (i) allows reducing considerably power losses, and (ii) facilitates the integration of RES with minimum number of power converters. Because PV panels produce direct current, the PV-powered charging system enables the direct charging of EVs from the DC bus [24].

This architecture represents a promising and cost-effective solution for EVs charging. Therefore, such system allows the charging of the EV by DC directly from the PV. In DC charging system a single bi-directional AC/DC conversion step can be used instead of the multiple conversion steps required in the AC charging system. The main challenge is to design a single power conversion step with high efficiency, high power density, bidirectional power flow and stable control. In this thesis, the integrated PV/grid/storage system based on an EV charger system is developed to cope with these challenges.

### ***1.3.2 Control and Power Management***

To establish a practical EVs charging structure, while mitigating the intermittent effects of PV generation, combining different power/storage devices is a feasible solution. Therefore, proposing appropriate control and energy management of such a hybrid power system is the most critical step in order to enhance the charging system stability, reliability and schedule the EVs load [25]. In this context, there are several challenges in designing a EV charging station. In terms of the electrical design of EV charging stations, the EV charging stations are either AC or DC micro-grids, equipped with various EV chargers. A hierarchical control structure can be introduced to demonstrate system control and energy management of EV charging

stations [26], as shown in Fig 1.3.

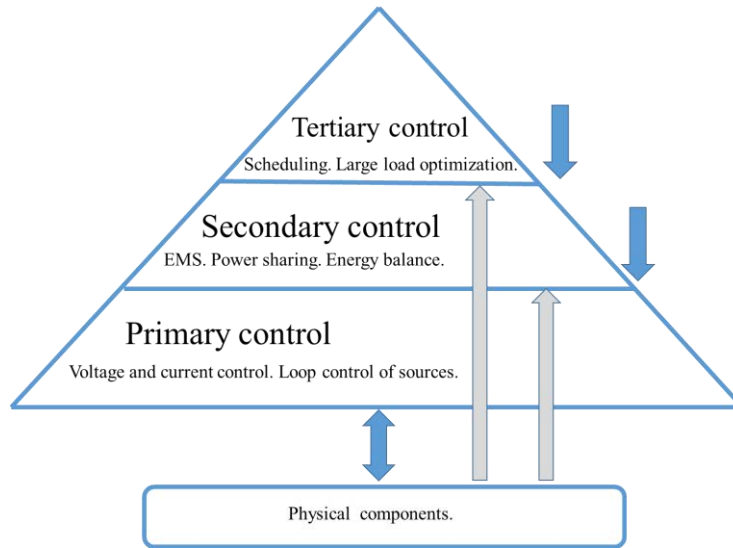


Fig 1. 5: Hierarchical control of EV charging station

The charging station as a micro grid are designed to operate in a stable mode under different scenarios, for instance in grid-connected mode and in stand-alone mode (in the event of a grid failure). In both cases, the system must be designed to ensure efficient EMS so that overall operating costs can be minimized [18, 27].

In this thesis, power management flow is built based on maximizing the use of PV and enhance the charging system voltage stability. Where an on-line strategy works in hierarchical manner, initializing from maximized utilization of PV source, then using BSS to supply power and utilize grid during intermittent conditions or when there is low amount of PV. The management strategy enables ensuring reliable operation of the overall system, while maximizing the PV utilization, meeting the EVs demand and maximizing the life cycle of the BSS.

## 1.4 Thesis outline

Based on the thesis objectives and outlines and the general framework is organized into 6 chapters as:

**Chapter 2:** deals with presenting review on EVs charging systems. The benefits and challenges of the existing EV charging technologies powered by solar energy and other sources are detailed. Besides, the different EV charging systems presented in the literature are compared. Based on this review and the analysis of the charging system configurations, the proposed hybrid system nominal power is selected together with the EV charging topology and components design.

**Chapter 3:** aims of the modeling and control of PV/BSS/grid-based charging station to meet EV energy requirements. The whole EVs charging station is designed and modeled using MATLAB® Simulink environment. The efficiency and the size of the power converters with closed loop controls for the charging conversion system are studied.

**Chapter 4:** represents the methods of battery parameters identification in order to determine the state of charge levels of the battery. An open circuit voltage method and extend kalman filter is presented within this chapter.

**Chapter 5:** considers studying EV charging station and EMS. The application of energy management strategy for EVs charging system are designed and examined to maximize the PV/BSS utilization and ensure a stable power for EVs load based on the change of solar irradiance, BSS energy level, and the difference of EVs load during day.

**Chapter 6:** presents the different conclusions and perspective recommendations for the future research direction.

## **Chapter 2: EV charging system and RES integration: An Overview**

## 2.1 Introduction

More recently, both battery and electric powertrain technology developments are being accelerated by intensive marketing and strong policy support. The cost of battery production has been decreased significantly in the last three years. EVs in the future vehicle market will probably take a more dominant role.

Under the EV transition scenario and as a result of the persistence of the roll-out schedule proposed in 2015, statistics show that the number of EVs exceeded one million in October 2018 [28]. In fact, the U.S. government has introduced several policies to encourage the public sector to set up EV charging infrastructures. In addition, the Canadian Ministry of Transportation reported that the Province of Ontario invested 20 million in 2017 to build approximately 500 EV charging stations in approximately 250 locations [29]. In addition, the German National Platform for Electric Mobility stated that by 2020, the number of EVs will reach practically one million, and demand will exceed 70 000 stations, particularly road charging points (CPs). In order to overcome the limitations of RES use and satisfy the growing energy demand for EVs, China established a model to specify a given number of charging stations with solar-based charging systems [30]. In May 2017, a group of 10 countries (China, Germany, Sweden, Netherlands, Norway, Japan, France, the United Kingdom, Canada, and the United States) organized intergovernmental meetings on initiatives concerning EVs (the EV Initiative) to encourage their global development. Automobile manufacturers in several countries have recently attempted to satisfy client demands by introducing novel EV models, such as the plug-in hybrid electric vehicle (PHEV) and battery electric vehicle (BEV) that are less expensive than ICEVs. Moreover, both utility and power firms have been partnering with stakeholders in order to enhance and enlarge the EV charging infrastructure market [31]. Despite the importance of the aforementioned reforms and laws, these countries do not have adequate and solid EV charging infrastructures.

As a random load, EVs will affect the overall load characteristics of the distribution network, increase the difficulty in load forecasting, and affect the distribution network substation planning and grid. Therefore, in the process of grid planning and design, the impact of EV load should be totally considered, and the constraints of planning must be supplemented so that the planned distribution grid can fully satisfy the varying EV requirements [32]. Although some research works have been implemented, the number of available comprehensive review papers that combine the questions raised on obstructions and problems relating to the sustainability of integrated PV-EV charging is limited [33, 34]. Furthermore, to date, there are no specific guidelines that cover the problems related to the charging system and EV charging scheduling. Thus, this chapter presents an overview of various configurations of charging stations and control topologies that can be utilized for the proper management of EV charging stations.

This chapter has three main objectives: (i) to determine the applicability of the common alternating current (AC) and direct current (DC) bus system in the EV charging stations; (ii) to analyze the integration of renewable energies into the charging systems (such as solar charging systems), the overall control and management framework, and the methods that can be employed including their impediments and sustainability; (iii) to identify the large-scale interaction of EVs with the grid and their charging schedule mechanisms.

The benefits from the chapter can be derived as follows. First, a literature review pertaining to state-of-the-art charging systems and electronic power converters is implemented; second, the interaction of equipment at the system level during various operating modes to determine the applicability of common AC and DC bus EV charging systems is assessed, and the objectives of various large-scale EV charging pattern mechanisms are evaluated. The insights acquired from this study are anticipated to aid in identifying the design criteria as well as.

## 2.2 EV charging framework and standards

Typically, the charging station is a micro-grid system that can be either: AC, DC, or hybrid micro-grid. In this context, high voltage AC or DC sources are used to supply the charging station while the charger converts electrical energy into the required level to charge the EV battery. The different power levels available for the various types of EV chargers are shown in Table 2.1[35].

Within the EV charging system, the power is converted from AC to DC or the DC power is transformed from one level to another and then supply the voltage and current at appropriate levels to charge the EVs battery packs which generally have several kWh capacities. DC power charging  $P_{ch}$  in the form of certain charging current  $I_{ch}$  for charging EV battery and specific voltage  $V_{ev}$  as:

$$P_{ch} = V_{ev} * I_{ch} \quad (2.1)$$

Thus, the energy supplied to the EV battery pack  $E_{ch}$  during a T time

$$E_{ch} = \int_0^{t_{ch}} P_{ch} dt \quad (2.2)$$

Given the global use of EVs, several international charging systems and standards operate at different power charging capacities worldwide. As summarized in Table 2.1, the main classifications of EV chargers are either AC or DC. Moreover, there are several global organizations that have established EV charging standards: Society of Automotive Engineers (SAE), International Electro-Technical Commission (IEC), and CHAdeMO. Tesla has set its own standards for EV charging [36-38]. On global levels, there are currently different types of AC and DC connectors in use.

Table 2. 5: Comparison between EV charging levels and international standards.

Charging Level	Type of Charging		Charging Time	Power Rating (kW)	Voltage (V)	Max Current Rating (A)		
	On-board	Off-board						
<i>AC Charging: SAE Standards</i>								
AC	Level 1	√	-	PHEV 7 h	BEV 17 h	1.4–1.9	120	12–16
	Level 2	√	-	PEV 0.4 h	BEV 1.2 h	19.2	208–240	80
	Level 3		√	0.5 h	1 h	>48	480	>100
<i>DC Charging: SAE Standards</i>								
DC	Level 1	-	√	PHEV 0.4 h	BEV 1.2 h	36	200–450	80
	Level 2	-	√	PHEV 0.2 h	BEV 0.4 h	90	200–450	200
	Level 3	-	√	-	BEV 0.2 h	240	200–600	400
<i>AC Charging: IEC Standards</i>								
AC	Level 1	√	-	Up to 2 h	Up to 3 h	4–7	250–450	16
	Level 2	√	-	1 h	2 h	22	250–450	63
DC	<i>CHAdEMO Standards</i>							
	Fast Charging	-	√	-	Up to 0.5 h	60	500	125
	<i>Tesla supercharging</i>							
	Fast Charging	-	√	Model S 80–90% soc; 0.5 h	Model S 20–80% soc; 1.25 h	>135	Up to 480	200

To charge the EVs at both levels 1 and 2, on-board chargers provide daytime charging at the workplace and overnight charging at home, whereas high-output power level 3 off-board chargers guarantee rapid charging. In fact, certain integrated on-board chargers used for fast-charging because they have the features of both on-board and off-board conventional chargers [6, 39]

### 2.2.1 AC Charging System

The AC charging system enables battery charging by converting AC to DC using the EV's integrated AC/DC power converter with a single or three-phase AC connection. According to SAE and IEC standards, the AC charging system can be classified into three level chargers as follows [40]:

**Level 1:** These chargers utilize a nominal single-phase AC rail of 120 V and 12-16 A and low power with charger 250-450 V, 16 A, and 4-7 kW to charge the batteries. Because these chargers effectively employ domestic plugs, no special installation of separate electronic components (e.g., on-board chargers) is required. Certain connectors, such as NEMA 5-15, SAE-J1772 and IEC are normally utilized at this level. In fact, the time of charging a small EV ranges 7–17 h, which is adequate for overnight charging. However, because of the cable size and thermal constraints of level 1 AC chargers, the charging current rating is considerably limited and results in a long charging time [41].

**Level 2:** These chargers use a direct connection from the main grid to charge the batteries. The main specifications of the single-phase connector are 240 V, 80 A, and a power level of approximately 19.2 kW with both SAE standards and Tesla supercharging and 400 V, 63 A, and 22 kW with IEC standards. In level 2, the on-board charger is usually utilized. Level 2 AC charging stations represent the majority of the typical charging stations. However, because of their rated voltage and superior power management capability, these chargers require dedicated installations at load locations.

**Level 3:** In these chargers, three phase 480 V connectors that support more than 100 A and power exceeding 48 kW are employed for EV charging using standard connectors, such as SAE standards and Tesla supercharging. This class includes rapid chargers of EV battery pack, which can be fully recharged within 30 minutes and 1 hour. The level 3 AC power, which is preferred by most EV owners, is the highest power level that affords fast and convenient charging. However, so far, the IEC standard for level 3 AC charger has not been introduced. Under the SAE-J1772 standard, the level 3 AC power is introduced and classified as off-board charger [42].

### **2.2.2 DC Charging**

DC charging systems are modelled and manufactured to be mostly utilized in outdoor stations compared to the AC equivalents. Although the DC charging systems necessitate more appropriate wiring, they are more efficient and of more rapid charging. DC charging is used for providing high charging power to EVs starting from 48 kW and increases with a purpose-design of the EV off-board charger to directly supply DC power into the EV's battery. As the off-board chargers are not restricted in terms of size and weight, high power charging rates can be achieved. Indeed, modern charging stations automatically convert AC voltages to more suitable levels for battery packs of EVs. These chargers are usually integrated into the connector of the EV supply equipment (EVSE) through Combined charging system (CCS/Combo), CHAdeMO and Tesla chargers [42, 43].

**Level 1:** This level provides charging power of up to 36 kW at 250–450V and 80 A.

**Level 2:** This level is the same as level 1, except that its current rating is 200 A, and its operating voltages can reach 450 V.

**Level 3:** The voltage rating of this system is 600 V. Its maximum current can attain 400 A, and its power rating is equal to 240 kW.

Different from their AC system counterparts, DC chargers provide rapid charging because of their high-power capacities. The standard connectors in DC systems can be classified into three categories: 1) combined charging systems that support power ratings of approximately 65 kW; 2) CHAdeMO connectors, which

provide rapid DC charging; 3) the Tesla vehicle super charger that supports a power capacity of 135 kW [44].

One of key advantages of DC charging system is implementing the V2G connection in bidirectional mode [45, 46]. Thanks to high power and DC-based charging system, EVs and other charging facilities have the potential to support multiple applications such as RES and to provide auxiliary services to the grid (e.g., frequency and voltage regulation). According to different EVs chargers, both single-phase and three-phase AC are widely used [47]. However, the DC charging is the preferred owing to:

1. PV and BSS electricity production is DC.
2. EVs energy flow is DC.
3. Possible smart charge of EVs over time.
4. Easier V2G protocol with DC charging.

### ***2.2.3 EV Charging Facilities and RES integration***

There are different charging architectures for EVs: hybrid power sources (renewable energy, BSS and grid), or one dedicated power source. This raises the question about the benefits behind using hybrid sources over single power source in charging EVs.

Many visions are introduced to enhance the use of RES with the electricity grid to charge EVs for many reasons, such as (i) reducing the charging cost of EVs through the free electricity generated by RES and simultaneously, (ii) reducing fuel consumption by the grid. Furthermore, the EV charging process will be ensured under unfavorable weather conditions through either the direct charging from the main grid or the RES in case of grid failure to meet the necessary electrical needs [48-50]. In addition, batteries can be installed as energy buffers to store excess RES energy. The energy can then be returned to the grid to provide ancillary service or/to assist EVs charging. However, the connection of renewable energies to the grid is used with higher penetration levels in comparison with stand-alone renewable installation [51, 52].

The dependance on the main grid as a stable source/load that can compensate the RES fluctuations. Among these RES sources, solar energy is a preferable source for EV charging thanks to its energy that can be generated during highly priced power grid tariff hours. Thus, the PV based EVs charging stations can reduce the power cost. The PV module has a simple structure, small size, lightweight, convenient transport and proper installation. Moreover, the PV system has a short construction period and can be combined flexibly depending on the electrical charging capacity. Therefore, it can be easily employed as an on-site source. In contrary, the production of PV energy is strongly influenced by ambient temperature and irradiation levels. Thus, PV power is discontinuous over one day of operation and has an intermittent nature that can occur over short time intervals (minutes to hours). Therefore, a direct connection of the PV panels to the load,

without any auxiliary system, negatively impacts the performance of charging system. Accordingly, the storage systems can be crucial in stabilizing and mitigating the variability of the solar power output energy [53-56].

This thesis proposes an energy storage device in combination to PV system to maintain the continuous power to the EVs load, however much the power fluctuations of the PV system. The integration of storage device with PV and the power grid enhances the utilization of renewable energy, which contributes to attaining lower operational costs with higher efficiency.

### **2.3 Hybrid sources-based charging system architecture: Literature review**

One of the main problems of the adoption of PV power sources is the lack of a stable and continuous electrical power production. The PV power sources suffer from an intermittent and stochastic nature that caused by the continuous variations in the solar isolation levels as well as the ambient temperature values. Additionally, the day-night cycles highly impact the ability of using PV sources in standalone configurations. Thus, PV source is considered as non-dispatch-able units. Consequently, different solutions should be adopted in PV systems to balance the electrical grid power flow and provide steady power to the connected loads.

Several works have analyzed the design of EV charging stations based on hybrid sources including the storage system. All aspects of the PV-EV charging such as topologies of power converters, charging mechanisms as well as the control and optimization of on-grid, off-grid modes and hybrid systems are summarized in [57-59]

The full architecture and multi-mode combinations of the EV solar charger and its performance have been studied in [6, 60-64], the authors have defined the mutual benefit of charging EVs from solar energy for providing the high level of penetration of both technologies.

One applicable solution is to design a charging system using a variety of RES that can compensate partially the local grid fluctuations. However, adequate selection of RES and storage devices together with adequate capacity sizing are required. The combination of PV with wind energy has been discussed in [65]. However, such system has required either storage system or a connection to the grid to continuously supply the load.

In [66] the use of PV with FCs for residential load has been presented. For this purpose, a reserve capacity had to be maintained at the PV to feed the load as the FCs delivers a slow dynamic response. This leads to a deviation between the PV maximum power point (MPP) and the system operating point. To accommodate those challenges, a hybrid power sources composed of PV/FC/ultra-capacitors has been studied in [67]. In the study, the ultra-capacitors have been used due to their fast-dynamic response, which leads mitigating the

fluctuations of the PV power while tracking the MPP. However, this configuration may not meet load demands during low irradiation hours.

Storage devices can play an essential function for integrating SERs. A variety of energy storage technologies were studied and analyzed in literature to deliver a constant power output to electrical loads.

In [68], authors have developed a hybrid system consisting of a WT combined to FCs and super-capacitors. In the study, the developed control system has coordinated the power exchange between the sources. The wind turbine can provide ancillary services to the electrical grid, a feature that has growing interest due to the deep penetration of RES in modern electrical grid system. Battery storage, ultra-capacitors, and hydrogen cells are some of the energy storage solutions have been analyzed for wind applications. The use of storage devices coupled with the PV sources can provide the necessary means to accommodate the functions. The careful selection of the energy storage technology along with a careful design of its size allows for a higher degree of deregulation on the demand side, thus, achieving lower running costs [69].

The authors in [70], have used the distributed battery storage in grid connection and PV system to improve power quality. Provide a stable power production for PV system was the objective of ESS in [71]. An energy management strategy was introduced in [72] to control PV system in combination with storage to generate constant power. Constant power generation allows the system participation in the electricity market pools. In [73], Battery storage was connected to the grid along with the PV system to minimize power fluctuations in order to maximize incomes. while maintaining utility restrictions on PV power that can be supplied to the grid. The battery sizing has been discussed in [74], where the objective was to maximize the cost associated with the power purchase from the electric grid. The authors in [75] have performed the battery sizing analysis with the same objective while accounting for the battery degradation cost in order to extend the system lifetime.

In context of hybrid system based EV charging schemes, the relevant and important literature published are summarized and reviewed as case studies in this section. Generally, each publication deals with a specific issue on the EVs charging subject.

In [76], the decentralized energy management scheme was applied on the designed EVs charging station. The charging system included a 119 kW PV system, a 23.9 kW BSS and a grid connection. The authors concluded that with the proposed control strategy, the charging system can operate in the stand-alone mode with occasional support from grid. Ref [77] proposed a parking lot for 1,500 vehicles at the workplace combined with a 500 kW PV installation. The authors demonstrated that rather than using the grid at peak hours, EVs can operate in V2G or V2V to minimize the impacts on the grid. A decentralized load management on several buses was also examined and it was found that EVs charging was successful in

minimizing power losses. The suggested pricing algorithm has accomplished its objectives to reduce price from 12 % to 16%. However, the authors of this model did not consider the effect of distributed BSS system on the efficiency of the proposed pricing system. With the low EVs load and a high output of the PV system, the BSS can be monitored and charged outside the peak hours of power grid. This way, PV consumption can be increased and reduction in the cost of EVs charging can be achieved. Within the scope of increasing the economic advantages.

The [78] have investigated the EV charging system in Shenzhen, China, to verify its technical and economic feasibility. The obtained results showed that the total present value of a PV charging station and the grid station satisfied the daily electricity demand of 4,500 kWh. The energy cost of combined system was equal to 0.098 kWh in this scenario. A sensitivity analysis was performed to determine the parameters that can influence the EV pricing mechanism, such as the capital cost of the PV system, carbon tax price, interest rate and feed-in tariff policy. The author concluded that an increase in the interest rate from 0 % to 6% increases the cost of energy from 0.027 kWh to 0.097 kWh. This is despite the investment value of the ESS, which can reward in each period. Thus, the presence of BSS can have a considerable effect on the charging cost of EVs.

Ref [79], the power balance between the two distinct charging systems of a 50 kW PV based EVs parking area has been analyzed. As part of a centralized management structure, V2G technology has been defined in terms of a mathematical algorithm including stochastic demand and EV charging time. The integration of the PV system introduce intermittency in the system, which is reduced when larger batteries are used. The authors summarized that V2G can provide economic benefits and improve the network stability. The PV system can also reduce grid voltage fluctuations by minimizing the impact of EV load and peak loads on grid side.

Using PV system, ref [80] investigated the feasibility of charging the EVs battery at the workplace in the Netherlands. The meteorological data is used to determine the optimal location of PV panels to obtain the highest energy production in the Netherlands. Seasonal and daytime variations in solar irradiation are examined to identify the power availability for EV charging and the necessity of a grid connection to work in a distributed or centralized configuration. Nevertheless, different dynamic load profiles of EVs are also compared to reduce grid dependency and maximize the utilization of solar power to charge the EV itself. The author found that the rated power of the PV generator could be over-sized by 30% in comparison to the rated power of the converter.

Based on PV production, the EV load can be supplied with 30 kWh for 7 days/week, which has allowed the exchange of electricity on the grid to be reduced and given the suggested size of the BSS, as it can decrease the flow of electricity into the grid by 25 %. The performance of a PV and a wind farm connected to a diesel

generator, overall designed to provide power to 1000 EVs have been analyzed in ref [81]. The simulations were carried out considering the meteorological conditions in Tehran, considering the worst-case scenario. A Weibull distribution function is being used to predict the EVs arrival time; the parking time is assumed to be 4 h. The most effective design consisted of 30 kW wind turbines, 190 kW PV panels and a 530 kW diesel generator in this study.

Ref [82] developed a hybrid charging system composed PV and electrical grid for workplace parking. The proposed distributed charging system was installed at two sites, Columbus Ohio and Los Angeles California, to investigate various scenarios of solar radiation and pricing behavior. Decentralized EV load scheduling is qualitatively compared to a centralized strategy. The intelligent planning strategy aims to minimize the energy purchased from the grid and maximize the use of PV energy. It is clear that smart planning improves economic performance. Likewise, Ref [83] presented the design of PV-based EV charge coupled with two micro gas turbines, used to charge EVs fleet. This work is intended to optimize the operator's economic viability. The scheduling of EV recharging, micro-turbine operations and rotating reserve supply is computed by calculating the fleet planning based on the information supplied by EV owners, market energy prices and the expected generation of renewable energy.

Ref [84] designed a PV-wind charging station for small electric tuk-tuks, located in Congo. The charging station is linked to wind energy system and a PV field, providing power to the BSS. In this case, the role of the BSS is crucial, as the proposed facility is intended for stand-alone operation. In this way, the BSS is utilized to deliver a stable energy distribution to the tuk-tuks, thus mitigating the variation due to weather conditions. The best layout includes 1.0 kW PV panels, a 7.5 kW wind turbine and 20 cell BSS. In this situation, the PV system produces 1518 kWh/year, the wind turbine 15.215 kWh/year. This system has an initial cost of 20,060, a current net cost of 39,705, an operating cost of 1,067 per year and a unit cost of energy produced 0.499 per kWh, with a corresponding expansion distance of 2.87 km from the grid.

Ref [85] proposed solar system-wind EV parking lot situated in Alberta, Canada. The aim of this research was to size the PV system, which could supply 17 kWh a day, corresponding to the daily energy necessary to achieve a range of 64 km in a fully electric EV. The investigation was performed in the worst and best irradiation conditions December and July, respectively. The best case led to a surface area of 20 m<sup>2</sup>; on the contrary, the worst case led to a layout of 78 m<sup>2</sup>. In [62], a solar park near Lisbon, Portugal is described. The purpose of this article is to investigate the energetic and economic viability of a distributed charging infrastructure for EVs. The relation between solar irradiation and parking lot usage is also investigated. In addition, the PV system is coupled with BSS to enhance the efficiency and effectiveness of the charging system. The author assessed that the 7-year refund period with a financial inducement of 40 % of the proposed pricing system has been achieved.

From the literature, multiple research points concerned/deal with advantages of integrating battery storage system with PV to realize a stable power at a minimal operating cost become important. In this dissertation, battery storage system is connected to PV panels and main grid forming a micro-grid to provide power for EV chargers. Independent power converters are used for PV, BSS, grid, and EVs chargers. In hybrid power sources based EVs charging, either DC/DC converters into a common DC bus then connected to the grid via a bidirectional AC/DC converter (DC micro-grid), or A common AC bus with independent stage rectifier for each source in the EVs charging station (AC micro-grid). or in a hybrid AC and DC micro-grid.

In the context of charging system classification, the authors in [41, 86], have been classified the charging systems configuration based DC or AC considering the installation place, the power rate, and time of charging as:

1. Decentralized AC charging station: The decentralized plug-and-charge type charging often appear in parking spaces, residential areas, or public places. It is characterized by a small current approximately 15 A slow charging mode, which requires about 5-8 h (or longer) for full EV battery charging.
2. Conventional charging station: It usually consists of three or more charging devices, located near the business district and offices areas. Most of the charging stations use medium or fast charging mode. The typical charging time is about 3-4 h. The fast charging (using DC charging) time is approximately 30 min-2 h. the state of charge (SoC) be can be over 80 %, and the charging current is 150-400 A.
3. Large charging station: It usually consist of many chargers and battery storage devices that can simultaneously charge many EVs. The large charging power station not only has the basic functions of the conventional charging station (such as regular charging and fast charging), but also can centrally charge the battery storage devices (mostly in the form of slow charging). The outstanding characteristics of large-scale charging power stations are that they can feed back energy V2G to the grid and participate in load peak-to-valley regulation, this type of mechanism it is not easy to be carried out for satisfying this load planning with equipment's of decentralized and conventional charging stations.

The power demand of EV users in the different regions depends on economic level, lifestyle, seasonal climate, location and type of load. The combination of different types of RES and distribution grid for enhancing EV charging and discharging facilities are a key issue of the integration technology. Based on the classification of charging systems, the integration of RES and charging installations can be carried out in each category as:

1. Decentralized charging stations and distributed RES's: Considering the possibility of installing RES in residential communities, residential units and public places, such as charging installations are most appropriate for integration with distributed PV systems that can be installed on building roofs, this type of integration is mainly adapted in rural areas, depending on its random and flexible charging characteristics.

2. Conventional charging stations and distributed RES's: The conventional charging station has a certain area. One or more distributed RES systems can be integrated into the charging station depending on the weather characteristics of the region. Owing to abundance of wind turbine (WT) resources in high latitudes cities, a number of small WT (a single machine 10-100 kW) can be installed in the charging station; solar radiation in the low latitudes city is strong. Therefore, both/either PV panels and/or WT can be installed in certain area depending on regional weather conditions.

3. Large and medium power stations and RES production: Under normal circumstances, certain commercial and passenger vehicles have relatively fixed driving characteristics and parking spaces, and fixed charging methods. Therefore, it is possible to establish a reasonable electrical connection with RES such as PV plants adjacent to the surrounding areas of the city. Therefore, local consumption and renewable energies can be accomplished.

Whatever the multi-criteria-based classification regardless of the energy sources in the literature, the hybrid source-based charging stations are still operating with different research idea in micro-grid configurations. In hybrid power sources based EVs charging, either DC/DC converters into a common DC bus then connected to the grid via a bidirectional AC/DC converter (DC micro-grid), or a common AC bus with independent stage rectifier for each source in the EVs charging station (AC micro-grid). or in a hybrid AC and DC micro-grid. From the literature, multiple research points concerned/deal with advantages of integrating battery storage devices with PV power to attain stable power supply at a minimal operating cost become important. In this dissertation, BSS are coupled to PV panels in a grid-tied system forming a micro-grid to provide means of charging for EVs. Independent power converters are used for PV, BSS, grid, and EVs chargers.

### ***2.3.1 Architecture 1: AC micro-grid structure and EVs charging system***

The diagram in Fig 2.1 illustrates the structure of AC based charging station, where the PV panels, BSS, and the EV charge/discharge are equipped with separate converters. As a DC/AC inverter, PV inverter includes maximum power point tracking MPPT, while the EVs chargers is AC/DC converters. Besides, the 50Hz AC grid is used where the most of power is delivered. The disadvantage is that the PV power is not available continuously to charge the EV with DC power. However, in the AC micro-grid the DC/AC power is converted at the PV inverter as well as AC/DC power at the EV charger. In the AC charging system, RES is connected to the AC bus via an inverter to provide electrical power to decentralize AC charging systems in EVs charging systems [87-89]. As the AC power sources is connected to the grid by an AC bus, no inverter is required to supply AC power to the other loads. The base load system can be integrated into the conventional electrical grid and can support AC equipment such as asynchronous motors. However, some

problems make it difficult to control and operate the AC charging system with many stages of power conversion.

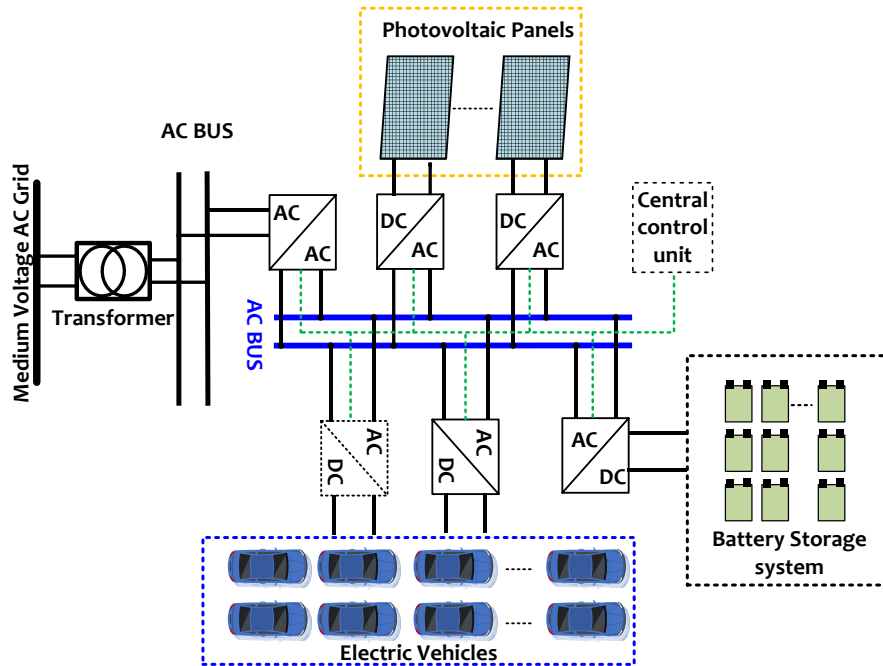


Fig 2. 8: AC micro-grid structure with EVs chargers.

Using the common connection point (PCC) switch on the AC bus, the charging system connection and island operation mode is performed. The EVs can be charged from the AC charging system, it can also be discharged into the distribution grid at certain times to achieve V2G functionality. Given the current situation of the characteristics of the AC charging system, this system remains the main form of integration of many kinds of RES installations and the charge/discharge of EVs [35, 90]. In [91], the AC micro-grid has been analyzed, including power generation units, WT, PV, intelligent charging/discharging, and controllable/uncontrollable loads. For small AC micro grids containing PV, WT and diesel generators. The literature [92] have evaluated the impact of multi-source on micro-grid frequency and voltage profile.

The analysis has suggested that EV applications can improve the performance of micro-grid systems and maximize the use of renewable energy. Considering the stochastic characteristics of EVs in renewable energy and AC micro grids, a semi-Markov decision process (SMDP) based real EV charging data has been proposed in [93]. The simulation results have shown that the strategy can better serve charging demand and improve the RES utilization.

### 2.3.2 Architecture 2: DC micro-grid structure and EVs charging system

The DC based EV charging system facility shown in Fig 2.2, mainly consists of PV with MPPT, BSS, EVs chargers, power converters, and central controller. Through the common DC bus, it is easier to use the

DC power of the PV directly for the DC charge of the EV without power losses, thus achieving high efficiency [94-96]. The DC bus is linked to the AC grid by a central inverter/rectifier, which is essential for the implementation of V2G and provides power (drawing/supply) in the charging system due to the difference between PV power production and EVs load. Accordingly, the cost and losses of the system can be reduced. Furthermore, the DC based charging station control is easier to implement compared to AC based charging system where the DC bus control is based on the DC bus voltage, while the power flow control is based on the current [97, 98]. In this way, a coordinated control between the different energy sources can be efficiently carried out.

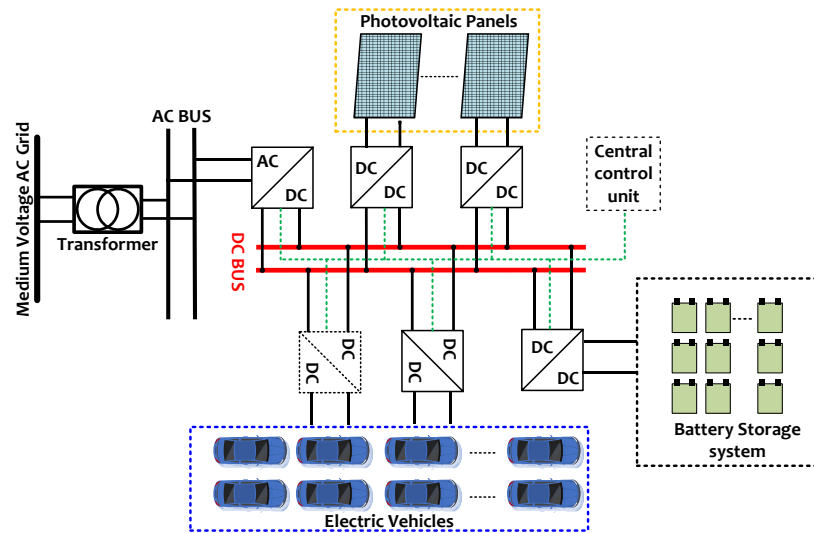


Fig. 2. 9: PV panels, BSS and EVs connected to the common DC bus with grid connection.

For decades, the discussion on the utilization of DC power as an alternative in energy distribution has been of great interest. More recently, the DC power systems in industrial systems, commercial buildings and residential witnessed more attractive and popularity than AC power system. The overall benefits of DC based charging system are (i) DC-based renewable energy sources require a single power conversion stage to connected to DC micro-grid and single-phase or three-phase inverters to connect to AC micro-grids. Meanwhile, AC-based renewable sources need a double power conversion. The reduction of energy conversion phases in sources entirely based on converters that can result in further decrease of the overall system cost; (ii) no reactive power in the DC systems. Therefore, a high-power transmission capacity and less power loss are reached; (iii) the reliability and the efficiency of DC power systems is high; (iv) the control of DC power systems is easy to perform by controlling the power supply by the common DC bus voltage. In [99], DC based charging system has enabled full use of renewable energy and EVs for electricity transmission and distribution. The simulation results have validated the feasibility of the different operating modes. In [100], the DC micro-grid based on solar energy has been designed to meet the changing needs.

The author has proposed a strategy for controlling the micro-grid under different DC voltage levels and load conditions.

### 2.3.3 Architecture 3: hybrid AC/DC micro-grid structure

With the development of smart grids, micro grids with EVs and RES become of hybrid AC/DC structure, as shown in Fig 2.3, where AC and DC loads at the same time can be supplied. The EVs are connected to the DC grid by primary DC-DC converter to achieve a fast DC charging in the charging station; or energy feedback by V2G technology if applicable. The AC grid can provide electrical power for the charging stations of the EVs and the AC charger on the parking space. Generally, this hybrid structure is still considered as an AC micro-grid and the DC grid can be considered as a particular source of DC power.

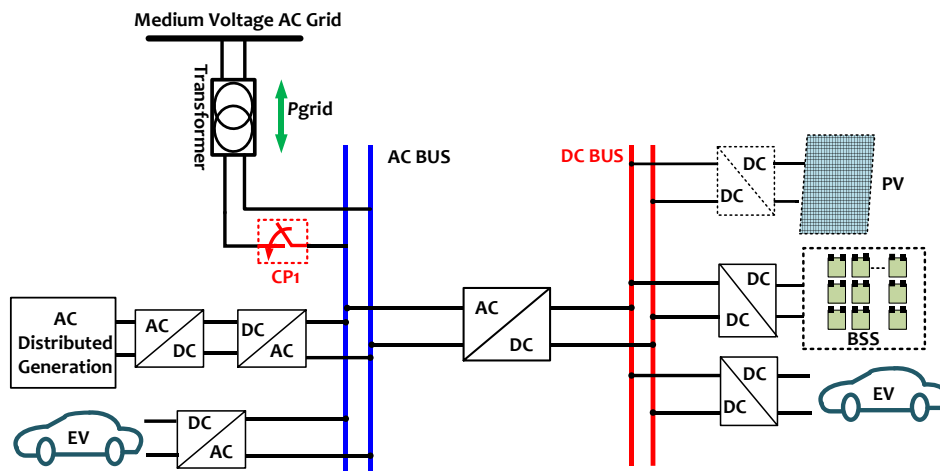


Fig 2. 10: Topology of AC-DC hybrid micro-grid structure.

In the AC/DC hybrid micro-grid, the interlinked power converter (ILC) is the key equipment for connecting the AC and DC grids. When the AC/DC hybrid micro-grid is working, the ILC starts the power transmission on both sides of the AC and DC and maintains the energy balance between the AC and DC sides. ILC can work in rectification or inverter mode according to the actual needs of load [22, 101].

In [21, 102], the influence of EVs on the internal characteristics of the micro-grid and the storage system has been investigated under the hybrid micro-grid structure. [57, 103], have been examined the battery SoC and the random charging demand of the EV user. The stand-alone decentralized V2G control strategy has been considered to establish a flexible EV charge/discharge and stabilize renewable energy power fluctuations and micro-grid charging. In [104, 105], three-layer coordinated control system has been integrated into the central micro-grid controller to control the interconnection between the three-phase AC and DC ESS EVs, alongside the analysis the impacts of homogeneous and heterogeneous of EVs load to observe balanced and unbalanced scenarios. In [106], the PV power generation and multiple sets of EVs have been considered into

a small DC micro-grid to access the charging stations. Other RES have supplied power to the station's AC load through the AC bus.

In the future AC/DC hybrid micro grid, further considerations for the regulation of EVs include “V2V”, “V2H” and “V2G”, and other modes to make the micro-grid facilities more controllable and interactive. The findings of numerous published studies have been implemented on EV charging stations and BSS to design and develop robust EV charging systems. Table 2 summarizes the various charging station architectures reported in literature that are rigorously examined. To achieve an efficient EV charging system, it is essential (i) minimize the total number of power conversion steps. (ii) to design appropriate and efficient control/energy management.

Table 2. 6: Charging station architectures presented in literature.

<i>Charging system architectures</i>		<i>Power rating (kW)</i>	<i>Power conversion and control</i>	<i>Review and Comments</i>	<i>Research papers</i>
<i>Common DC bus</i>	<i>Common AC bus</i>				
-	√	16–24	MC68HC microcontroller for maximum point tracking (MPPT); three-phase bi-directional DC/AC inverter.	A distributed charging architecture was tested, the paper did not introduce the energy management of the charging system.	[51]
√	-	48	AC/DC rectifier transforms the three-phase AC input power to an 800-V DC output; the DC/DC converter adjusts the DC output to an appropriate level to charge the EV battery; the bi-directional DC/DC converter charges and discharges the BSS in the charging station.	Model predictive controllers were proposed to implement decentralized energy management in the introduced system; a unidirectional AC/DC inverter was implanted. To examine the developed EMS of this model, a bi-directional converter at grid side was used to test the system under peak load conditions. The model did not consider electricity cost.	[76]
√	-	20	Bi-directional converter AC/DC grid connected to two DC/DC converters with a similar nominal power rating.	A schematic of the charging station was created. The VDC bus, which is the control logic of the AC/DC bi-directional converter, indicated the difference between the reference voltage and measured voltage. The closed-loop control of each power converter was used in the charging station under several operating conditions.	[24]
-	√	33	AC/DC rectifier transforms three-phase AC input power to an 800- V DC output; DC/DC converter adjusts the DC output to an appropriate level for battery charging.	A centralized control and a charging schedule were proposed to solve the voltage drop problem, which resulted from the charging process at the grid peak load.	[107]

√	-	0.2	Smart fuzzy logic employed for the MPPT algorithm based on discrete proportional integrated derivative (PID); PID-controlled buck converter charges the battery under various conditions.	A comparative analysis of the MPPT controller was performed and different MPPT techniques were introduced.	[108]
---	---	-----	---	--	-------

## 2.4 A comparison of charging systems architectures

At the micro-grid and EVs control level, the operating mode of the charging and discharging facilities of the EVs connected to the micro-grid can be set by identifying specification of EV batteries, Simultaneously, it is necessary to study the battery charging/discharge requirements and capacity of the different micro-grid models, combined with the control characteristics of RES, analyze the typical micro-grid, and the control strategies of the micro-grid within the EVs and RES. Several publications have been published in this field.

In AC micro-grids, the difficulty of research lies in the stability of indicators such as buses voltage and frequency. In [109], a micro-grid simulation model consisting of distributed power generation, EVs, conventional load, central controller and other base units has been initially established and studied under grid-connected, stand-alone and transient mode. EVs have been used as load and power sources. The effect of the bidirectional flow of the active load on the voltage and frequency of the micro-grid has been analyzed. In [79], a micro-grid has been established with different levels of renewable energy production penetration. The EV can control and regulate the voltage and frequency of the micro-grid by V2G to ensure the safety and reliability of the micro-grid's energy.

In DC micro-grids, voltage stability, load requirements and energy conversion efficiency are the most significant issues to be considered. In [27], the back-up power supply has been used for stabilizing the bus voltage. The strategy for controlling power transmission has been proposed. The micro-grid is operated in different distribution modes to meet the demand of EVs and other loads. In [110], the author has proposed a control method to ensure the conversion efficiency of the EV charging systems while reducing the energy conversion phase between power supply and load.

In AC/DC hybrid micro-grid, the main concerns are power balance, system stability and coordinated control of each component in the micro-grid. In [81], the energy status of the different batteries in EVs has been virtually defined as a "power package". The balance of active power in near-real time has been considered to reduce random charging and intermittent power fluctuations caused by RES.

Although the establishment different types of charging and discharging fatalities, their simulation models for the micro-grid access are not yet optimal because of the different factors: (i) for decentralized EV charging system, the charging and discharging power can be regulated by demand-side response measures,

under partial control only; (ii) in fast charging mode, the user needs to meet the fast charging requirements of the plug-and-charger and charging power basically uncontrollable ; (iii) In power exchange mode, due to the centralized charging of the BSS, the charging and discharging process is partially controllable.

Therefore, it is essential to examine the control diagrams of the different charging and discharging facilities according to the specific application conditions and to carry out related modelling research appropriate to the micro-grid framework.

At the hybrid grid level, the primary control techniques and energy management strategies are still performance deficient, the feasibility and scope of the master-slave control and hierarchical control of the micro-grid in the integrated system need to be studied. According to the power regulation characteristics of distributed renewable energy, the SoC of EVs battery, the BSS, and the control mode of the charging and discharging architectures, the local control strategy for renewable energy is studied, and explore the EVs batteries characteristics to regulate the voltage and frequency of the micro-grid buses. The technical analysis of the feasibility of various real-time consumption strategies, and the testing and validation of the negative impact of various collaborative control strategies on the availability of charging services and the micro-grid self-smoothing rate.

Table 2.3 presents a qualitative comparison of EVs charging system architectures where the advantages and disadvantages of both types of systems are presented. The DC charging of EVs with hybrid power sources reduces the number of conversion steps and power losses associated with the use of AC power, which includes additional power conversion steps. A major advantage of the DC charging architecture over the AC charging system is that it provides a more efficient way for the charging system to operate. Only the power conversion in the charge based on DC power at the grid side leads to a lower number of components, higher system efficiency and power density compared to the multiple power conversion steps in the AC charging architecture.

Table 2. 7: A qualitative comparison of AC and DC based charging system architectures.

<i>Architectures</i>	<i>Advantage</i>	<i>Disadvantage</i>
<i>AC bus-based charging system</i>	<ul style="list-style-type: none"> <li>• Represent a simpler concept, well-developed standards and technologies are available.</li> <li>• Reliable switching and control considering the zero crossing.</li> <li>• Active/reactive power management can be decoupled which simplifies the AC voltage/frequency control.</li> <li>• Charging unit can be individually connected to grid.</li> </ul>	<ul style="list-style-type: none"> <li>• Fast chargers with separate rectifier stages can cause undesirable harmonic effects on the power grid.</li> <li>• The cost of multiple converters with low rated power is greater than that of a single high-power converter, due to the large number of control stages and filters.</li> <li>• Renewable that are inherently DC, will require an independent DC/AC stage, consequently, the system's cost and complexity.</li> <li>• The power quality and stability of indicators such as bus voltage and frequency, control and operation are difficult to find and achieve.</li> </ul>
<i>DC bus-based charging system</i>	<ul style="list-style-type: none"> <li>• Provides a more flexible structure, which can easily integrate RES and ESS.</li> <li>• Higher power density and overall efficiency, low losses, low component number and cost reduction.</li> <li>• Promotes the concept of a central charging station serving which minimize the impact of the high density EVs loads in public locations on the grid.</li> <li>• No issues with control nor reactive power and frequency exists</li> </ul>	<ul style="list-style-type: none"> <li>• Requires more complex protection devices because no zero cross points of the voltage exists.</li> <li>• Switching frequency is restricted because the switching losses become relevant when the power range is high.</li> <li>• The increase in the nominal power of the central converter causes more severe requirements for the grid, in terms of harmonic component amplitude and overall harmonic distortion.</li> </ul>

Based on the comparison between the two systems architecture, the scope of this thesis will focus on DC-based charging architecture and its applicability and feasibility with medium voltage high power rating in charging system-based hybrid power systems. The direct DC charging of EVs from PV and BSS in stand-alone mode with only one inverter required for the AC grid will be comprehensively studied. For energy exchange between chargers and the grid, V2G can be used with the existing AC grid infrastructure available worldwide using a DC interconnection.

## 2.5 Hierarchical Control for EVs Charging System

The EVs charging station plays the pivotal role to provide the power link between EVs user and the main grid. Proper design of the charging station, primarily dependent on renewable energy and assisted by electrical storage enables cost effective operation of the grid [111, 112]. The main points related to the hierarchical control of the EVs charging station are given as:

1. Energy management: reference generation constrained to the SoC of the storage elements to drive the primary controllers.
2. Power balance: to provide a sustained balance between generation and load

3. Output regulation: tracking of the reference voltage and currents of various charging system components.

The hierarchical control is depicted in Fig. 2.4.

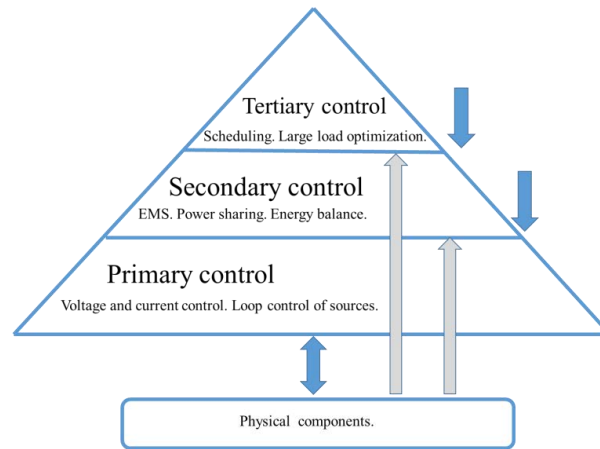


Fig 2. 11: Hierarchical control of EV charging stations.

### 2.5.1 Primary Control Structure

Primary control structure is the primary level of control mechanism. It is driven by the appropriate secondary control or energy management strategy. It controls the dynamic response of the controllers attached to individual power conversion stages of all the components. So, the input of primary control structure is the reference generated by secondary control/energy management. Primary control includes the voltage and current droop controllers, classical PI controllers and nonlinear switch mode controllers.

#### 1. Centralized Control Structure

A centralized control approach consists of a central controller to maintain the bus voltage. In the DC micro-grid, the grid-tied AC/DC interlinking converters are responsible for the DC-link voltage stability, and the DC load and DC sources can operate in the constant power mode without supporting the DC bus voltage [113-115]. The grid-tied interlinking converter controller typically employs a double loop structure that consists of an inner current loop controller and an outer voltage loop controller [116]. A common method of designing the control loop is to use a PI controller to improve the current regulation performance with an additional feed forward compensation. In [117], a model predictive control is proposed for the interlinked power converter in both grid-tied or islanded conditions in which the switching vector can be directly determined through the model predictive control technique. A centralized controller is proposed in [115, 118] where the load current is measured and transmitted to a central controller. Then, based on each distributed energy resources (DERs) characteristics, the output contribution of each source can be determined and the output current reference are sent back to the sources, while an outer voltage loop

simultaneously controls the bus voltage. This scheme can realize fast mitigation of transients. A voltage controlled power sharing is suggested in [119]. Here the equivalent current sharing between different power sources is based on central communication blocks. This is an efficient method of hierarchical control mechanism.

## ***2. Decentralized Control Structure***

The decentralized control structures are gaining more attention in the past decades due to more resilient nature, ease in implementation and better safety provision during the grid connected and islanded operation [76]. In the decentralized control, the major portion of control consists of droop controllers. Mostly the droop controller provides satisfactory performance to meet the desired objectives.

### ***2.5.2 Secondary control for EVs Charging unit***

The secondary control level is referred to EMS of EV charging stations as shown in figure 2.5. The EMS generates the reference signals for the primary control structure. The main objective of secondary control is realizing the maximum utilization of renewable energy, reduce the stress from electrical storage and main grid, reduce the operational cost and satisfying the necessary constraints. The economic operation is the major concern of the EMS. At present, the dynamic electricity price, the controllable EV charging load, and the ancillary service market are the main tools that can be used to minimize the operation costs. Besides, the EMS can also take advantages of the local generation units and the local ESS to generate extra revenue [48, 120-122].

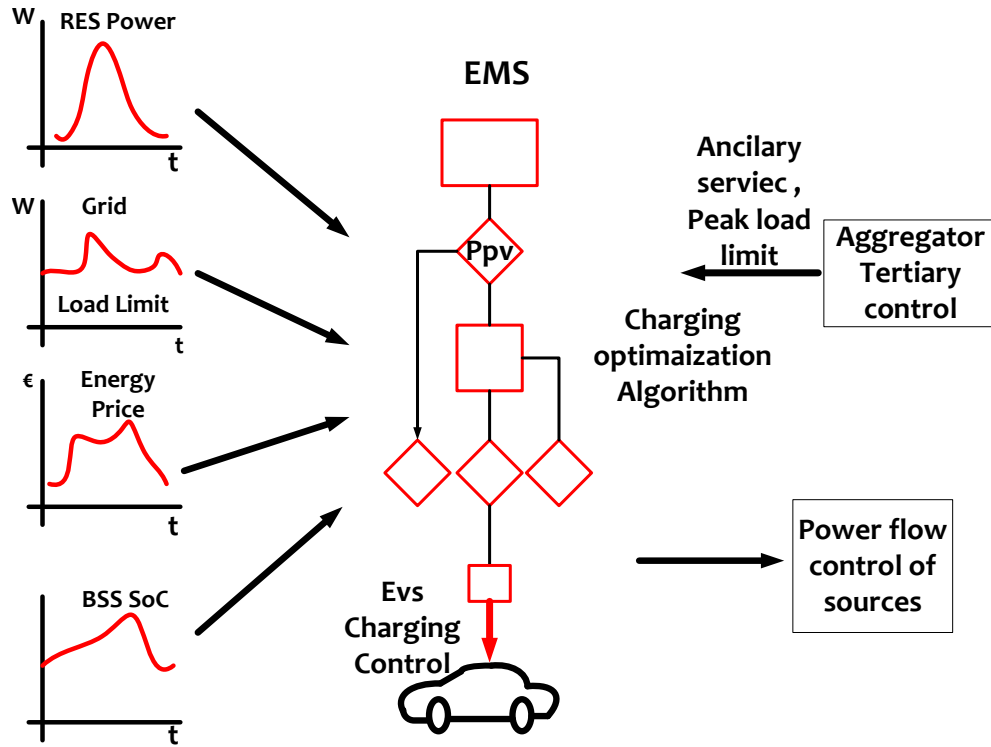


**Fig 2. 12: EMS structure for EV charging station.**

To design EV charging system, the flow of the power among the main sources of the system needs to be explored. The decision on the needs and the types of bi-directional power electronic systems together with their sizing requirements can be performed based on the power flow management. Accordingly, the research attempts to solve the power flow management problem and the applicability of the power flow management to the proposed charging system. The combination of the battery storage with the PV offers different solutions to power flow problems during different time intervals while supplying the connected load with the demanded power.

Solving the operation issues of the hybrid system has been the main interest of research in several publications. The power flow in grid/ PV/BSS have been conventionally predefined by heuristic rules that consider the load demand, the PV irradiation levels and the utility off-peak hours [123]. However, a dynamic grid tariff complicates the proposed solution. In the dynamic grid tariff system, the operation of the PV/BSS using the simplified heuristic rules has provided running cost solutions that largely deviate from the minimal cost operation. Thus, the research in this area has taken an accelerated path. In [124], the Lagrangian relaxation technique has been applied to determine the optimal hourly battery charging/discharging current. The objective was to maximize the contribution of the hybrid system to the grid. The proposed technique in [125] has assumed zero dispatch cost associated to the PV/BSS output power. This leads to the neglecting

of the battery degradation cost and its advisable operating conditions. In [56], the power flow management has been proposed based on charging schedule method through EVs load forecasting. By adjusting the charging start time to maintain the charger power rate, on the basis of satisfying the user's demand, the low-voltage electricity has been used for charging the EVs as much as possible to stabilize the load fluctuation and to reduce the difference between peaks and valleys. Besides peaks load in the charging process can be avoided.

In [31], the linear programming (LP) has been used for obtaining the optimal EV charging strategies for multiple EV aggregators, the author has been considered LP based on the PV generation forecasting technique to reduce the charging costs and improve the PV utilization rate. The rule-based energy management scheme has been proposed for EV charging with a PV-grid system [126]. The continuous charging process has been ensured with defined the operation rules to achieve the charging cost reduction. However, the techniques suggested in [127], [128] have been developed for constant electricity price market. Considering certain incentive policies (time of use tariff, dynamic price, etc.) may require further improvements in terms of energy management strategies. Regarding the ancillary services, V2G EV charging stations can play an important role in the future of smart grid by offering charging and reserve services in a sustainable way [129], the LP and the rule-based energy management methods have been presented for small-scale micro-grid with multiple EVs. The self-consumption of PV power has been increased and the power peak was shaken through the V2G technology. In [130], the mixed-integer linear programming (MILP) framework-based models has been developed to investigate the cooperative EV charging with the V2G provision. In order to utilize the potential energy storage of EVs, the EVs have been modelled to provide the frequency regulation capacity [14, 131, 132]. The battery energy storage has been integrated into the RES for enabling the PV source to act as a dispatch-able unit on hourly basis. The objective of the battery storage utilization has resulted in reducing the running cost. The proposed system was sensitive to the solar power forecasts.

From the ongoing research in the field of power flow management of PV/battery grid-tied systems, different conclusions can be drawn. The problem formulation should account for maximizing the use of PV and enhance the local BSS capacity to extend the battery lifetime. Thus, the system reliability can be increased. Moreover, the PV is known by its stochastic nature and non-linear performance; in such a system, EV batteries must recharge at specific voltage and current limits. Consequently, the coordinated control of the energy conditioning system is necessary in this process to control the power flow. As the desired power flow management topology has to accommodate non-linear functions, the generalization of the developed topology on different operating scenarios become necessary. The energy management approach should consider weather information and load demand statistics to optimize the use of solar and grid energy by the

charging station. Hence, instead of immediately recharging the battery to a fixed SoC after each EV charging, the target charge level of the buffer battery can be optimized according to the estimated PV electricity generation and the projected EV charging load. Therefore, the usage of solar energy will be maximized. Consequently, the impacts of solar availability and EVs charging on the utility grid will be reduced. From the literature review, focusing on hybrid charging systems, power balancing issues, energy storage sizing and aging problems and coordinated control between the sources has become a matter of great interest for the researchers. Therefore, this thesis deals with the charging system based on the hybrid sources. The hybrid sources considered in this thesis are PV, power grid and BSS alongside their uni/bidirectional power conversion steps.

### ***2.5.3 Tertiary control Large-scale Management of EVs in Power system***

This control is the top-level management strategy provided to generate reference signals considering the present condition of main grid. This control is only relevant to main grid and therefore not interlinked to micro-grid [133-135]. The tertiary control coordinates different charging stations to provide the global power management. It typically provides the control signal to the secondary level controllers of micro-grid systems. The main aim is to coordinate the multiple aggregators to achieve various objects related to grid such as (low transmission losses, low maintenance costs, low peak power, etc.). The EVs are connected to a charging station through charge outlets. They operate as a load on the distribution grid during charging and an energy supplier to the grid during discharge. In contrast, the EVs can be operated without any start-up or shut-down costs during the charging or discharging mode [136]. Evening hours are preferable for charging EVs; this period provides grid operators the appropriate opportunity to fill the loading valley. However, this scenario may not always be feasible. With the possibility of switching the EV charging time based on the real charging time, the charging system supplies ancillary functions, such as frequency regulation; on the other hand, the charging of EVs at specific points in time leads to the smart charging schedule concept. Nevertheless, the EV charging schedule depends largely on the parameters and characteristics of the EVs and their loads. Specifying the nature of the EV charging and its appropriate control mode is a complex process that generally depends on the following factors [32, 137].

1. EV travel time: This time mainly refers to the user's mileage or travel interval; this parameter defines the user's charging time, power demand, and access to charging facilities.
2. EV driving pattern: This parameter reflects the user's charging preferences; when the difference in usage patterns is considered, a certain amount of charge load dispersion results.
3. EV battery characteristics: These include battery capacity, charging/discharging rate, and SoC.
4. Number of EVs: This number defines the overall regulation of the load profile.

5. Charging facilities and their standards.

6. Charging control strategy: This can be divided into centralized and decentralized control strategies also known as direct control and distributed control. The centralized control strategy refers to the EV charging schedule, which is performed centrally at the aggregate level after collecting the information and parameters. The decentralized control strategy on each EV is that in which there is a certain computing capability in collaboration with the aggregator.

### 1. Centralized management strategy

In the centralized control strategy, the EVs provide the local aggregator with information on their electrical parameters, such as battery capacity level, charge rate, and SoC. Based on the aggregated energy requirements, each local aggregator concludes a contract with the grid operator [138]. Once the contracts from different local aggregators are received, the grid operator decides on the appropriate share of energy for each aggregator within its contractual scope, considering other loads, power production capacity levels of various sources, and other system constraints. Thereafter, each aggregator performs optimization to schedule each EV load so that the expected energy requirement of the vehicle is satisfied [139]. However, the problem with centralized charging is that the system is dynamic, and EVs arrive and leave all the time; hence, it is not possible to achieve a long-term stationary planning profile. Figure 5 shows the centralized control strategy architecture.

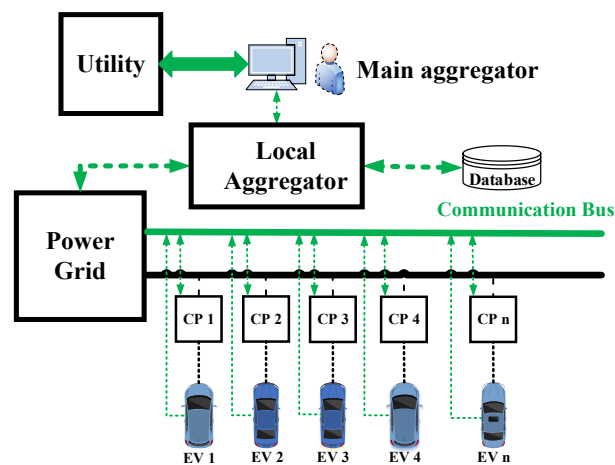


Fig 2. 13: Centralized control architecture.

The local aggregator, which is added to the technical management, is generally responsible for the involvement of EVs in the electricity market [140]. As such, it is important to forecast daily demand based on historical data, customer preferences, etc. As soon as the load demand profile, including the electricity price for all EVs, is collected through the local aggregator, it is sent to the main aggregator or grid operator for approval. The main aggregator verifies and assesses whether the load demand profile is appropriate for

the safe operation of the distribution system. Once the demand profile is approved by the main aggregator, the local aggregator provides a charge set point to each EV in real time. In real-time operation, the aggregator collects data from the EVs that are connected to the grid. Such data can be saved in a database relevant to the EV profile for the next charging process. Thereafter, the aggregator uses algorithms to achieve the proposed objectives while satisfying the requirements of EV owners. To achieve this goal, all set points will be sent to the CPs via a communication system. Inside each CP, the control unit receives the command signal and operates on the charger/inverter in order to provide the required charge/discharge power [139, 141].

## 2. Decentralized management strategy

In the decentralized control strategy as shown in Fig. 6, every EV directly shares its energy requirement with the main aggregator while using some of the information compiled with the aggregator to decide on an optimal schedule; each EV owner can potentially decide when to charge the vehicle battery and how much energy is required. This decision could be influenced by the aggregator through signals that indicate the cost of electricity, such as time of use (ToU) rate[142]. The introduction of a ToU rate affords an incentive by reducing the charging price; the aggregator uses a static ToU rate that is assigned to the EVs [143]. The amount of energy that is charged into the batteries is evaluated because the EVs are connected until their departure. The number of steps required to charge the EV battery is calculated as a function of the EV charging power and energy demand. During the period during which the cost of connection to the grid is between the highest and lowest price, the tariff is ordered to evaluate the time steps with the lowest possible electricity prices. The main benefit of decentralized control is its flexibility to accommodate many EVs and allow the penetration of the scheduling process. However, because of the absence of complete EV information, the charging scheme is sometimes sub-optimal [142, 144, 145].

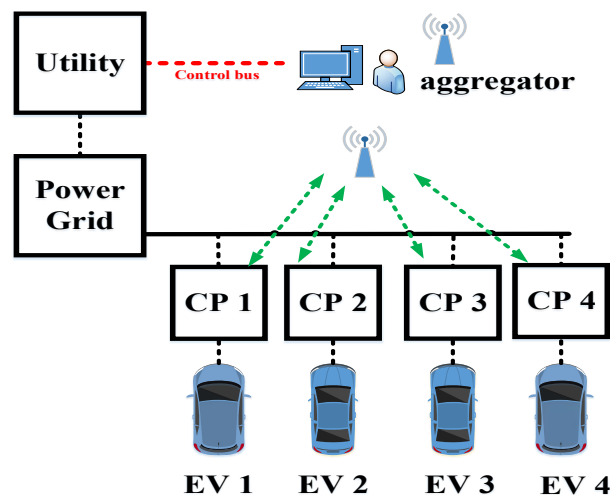


Fig 2. 14: Decentralized control architecture.

From a critical point of view, EV charging scheduling is solely based on the assumption that a group of EVs is involved; however, it actually relies not only on this assumption but also on different parameters on the grid (both on the user and operator sides), the amount of power involved, and the starting and ending times of the charging of each EV in the group. This is an optimization problem where some parameters are improved on the grid (at the user side or aggregator side or both) under different constraints. Because the parameters, constraints, and objective functions are considered to cover a wide spectrum, different forms of optimization problems arise; hence, in general, there is no single mathematical formulation for the problem. The parameters and constraints involved and the methodology used to establish the scale of charges vary considerably although they all pertain to the same fundamental problem the implementation of EV charging schedule. Table 2.4 summarizes the centralized/decentralized characteristics and shows the capacities of the charging facilities used in charging topologies alongside the charging behavior of EV owners at different locations [141, 145].

Table 2. 8: Centralized/decentralized characteristics.

		<i>Characteristics of the EV owner's</i>		<i>Characteristics of electricity facilities</i>		
		<i>Distribution Time</i>	<i>Charging time</i>	<i>Capacity (kVA)</i>	<i>Voltage level (kV)</i>	<i>Load characteristics</i>
Centralized charging	Charging according to the running time of the vehicle		min ~ few hours	Hundreds ~ thousands kVA	Up to 10	Generally during the low electricity period.
	Daytime charging use is greater than nighttime		10 min~1 h	600	Up to 10	The charge impact is more greaten during day than nighttime
Decentralized charging	Fast charging: distributed time evenly		10 ~ 30 min.	70	0.4	The Impacts is more is greater during daytime than nighttime
	Slow charging during day and night		Hours	8	0.4	Generally superimposed with the peak period of grid load during daytime
	Daytime (Workplace) or night (residential area)		Hours	4-8	0.4	Charging Impact at daytime. Load valley at nighttime

## 2.6 Conclusion

The large-scale integration of EVs in the conventional power system can lead to increment in power demand and can therefore threaten main grid. Thus, appropriate control mechanism and energy management should be designed to smoothly integrate the EVs into the local grid, and minimize the total operation costs, as well together with maximizing the local utilization of renewable energy. This chapter presents the state of the art of the system control and energy management aspects of Level 2&3 charging infrastructures (i.e. EV

charging station). The hierarchical control of EV charging station is outlined, which offers decoupled control objectives in different layers of the EV charging micro-grid system. Some important contents of charging infrastructure standards, basic power architectures, energy storage technologies are highlighted in this chapter. Various coordinated primary control techniques and basic energy management strategies are also introduced. Subsequently, the power conversion stage plays an important role to achieve an efficient and stable hybrid charging station.

## **Chapter 3: EV charging system modelling and control**

### 3.1 Introduction

In this chapter, the primary control and energy management is developed and analyzed. The primary control plays the most essential role in EVs charging system. The EV charging system as a micro-grid system mainly includes several components [2, 60, 146]: EV chargers, AC/DC power converter, local generation units and ESS as shown in Fig 3.1. Thus, appropriate coordinated control is generally required for all the components of the system. Power conversion stage indicates one of the most important components inside the charging system. The major purpose of power processing stage is to develop a compatible common connection between sources and load. Reliability and high efficiency are associated with conversion stage while processing the power under various uncertain conditions. Therefore, choosing the most appropriate processing stage in accordance with the designed system, nature of sources and requirement of load is an interest research challenge. Since, PV and batteries are sources of DC, a DC/DC conversion stage is required [147]. In case of central grid, due to AC production of grid, a universal AC/DC converter is required [148]. Furthermore, bidirectional processing is required depending on the power flow between storage and load. All of these converters are connected to a common DC bus [149]. This chapter illustrates the design criteria, steps of development and the control related to the power configuration/management of DC bus composed of hybrid power sources for EVs charging. The proposed charging architecture is selected by comparing the main characteristics of charging systems that are mainly based on AC and DC common bus while considering the integration of PV generation system with local grid, stationary BSS, EVs load and the power conversion steps based on the interleaving converter alongside with the AC/DC interlinked converter. The detailed parameters are listed in Table 3.1

Table 3. 1 charging system component parameters.

Parameter Description	Value
Rated AC Line Voltage	380V
Rated DC Bus Voltage	750V
DC Charger Power	45kW
PV Power Capacity	100kW
BSS Capacity	60Ah
EV battery Capacity	50Ah
EV Charging current / Discharging current	65 A

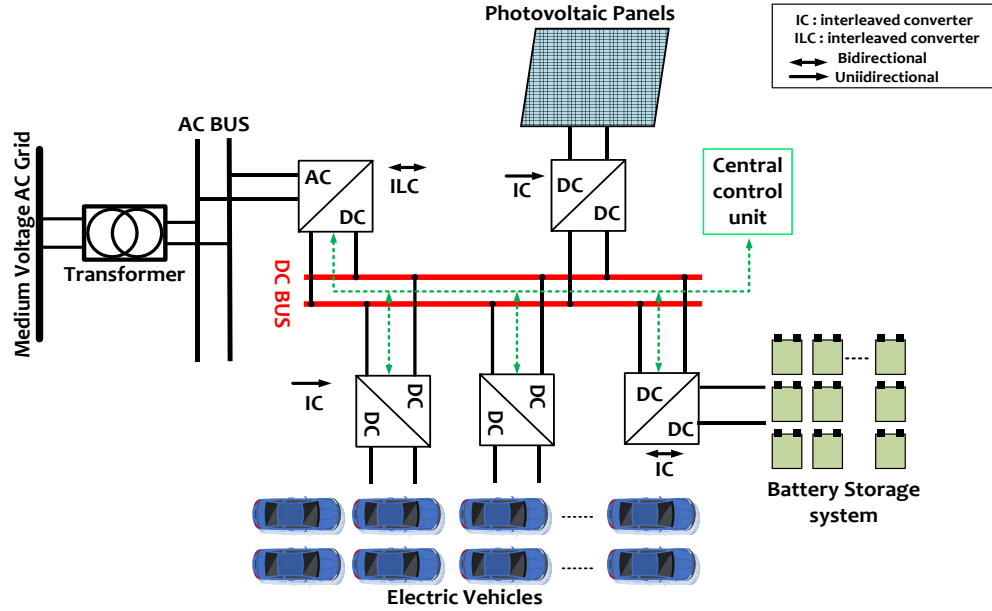


**Fig 3. 5: EV charging station module based on DC micro-grid.**

In the proposed EVs charging architecture as shown in Fig 3.1, the AC/DC converters realize a DC bus at 750V. In sequence, other power conversion units allow charging of EVs and charging/discharging of BSS during the intermittent operations. To achieve an overall stable operation, an efficient coordinated control for charging is proposed considering the stability issues related to both DC bus voltages and AC grid. In this chapter, the EVs charging system based on hybrid power sources, the power conversion architecture, and the evaluation of EVs charging are implemented and investigated. In addition, proper control strategy is implemented, allowing the proposed charging architecture to follow the required operation under different scenarios. Therefore, this chapter focus on the primary control level of the DC-EV charging system, where the EV chargers, AC/DC interlinking converter, local PV system and BSS are connected to a common DC bus.

### 3.2 PV system modelling and MPPT control

Power electronics structures dedicated to PV system are numerous, several criteria make it possible to classify them into different groups. The first characteristic of the converter chain is the presence or absence of galvanic isolation between the PV modules and the grid. The second distinguishing characteristic of the conversion chains is the number of power conversion stages. Two types of conversion are possible: converting DC to AC in one step, or a DC/DC conversion stage needed to increase the voltage before turning it into AC voltage. The last characteristic of a conversion chain is its number of phases [150, 151]. Fig 3.2 presents the equivalent circuit of the PV cell consisting of an ideal current source, a reverse parallel diode, a

series resistor  $R_s$  and a parallel resistor  $R_{sh}$ . The current of the PV system is dependent on solar irradiance and is proportional to temperature. The current-voltage curve of the PV cell can be described as:

$$I = I_{sc} - I_s \left( \exp^{(q(IR_s + V)/c_d B \theta)} - 1 \right) - \frac{IR_s + V}{R_{sh}} \quad (3.1)$$

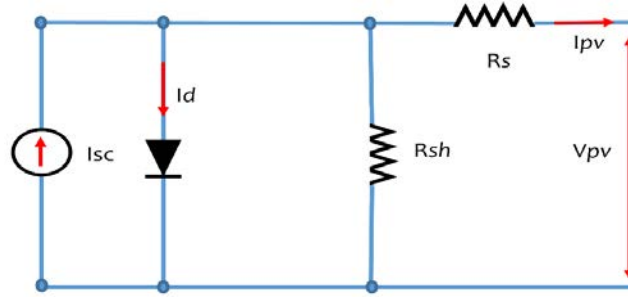


Fig 3. 6: Equivalent circuit model PV panel.

In equation (3.1),  $V$  is the output voltage of the PV cell;  $I$  is the output current of the PV cell;  $I_{sc}$  is the short current of PV cell;  $I_s$  is the saturation current of the diode;  $C_d$  is the coefficient of diode;  $B$  is the Boltzmann constant  $1.38 \cdot 10^{-23}$  j/k,  $q$  is the charge of electron  $1.6 \cdot 10^{-19}$  c, and  $\theta$  is the inner temperature of the PV cell. Due to difficulty to estimate the accurate values of these parameters, a generalized approximated model is given in (3.12-3.14).

$$I = I_{sc} \left[ 1 - C_1 \left( \exp^{(V/(V_{oc} C_2))} - 1 \right) \right] \quad (3.2)$$

$$C_1 = \left[ \exp^{(-V_o/(V_{oc} C_2))} \times 1 - \frac{I_o}{I_{sc}} \right] \quad (3.3)$$

$$C_2 = \left[ \ln^{(1 - \frac{I_o}{I_{sc}})^{-1}} \times \frac{V_o}{V_{oc} - 1} \right] \quad (3.4)$$

Here,  $I_{sc}$  is the short circuit current,  $V_{oc}$  is the open circuit voltage,  $V_o$  and  $I_o$  are the output voltage and output current at MPP respectively. The performance of this model is dependent on both the temperature and irradiance.

To obtain the I-V and P-V characteristics based on the PV model, SimPowerSystems package from Simulation is used. The P-V and I-V characteristics of the PV model are similar to a PV system with proportionality ratios. These ratios depend on the number of cells connected in series and the number of branches of associated cells in parallel. This characteristic is non-linear, it has a MPPT characterized by a current ( $I_{max}$ ) and a voltage ( $V_{max}$ ).

To maximize the utilization of PV generation, the MPPT technique is applied to the PV-Interleaved system. The MPPT is achieved by regulating the PV output voltage through controlling the IBC. The classical perturbation and observation method is adopted to harvest the maximum solar power [152, 153]. Fig 3.3 illustrates the principle of the MPPT technique. This technique consists of imposing an initial duty cycle " $\alpha_0$ " and an initial power  $P_0$ . After measuring the  $I_{pv}$  current and the  $V_{pv}$  voltage across the PV, the product ( $V_{pv} * I_{pv}$ ) is calculated. The latter is the image of the instantaneous power  $P_{pv}(k + 1)$  delivered by the PV generator when the measurement is made. This value is then compared to the previous power  $P_{pv}(k)$  and  $\alpha$  is incremented. Once  $\alpha$  has been modified,  $P_{pv}(k)$  takes the value of the previous power  $P_{pv}(k + 1)$  and  $\alpha_0$  takes the value of  $\alpha$ . Finally, a new measurement of  $V_{pv}$  and  $I_{pv}$  is performed to calculate the new power  $P_{pv}(k + 1)$ .

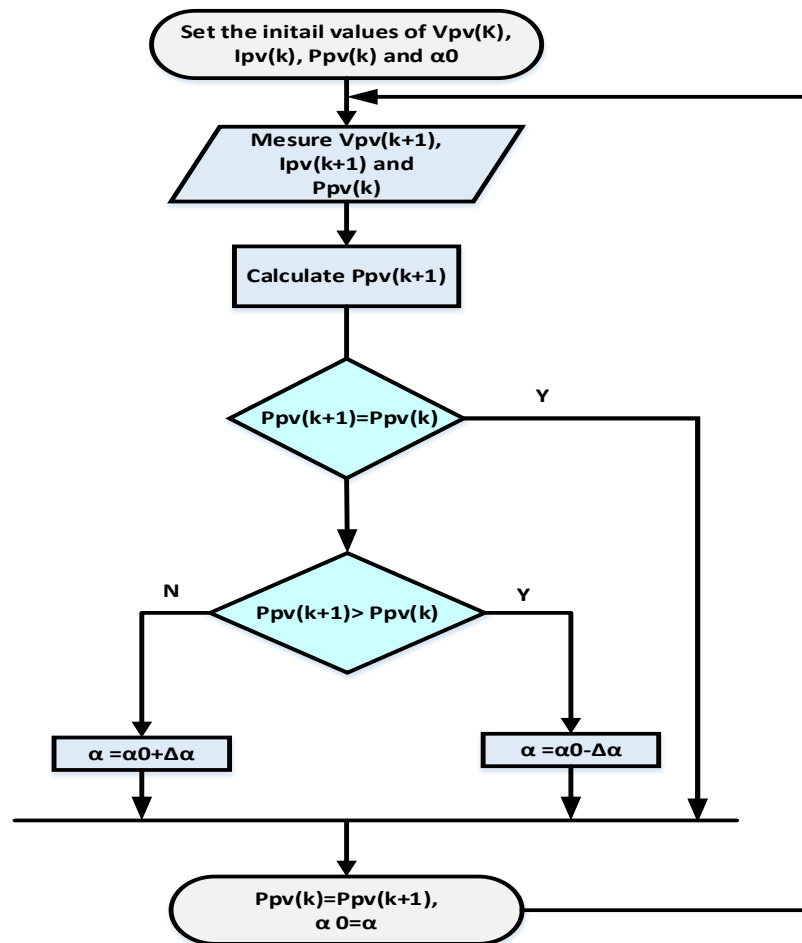


Fig 3. 3: Flow chart for the MPPT control.

### 3.2.1 Interleaved boost converter for PV system

Generally, the DC/DC boost converter is used to connect the PV panel to the DC bus thanks to its simplicity. Meanwhile, it is used for the battery with converter in bidirectional mode. However, several drawbacks concerning this topology in terms of vehicle battery charging applications should be considered, mainly: (i) low efficiency for high voltage gains; (ii) low elevation gain; (iii) weight and volume of the inductance (low compactness); (iv) high current ripple; (v) sensitivity to faults (operating shutdown).

Since the boost converter has no redundancy [154], the operation of the converter is no longer ensured in case of a switch fault that may result in system disturbance and/or failure of power conversion step. Because of these disadvantages, more research has been carried out to propose new architectures to meet the requirements of application, ensure the power supplied as well [155, 156].

The proposed power conversion of the PV panels used in this work is shown in Fig 3.4. Interleaved boost converter (IBC) has been introduced in the literature, including 2-phase, 3-phase and 4-phase [157-159]. The interleaved topology provides different features as: (i) minimize the size and volume of passive components; (ii) reduce the Input ripple current ;(iii) increase the frequency of the input current; (iv) improve the reliability of the system due to the higher voltage gain; (v) Increase the output power of the converter due to the parallel phases; (vi) Provide simple thermal management, the parallel of IBC and IBDC converters phases allow a better thermal distribution

The IBC, in this type of assembly's inductors, switches and diodes are connected in parallel; a single capacitor is placed at the output of the converter. The control of the switches  $S_1, S_2, \dots,$  and  $S_n$  is successively shifted by  $T_s/N$ ;  $T_s$  is the switching period,  $N$  is the number of branches constituting the converter.

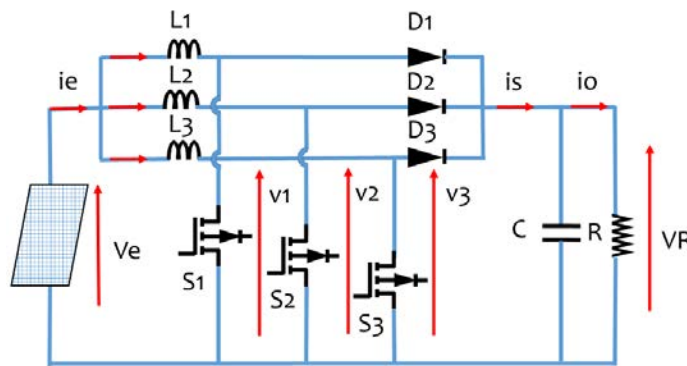


Fig 3. 4: Interleaved (DC/DC) Converter.

The switching sequences of the switches may or may not overlap, causing variations in the ripple of the input current. The frequency of the input current is  $N$  times the frequency of the current in each inductance [160, 161].

The analysis of the voltage ripples and the current according to the duty cycle is obtained under the following simplifying assumptions:

1. The resistances of the coils and the capacitor are negligible.
2. Inductances and parasitic capacitances are negligible.
3. Switches are ideal.

The equations of the proposed circuit of IBC converter depicted in Fig 3.5 are:

$$\begin{aligned} V_1 &= L_1 \frac{di_1}{dt} + V_e \\ V_2 &= L_2 \frac{di_2}{dt} + V_e \\ V_3 &= L_3 \frac{di_3}{dt} + V_e \end{aligned} \quad (3.5)$$

The inductances for IBC circuit are identical  $L_1 = L_2 = L_3 = L$ . Therefore: -

$$i_e = i_1 + i_2 + i_3 \quad (3.6)$$

$$V_1 + V_2 + V_3 = 3V_e - L \frac{di_e}{dt} \quad (3.7)$$

To determine the current  $i_e$ , three cases must be examined according to the value of ( $\alpha$ ).

**Case 1:**  $\alpha < \frac{T}{3}$

In this case, the operating state of each switch is less than  $T/3$ , the timing of conduction of the switches is given Fig 3.5:

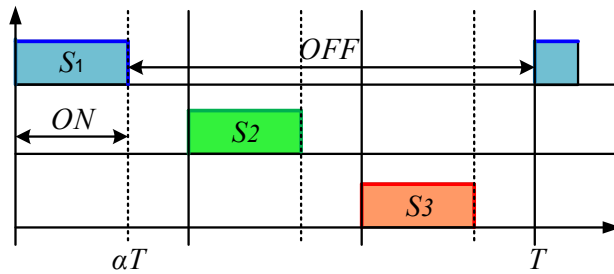


Fig 3. 5: Switches conduction timeline, case 1.

Each interval of  $T/3$  can be sub-divided into two intervals to determine the input current, based on equation (3.6, 3.7). Therefore, the equivalent circuit diagrams for each interval are given in Fig 3.6. Only one switch

is in a conducting mode for each first phase of a  $1/3$  of the switching period. The voltage  $(V_1+V_2+V_3)$  is alternatively equivalent to  $2V_R$  and  $3V_R$ . Defining  $i_{e \min}$  as the value of  $i_e$  for  $t = 0$ .

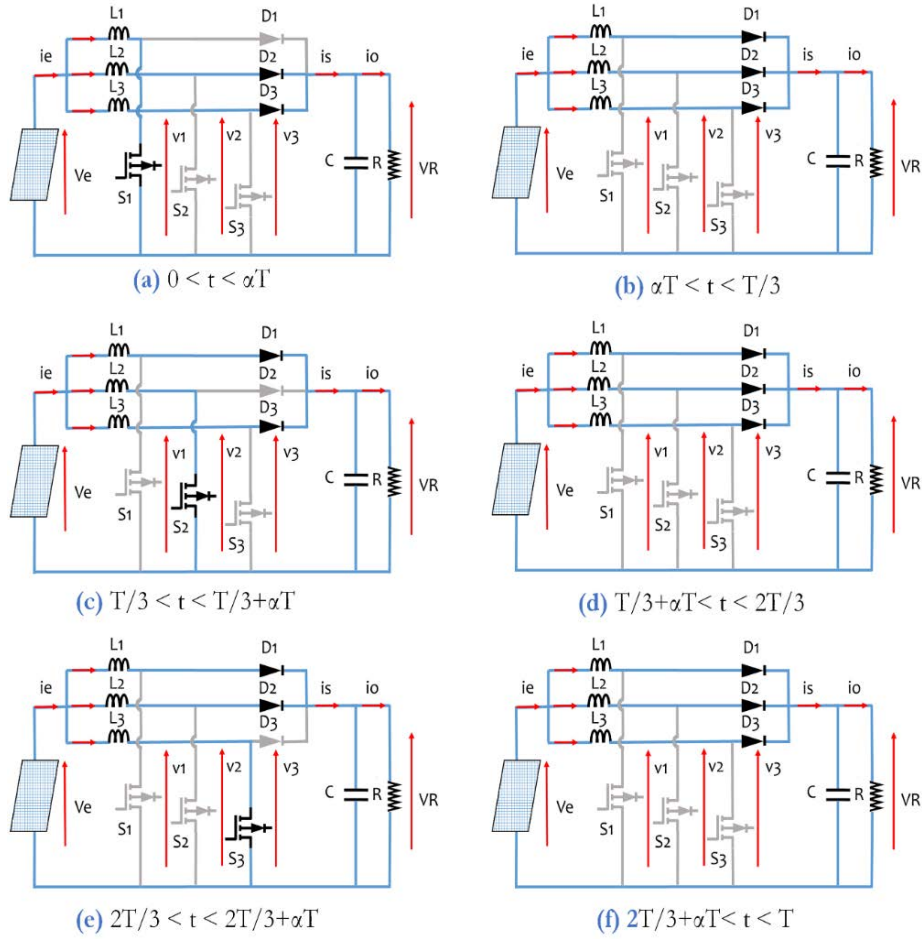


Fig 3. 6: Behavior of interleaved converter in each small interval case 1.

For each conduction interval,  $\alpha < \frac{1}{3}$ , the input current of each interval is given by the equations (3.8 - 3.13):

$$i_e = \frac{3V_e - 2V_R}{L}t + i_{e \min}, \quad 0 < t < \alpha T \quad (3.9)$$

$$i_e = \frac{3V_e - 3V_R}{L}t + \frac{V_R}{L}\alpha T + i_{e \min}, \quad \alpha T < t < T/3 \quad (3.10)$$

$$i_e = \frac{3V_e - 2V_R}{L}t - \frac{V_R}{L}\frac{T}{3} + \frac{V_R}{L}\alpha T + i_{e \min}, \quad T/3 < t < \alpha T + T/3 \quad (3.11)$$

$$i_e = \frac{3V_e - 3V_R}{L}t + \frac{2V_R}{L}\alpha T + i_{e \min}, \quad \alpha T + T/3 < t < 2T/3$$

$$i_e = \frac{3V_e - 2V_R}{L}t - \frac{2V_R}{L}\frac{T}{3} + \frac{2V_R}{L}\alpha T + i_{e \min}, \quad 2T/3 < t < \alpha T + 2T/3 \quad (3.12)$$

$$i_e = \frac{3V_e - 3V_R}{L}t - \frac{3V_e - 3V_R}{L}T + i_{e \min}, \quad \alpha T + 2T/3 < t < T \quad (3.13)$$

The waveforms of the currents and voltages within the converter and at the load side are illustrated in Fig 3.7.

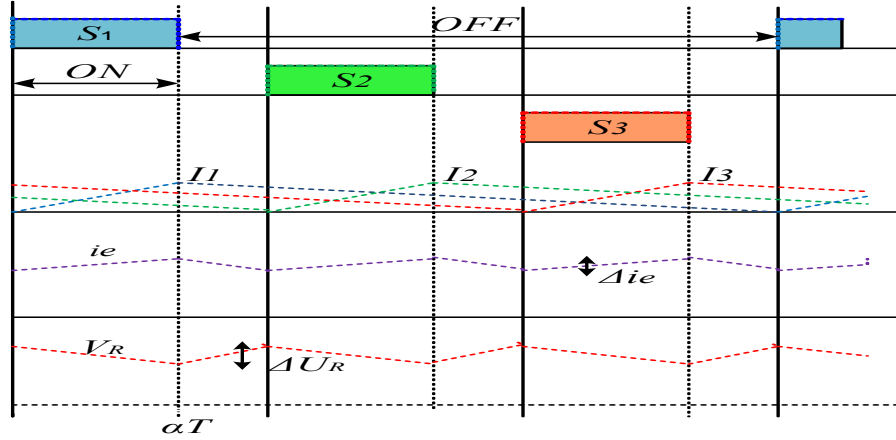


Fig 3. 7: Waveforms of different signals, case 1.

**Case 2:**  $\frac{T}{3} < \alpha < \frac{2T}{3}$

Each switch has a conduction time greater than  $T/3$  and less than  $2T/3$ . The timing of the switch's conduction is shown in Fig 3.8.

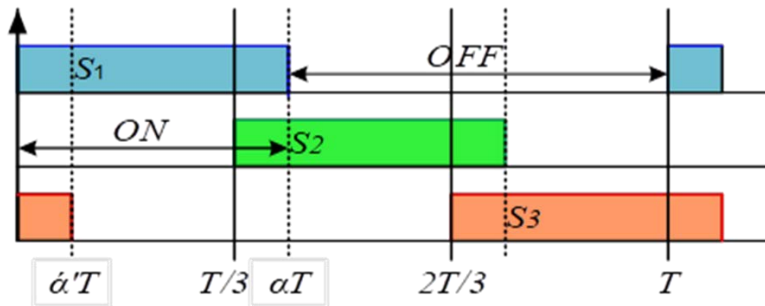


Fig 3. 8: Switches conduction timeline, case 2.

If  $\alpha'T$  is assumed to be equal to  $(\alpha T - T/3)$ , and considering the intervals  $[0, \alpha'T]$ ,  $[T/3, T/3 + \alpha'T]$  and  $[2T/3, 2T/3 + \alpha'T]$ , the two switches are conducted in each first phase of a  $1/3$  switching period. The voltage  $(V1+V2+V3)$  is alternatively equivalent to  $V_R$  and  $2V_R$ , therefore the frequency of  $i_e$ , is three times of the switch's frequency. Thus, the equivalent circuit diagrams for each interval are given in Fig 3.9.

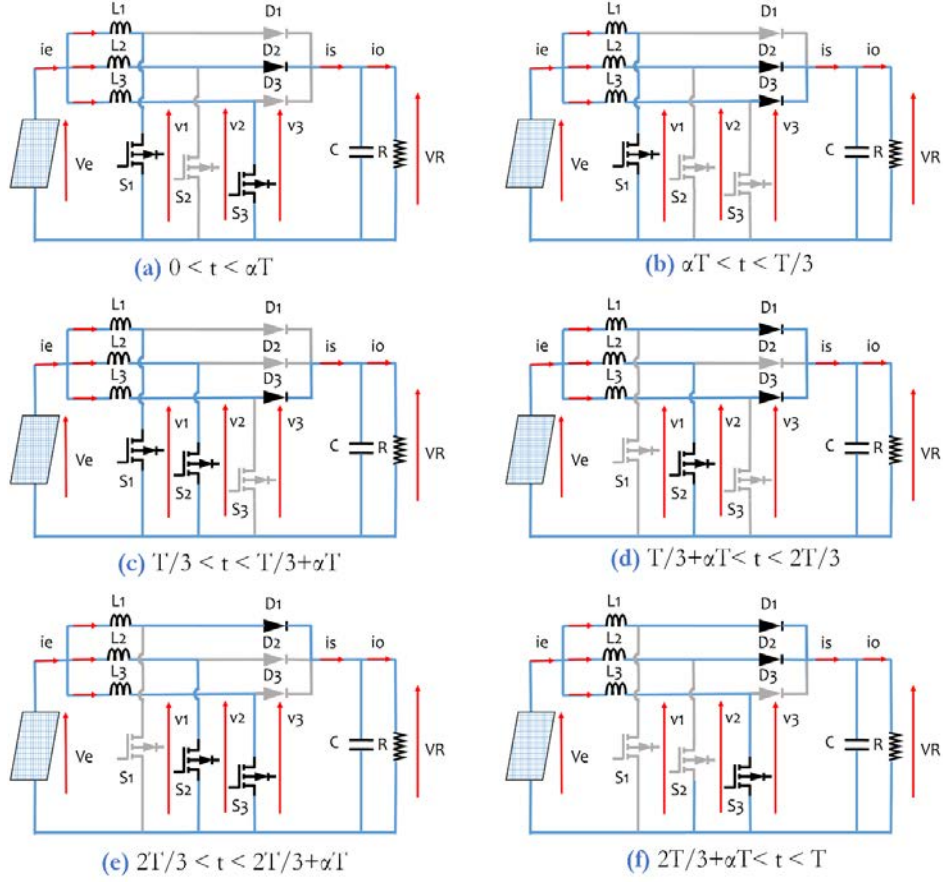


Fig 3. 9: Behavior of interleaved converter in each small interval case 2.

The input current value of each conduction interval, for  $1/3 < \alpha < 2/3$  are given by the equations (3.14 - 3.19):

$$i_e = \frac{3V_e - V_R}{L} t + i_{e \min}, \quad 0 < t < \alpha T \quad (3.14)$$

$$i_e = \frac{3V_e - 2V_R}{L} t + \frac{V_R}{L} \alpha T + i_{e \min}, \quad \alpha T < t < T/3 \quad (3.15)$$

$$i_e = \frac{3V_e - V_R}{L} t - \frac{V_R}{L} \frac{T}{3} + \frac{V_R}{L} \alpha T + i_{e \min}, \quad T/3 < t < \alpha T + T/3 \quad (3.16)$$

$$i_e = \frac{3V_e - 2V_R}{L} t + \frac{2V_R}{L} \alpha T + i_{e \min}, \quad \alpha T + T/3 < t < 2T/3 \quad (3.17)$$

$$i_e = \frac{3V_e - V_R}{L} t - \frac{2V_R}{L} \frac{T}{3} + \frac{2V_R}{L} \alpha T + i_{e \min}, \quad 2T/3 < t < \alpha T + 2T/3 \quad (3.18)$$

$$i_e = \frac{3V_e - 2V_R}{L} t - \frac{3V_e - 2V_R}{L} T + i_{e \min}, \quad \alpha T + 2T/3 < t < T \quad (3.19)$$

The waveforms of the currents and voltages at the converter and at the load terminals are illustrated in Fig 3.10.

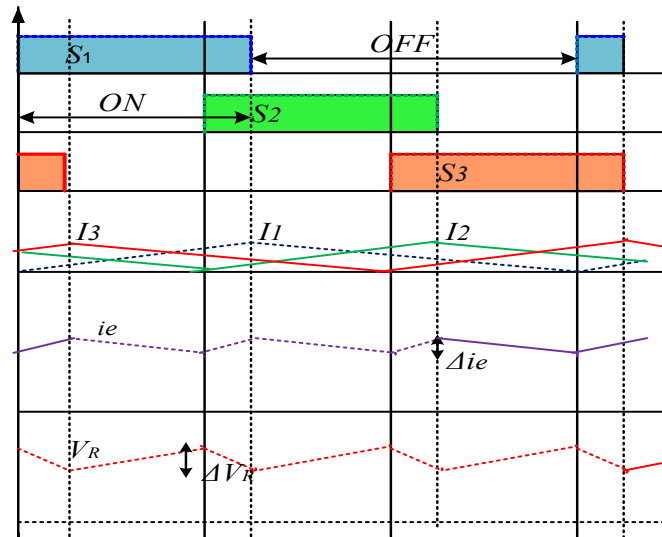


Fig 3. 10: Waveforms of different signals, case 2.

**Case 3:**  $\alpha > \frac{2T}{3}$

In this case the switches have a longer conduction time than  $2T/3$ . The conducting time of the switches is given in Fig 3.11. Assuming  $\alpha'T$  is equal to  $(\alpha T - 2T/3)$ , and considering the intervals  $[0, \alpha'T]$ ,  $[T/3, T/3 + \alpha'T]$  and  $[2T/3, 2T/3 + \alpha'T]$ , it is observed that three switches are driving in each 1/3 first phase during the switches time. The voltages  $(V1+V2+V3)$  are alternating between 0 and  $V_R$ . The frequency of current  $i_e$ , is equal to three times the switching frequency.

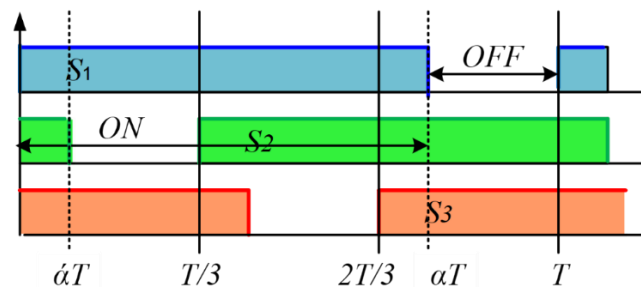


Fig 3. 11: Switches conduction timeline, case 3.

Consequently, the equivalent circuit diagrams for each interval are given in Fig 3.12.

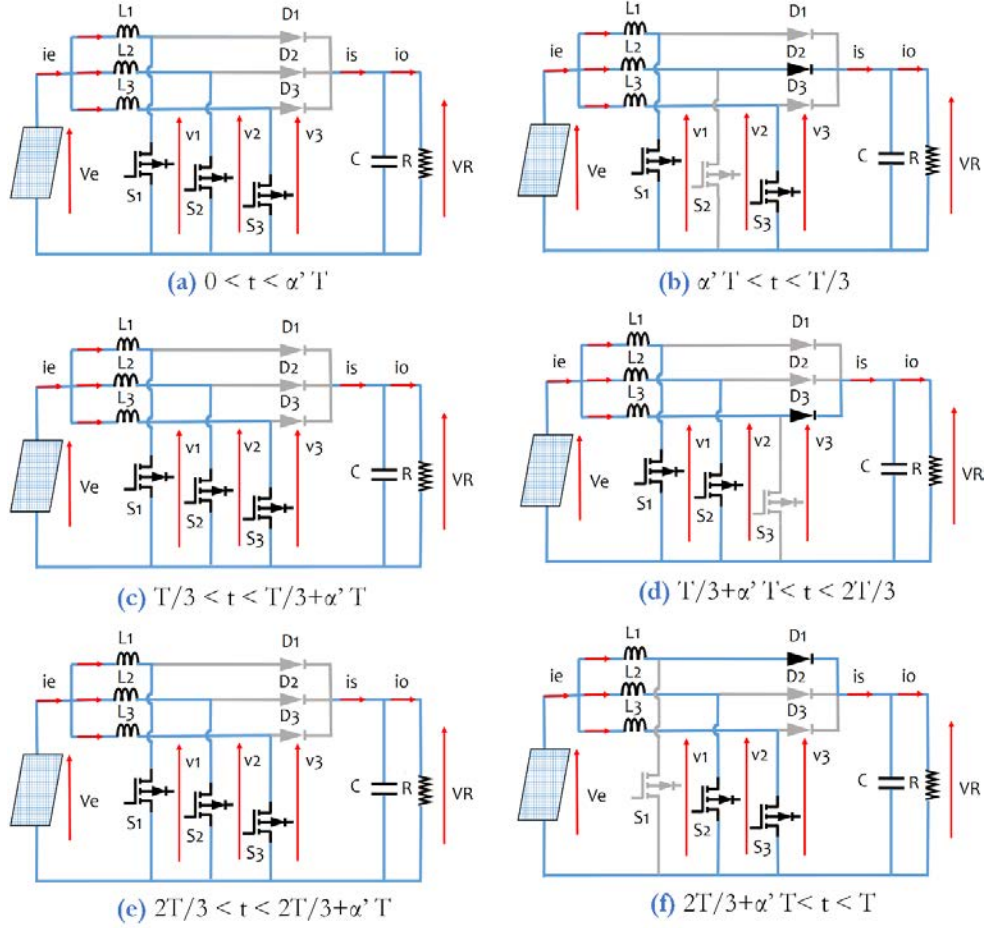


Fig 3.12: Behavior of interleaved converter in each small interval for case 3.

The input current value of each conduction interval, for  $2/3 < \alpha < 1$  are given by the equations (3.20 - 3.25):

$$i_e = \frac{3V_e}{L}t + i_{e \min}, \quad 0 < t < \alpha' T \quad (3.20)$$

$$i_e = \frac{3V_e - 2V_R}{L}t + \frac{2V_R}{L}\alpha' T + i_{e \min}, \quad \alpha' T < t < T/3 \quad (3.21)$$

$$i_e = \frac{3V_e}{L}t - \frac{2V_R T}{L} + \frac{2V_R}{L}\alpha' T + i_{e \min}, \quad T/3 < t < \alpha' T + T/3 \quad (3.22)$$

$$i_e = \frac{3V_e - V_R}{L}t + \frac{3V_R}{L}\alpha' T - \frac{V_R T}{L} + i_{e \min}, \quad \alpha' T + T/3 < t < 2T/3 \quad (3.23)$$

$$i_e = \frac{3V_e}{L}t - \frac{3V_R T}{L} + \frac{3V_R}{L}\alpha' T + i_{e \min}, \quad 2T/3 < t < \alpha' T + 2T/3 \quad (3.24)$$

$$i_e = \frac{3V_e - V_R}{L}t - \frac{3V_e - V_R}{L}T + i_{e \min}, \quad \alpha'T + 2T/3 < t < T \quad (3.25)$$

From the Fig 3.13, the waveforms of the currents and voltages at the converter and across the load side are depicted as:

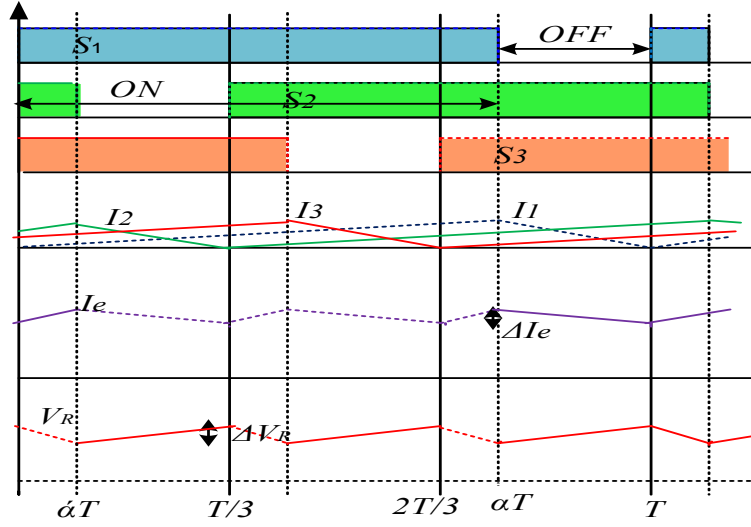


Fig 3. 13: Switches conduction timeline, case 3.

### 3.2.2 Calculation of IBC ripple current

Unlike the conventional boost converter, the ripple of the input current of 3-phase IBC consists of three parts based on the duty cycles. The Fig 3.7, 3.10 and 3.13 represent the waveforms of input current and output voltage according to the duty cycle, where the frequency of input current is three times of the switches frequency [162-164].

In the case 1,  $0 < \alpha < 1/3$ , one current of the three currents in the inductances is increased during  $[0, \alpha T]$ , because only one switch is in conductive mode. Accordingly, the currents  $i_1$  and  $i_2$  will decrease. In the other cases where  $1/3 < \alpha < 2/3$  and  $2/3 < \alpha < 1$ , the variation in current ripple can be explained in a similar way. Consequently, the ripple of the input current can be calculated by:

$$\Delta I_e = \frac{V_R}{L}(1 - 3\alpha)\alpha T, \quad 0 < \alpha < 1/3 \quad (3.26)$$

$$\Delta I_e = \frac{V_R}{L}(2 - 3\alpha)\left(\alpha - \frac{1}{3}\right)T, \quad 1/3 < \alpha < 2/3 \quad (3.27)$$

$$\Delta I_e = \frac{V_R}{L}(3 - 3\alpha)\left(\alpha - \frac{2}{3}\right)T, \quad 2/3 < \alpha < 1 \quad (3.28)$$

The effect of interleaving currents of each (phase) can be described by  $\Delta I_e$ . The variation trajectory of the ripple current as a function of the number of parallel branches and the value of the duty cycle makes it easy to highlight this characteristic: the increase in the number of branches placed in parallel obviously leads to a reduction in inductance value. To investigate changes in the current ripple as a function of duty cycle, by examining the derivative of the latter with respect to  $\alpha$ . The value of the maximum waviness is obtained by differentiating one of the equations (3.26, 3.27, 3.27). Taking for example the equation (3.26).

$$\frac{d\Delta I_e}{d\alpha} = \frac{V_R}{L} \frac{d}{d\alpha} \{(1 - 3\alpha)\alpha T\}, \quad (3.29)$$

$$\Delta I_{e \max} = \frac{V_R}{L} \frac{1}{12} T \quad (3.30)$$

To compare the ripples current in the case of a boost converter and in the case of 3-phase interleaved boost converter, it is adequate to consider the same values of the inductance [165], whereby according to the relation (3.30), the current ripple in 3-phase IBC is three times smaller compared to that of a boost converter.

### 3.3 BSS /EV battery and their power conversion step

The ESS is used to store the extra energy from renewable sources or to compensate for the energy deficit. Therefore, in the proposed design of charging station, the bi-directional converter is used to interface the BSS, if necessary. Similarly, the EV charger can be designed as a bi-directional converter. In this context, the application of multi-phase parallel interleaving technology in BSS should be extended; this technology gives full advantage of its wide voltage transformation range, low current ripple, high efficiency, and fast response to make it widely used.

The converter consists of 3-phase interleaved Buck-Boost converters (IBDC) to provide efficient, reliable power conversion stage and high voltage gain and reduce ripple current is selected to interface the BSS and used to charge EV. Within this section the lithium-ion battery modelling and the SoC estimation which represent an important parameter, the BSS are presented beside the used power conversion step to interlink BSS to the charging station.

#### 3.3.1 Power conversion step of BSS and EV charger

##### A. Modelling and control of IBDC for BSS charger

BSS provides a rapid response to system variations, however, there are two significant challenges with bi-directional converters. The first issue is an extreme duty cycle operation. To bridge the huge voltage gap between the DC bus (750V) and BSS, a conventional non-isolated converter must operate with high duty cycles (e.g., duty cycle greater than 0.9). However, conventional converters with such extreme duty cycles

are exposed to high voltage and current stresses and are known to suffer from increased losses and reduced controllability [157, 169]. The second issue is a large current at the low-voltage battery side. A current of the low-voltage side is greater than that of the high-voltage side, increasing current stress as well as associated losses.

Fig. 3.14 shows the proposed IBDC. 3 Inductors,  $L_1$ - $L_3$ , are connected to the battery and sharing the input current. The control of this converter is directly related to the EMS on the charging system. Control of current (level of current to be supplied or absorbed according to the power profile). The switches on the upper and lower sides, respectively, where  $i = 1, \dots, 3$ ) are operating in a complementary mode. Three switch pairs (S1, S2 and S3) (S1, S2 and S3 and inductances) are operating in interleaved  $120^\circ$  phase-shifted modes, and therefore, the converter can be considered as an interleaved 3-phase converter when considered at the battery side.

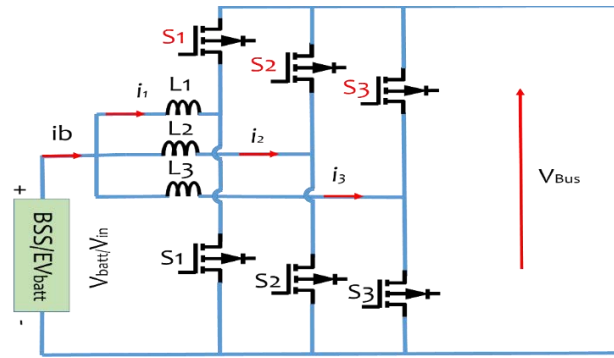


Fig 3. 14: bidirectional interleaved converters for BSS and charger side.

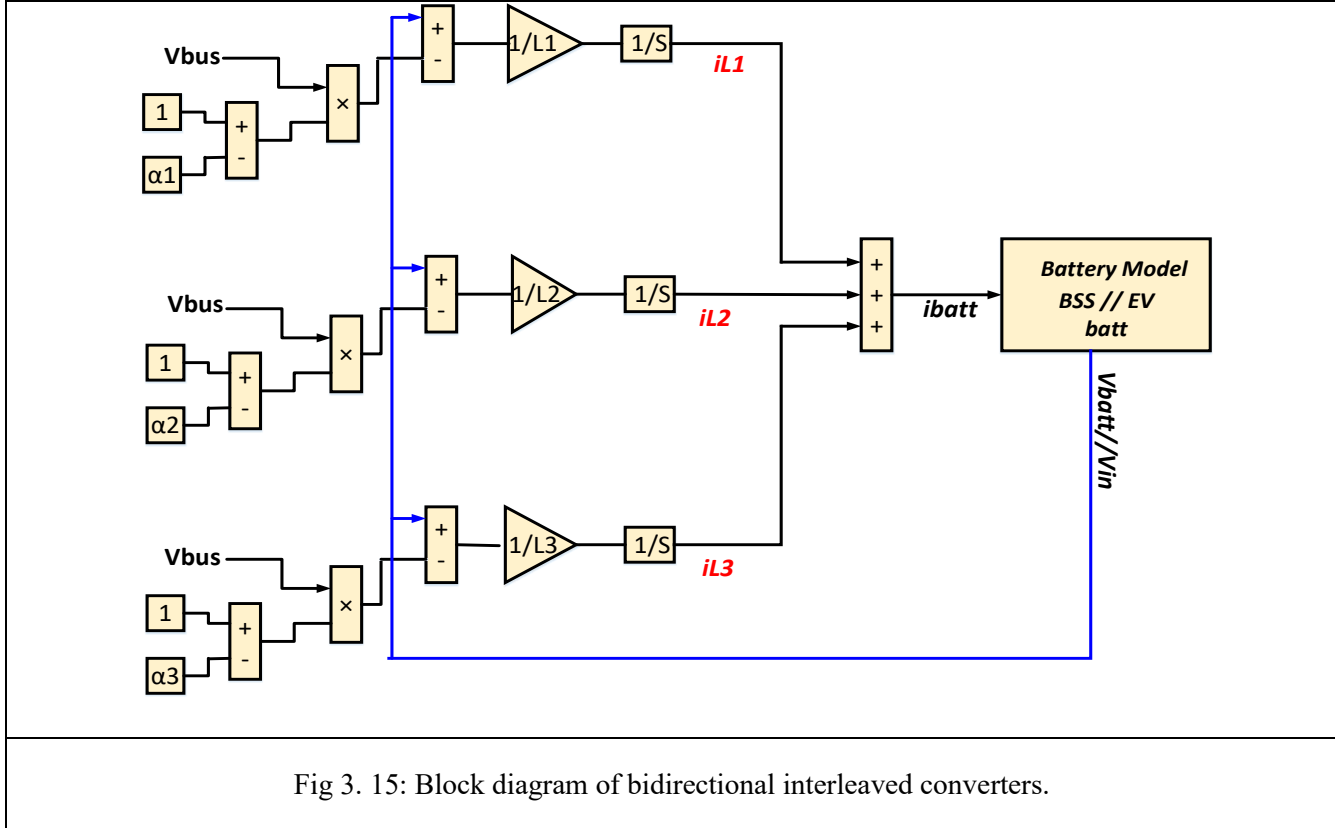
Despite the constraints related to power demands that may will be appear due to the variation on load, the DC bus voltage can be controlled through the bidirectional AC/ DC converter and/or IBC of PV system. Accordingly, a similar analysis of IBC can be performed on IBDC for the BSS. Either a buck operation when the BSS receives power from the DC bus or a boost operation when the BSS supplies power to the DC bus. By applying the modeling approach used for the IBC converter, analysis of the operating sequences and by putting the variables representing the conduction state of the converter switches, differential equations can be obtained as the following:

$$V_{in} = L_1 \frac{di_1}{dt} - (1 - \alpha_1)V_{bus} \quad (3.31)$$

$$V_{in} = L_2 \frac{di_2}{dt} - (1 - \alpha_2)V_{bus} \quad (3.32)$$

$$V_{in} = L_3 \frac{di_3}{dt} - (1 - \alpha_3)V_{bus} \quad (3.33)$$

This model can be directly used to carry out a simulation of the converter in a Matlab Simulink environment as shown in Fig 3.15.



The connection of the storage systems BSS to the DC bus must be carried out throughout two IBDC converters since the BSS can be charged or discharged. The control of this converters is directly linked to the EMS. These converters are controlled to supervise the power flow between the DC bus and the storage elements. For this purpose, the current references are calculated from the DC bus power and the voltage of each storage source as shown in Fig 3.16a. and 3.16b. The reference powers,  $P_{ref}$ , can be derived from the EMS and applied to the BSS in order to control the DC/DC converters.

$$i_{batt} = P_{ref} / V_{batt} \quad (3.34)$$

The control structure of the system is mainly based on reference [170, 171]. Which includes a summary for the controller design on internal model control (IMC). The method is used to implement controller design, the controller becomes directly parameterized in terms of the model parameters and the desired closed-loop bandwidth. The carried-out controller is a loop of current that could be able to ensure the control of the power in the converter. To be able to define a simple current regulator, the system behavior can be linearized. The

linearization will be made by an opposite model, in this case an expression to permit the unity transit between controller output and voltage is required.

$$\alpha = \frac{V_{Ln} - V_{batt}}{V_{bus}} + 1 \quad (3.35)$$

Where:  $V_L$  'is a new control variable representing the voltage reference across the inductor. Based on IMC method a linear transfer function between  $v_L(s)$  and  $i_{batt}(s)$  can be expressed as:

$$G_{batti} = i_{batt}(s)/V_L(s) \quad (3.36)$$

Where  $G_i(s)$  is the decoupled system transfer function of each leg of converters from  $v_L$  to  $i_{batt i}$ .

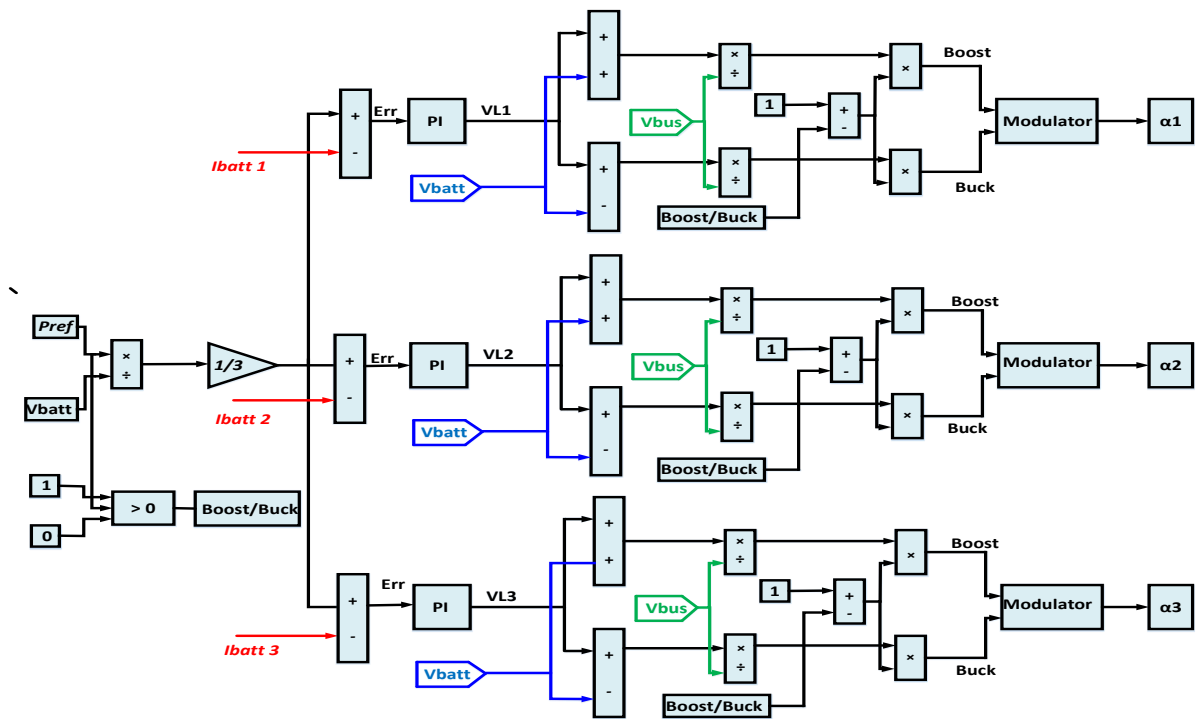


Fig 3. 7a: Control scheme of IBDC.

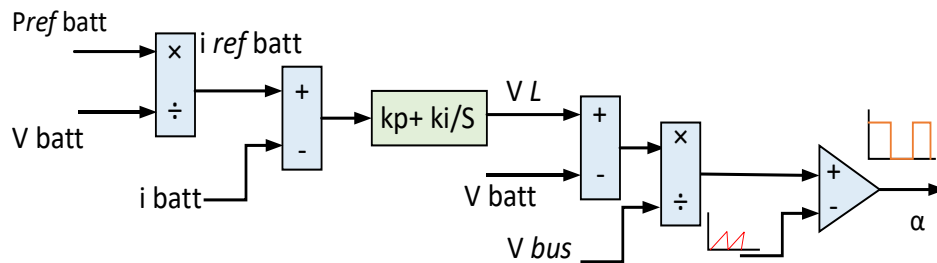


Fig 3. 16b: Controller scheme of IBDC.

## B. Modelling and control of Buck converter for EV charger

In the charging of EVs, the DC/DC converter is the conversion interface between the DC bus and the EV battery as shown Fig 3.17, realizing flow of energy between the charging station and the EV battery. The buck converter has the advantages of simple structure, easy control, few components, small size, and high conversion efficiency [9], and can be applied to high-power applications. Therefore, in this work a selection and design of the topological structure of buck converter. The proposed buck model for EV charging uses a two-stage charge control strategy of constant current first and then constant voltage for the charging of the battery pack of EV.

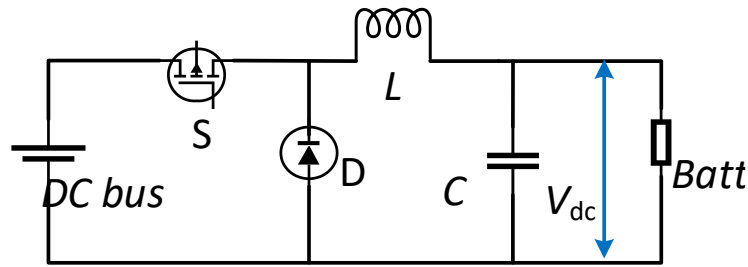


Fig 3.17: buck DC/DC converter.

Since EVs battery starts charging, a constant current is used for charging process. As time increases, the state of charge SoC of the battery gradually increases, the acceptable charging capacity gradually decreases, and the temperature of the battery continues to rise. When the battery terminal voltage reaches the maximum allowable or the temperature reaches the upper limit, it needs to stop immediately the constant current charging, switch to constant voltage charging. After that, the charging current will gradually decrease until the battery is fully charged and automatically stop charging. Therefore, to prolong the life of the battery and shorten the charging time as much as possible, the proposed DC/DC converter adopts a charging control strategy of constant current first and constant voltage. The control block diagram of constant current charging, constant voltage charging is shown in Fig 3.18. Among them, the constant voltage stage charging adopts the dual-loop control of the voltage outer loop and the current inner loop. The outer loop compares the measured battery terminal voltage  $V_{bat}$  with the given voltage  $V^*_{bat}$  and sends it to the PI regulator for adjustment to generate current Set the value of the loop and compare it with the charging current  $i_{cha}$ . After the PI regulator adjusts and limits the amplitude, it is compared with the triangular wave to generate the control pulse of the bidirectional DC/DC converter and control the turn-on and turn-off of VD1, it can realize the constant voltage charging of the battery pack.

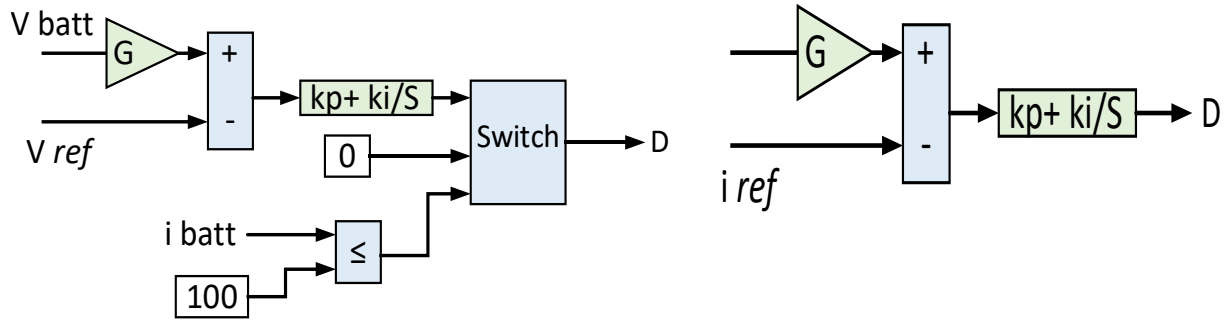


Fig3.18: PI controller scheme of EV c charger.

Constant current charging stage proportional coefficient KP, integral coefficient KI; and the proportional coefficient of the voltage outer loop of constant voltage charging stage KP, integral coefficient KI in table 3.2.

Table 3.2: Parameter of PI controller for the EV charger.

	kp	ki
Constant current charging	0.75	50
Constant voltage charging	5.65	0.150

The initial state of the battery is set to SOC=60%, the given value of charging current  $i_{cha}^*=100A$ , and the simulation results of the terminal voltage and charging current of the battery pack are shown in Fig 3.19.

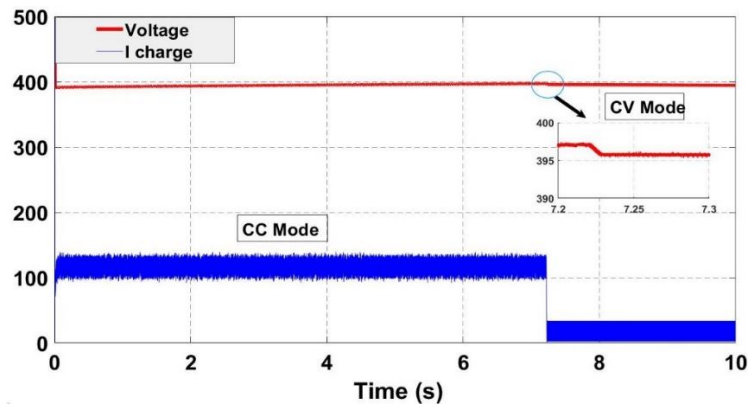


Fig.3.19: Voltage and current waveforms of the charging battery.

### 3.4 AC/DC interlinking converter for the EVs charging station

The development of micro-grid technology has brought more attention to the hybrid AC/DC micro-grids [172, 173], since it has the characteristics of AC and DC micro-grids; (i) includes both the AC subsystem, the DC subsystem, the AC/DC Interlinked converter (ILC) bidirectional 3-phase AC/DC converter ; (ii) it can supply power to the AC and DC load simultaneously, reducing electronic power conversion stages

besides energy losses; (iii) the power flow between the AC and DC systems is bidirectional. Fig 3.20 shows the ILC in connection with the AC and DC bus [174].

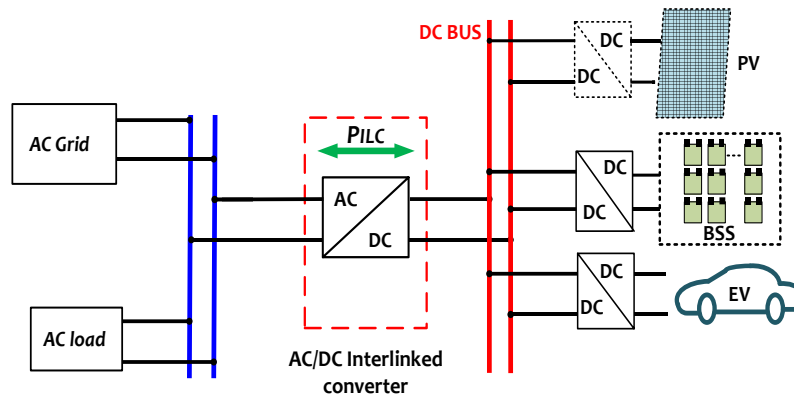


Fig 3. 8: AC/DC micro-grid with DC charging station.

The ILC can provide more efficient in integrating RES, energy storage devices and various types of loads into the distribution grid, all of this based on generation/load layers, and the main power grid requirements. Typically, most micro-grids are installed at low load levels. Therefore, the power conversion rate is relatively low, which reduces the cost of investment [52]. ILC at the micro-grid provides the bidirectional power flow between the AC grid and the DC grid, the latter representing an outstanding part of the system's voltage stability and power quality improvement. The DC/AC converters play a dual function as inverters when the power is transmitted from the DC side to the AC side; when the power is transmitted from AC side to the DC and used as a rectifier.

### 3.4.1 Topology and model of bidirectional ILC

The voltage-type PWM rectifier is composed of fully controlled devices and has the advantages of bidirectional energy flow, unit power factor, low harmonic pollution, etc. [116, 174]. The topology of the main circuit is shown in Figure 3.21.

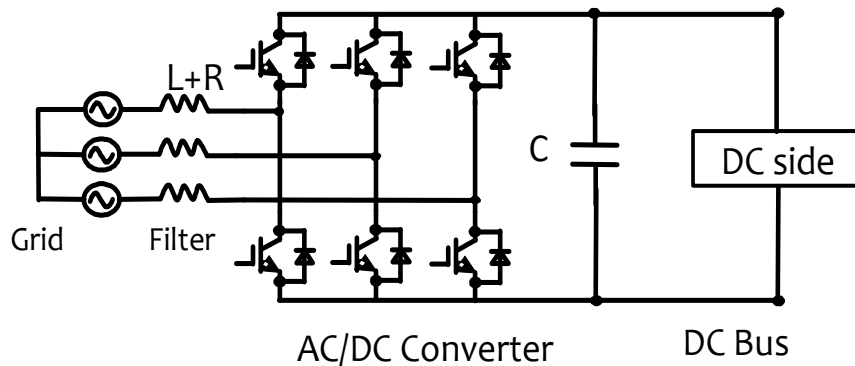


Fig 3.21: AC side of the micro-grid.

In the Figure 3.21, ea, eb, and ec represent the three components of the power grid. Phase AC voltage represents the three-phase AC current of the power grid. L and R represent the equivalent inductance and equivalent resistance of the grid side, respectively. L can filter the grid side and converter side current harmonics. C represents the DC side filter capacitor, which can reduce the pulsating component of the DC voltage, and Udc represents the rectified DC voltage [116, 175]. Due to the coupling between the coordinates of the mathematical model in the three-phase static coordinate system, which is unfavorable to the design of the control system, the mathematical model of the PWM converter in the three-phase static coordinate system (a, b, c) can be converted to Under the synchronous rotating coordinates (d, q) synchronized with the grid frequency, its mathematical model can be expressed as:

$$\begin{cases} e_d = L \frac{di_d}{dt} + Ri_d - \omega Li_q + u_d \\ e_q = L \frac{di_q}{dt} + Ri_q + \omega Li_d + u_q \end{cases} \quad (3.37)$$

Where ed and eq respectively represent the d and q components of the grid electromotive force; ud and uq respectively represent the d and q components of the AC side voltage vector of the three-phase PWM rectifier; id and iq represent the d and q components of the AC side current of the three-phase PWM rectifier respectively q component.

### 3.4.2 Control of ILC

In order to make the power factor of the PWM rectifier circuit work approximately 1, the input current is required to be a sine wave and the same phase as the input voltage, and the switching devices need to be controlled. According to whether the AC current feedback is introduced, the control method can be divided into indirect current control and direct current control. Due to the simple structure of the direct current control system, the fast current response speed, the circuit parameters are not used in the control operation, and the system has good robustness [175], so this article adopts the direct current control method. From equation (3.37), it can be found that due to the current coupling of the d and q components of the grid electromotive force, it is not conducive to the design of the control system. Decoupling control can be used to facilitate the realization of the control strategy. When adopting the feedforward decoupling control strategy based on PI controller [174,175], the decoupling control equation becomes:

$$\begin{cases} u_d^* = -(K_{iP} + K_{iI}/s)(i_d^* - i_d) - \omega Li_q + u_d \\ u_q^* = -(K_{iP} + K_{iI}/s)(i_q^* - i_q) + \omega Li_d + u_q \end{cases} \quad (3.38)$$

In the equation (3.38), Kp and KI respectively represent the proportional coefficient and integral coefficient of the current inner loop; ud\*, uq\* represent the command value of the d and q axis voltage respectively; id\*,

$i_q^*$  represent the command value of the d and q axis current respectively. The control structure diagram of the system after decoupling is shown in Figure 3.22.

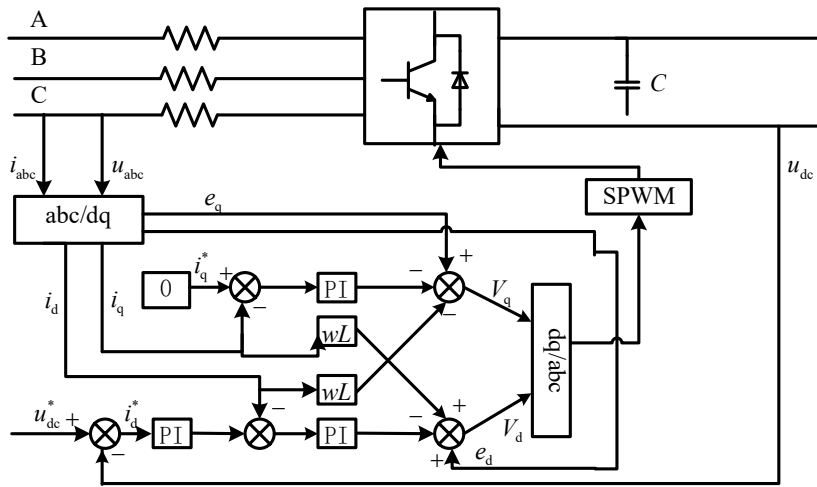


Fig 3. 22: Block diagram of voltage and current double closed-loop control for PWM rectifier.

According to the typical second-order system, the current inner loop is designed, according to the PI parameter design method [175]. The modification based on the actual application, the PI parameters of the d-axis current loop are calculated  $K_iP=320$ ,  $K_iI=0.5$ . Similar to the current inner loop, after simplifying the current closed loop and merging the small inertia links, the voltage outer loop parameters according to the typical second-order system are:  $K_vP=0.2$  and  $K_vI=4$ .

When charging, the reversible PWM rectifier works in the rectifying state. Since the system is three-phase symmetrical, phase a is used to analyze the voltage, current waveforms and harmonics of phase a on the grid side as shown in Fig 3.23.

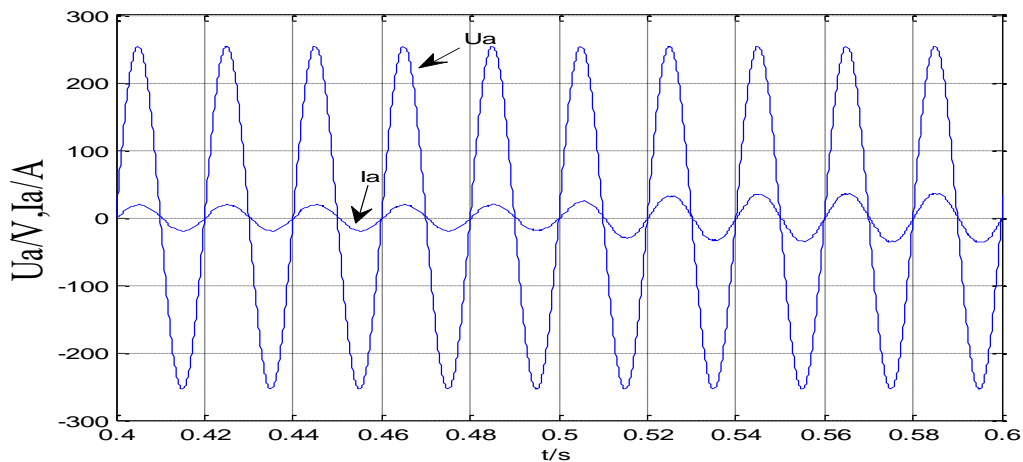


Fig 3.23: Voltage and current waveforms of phase a on the grid side during rectification.

In order to verify of the proposed control strategy, when  $t=0.5s$ , the load is suddenly increased, and the DC side voltage waveform and the grid side a-phase current waveform changes during load fluctuation are shown in Fig 3.24, where the waveform can quickly return to a stable state.

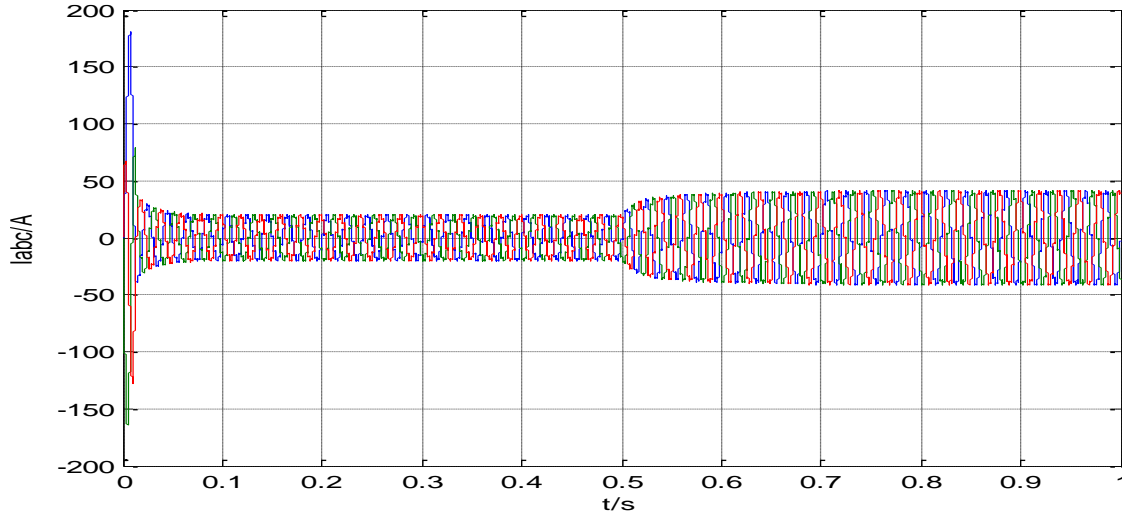


Fig.3. 24: The grid side current during load fluctuation.

The grid side voltage and current are shown in Fig 3.23. The grid voltage remains constantly stable, while the grid current. Here, the bus voltage can be maintained at 750VDC. While the voltage will fluctuate when the power balance changes, especially when the AC/DC converter is disconnected from the grid. The simulation verifies the two typical power balance conditions such as the AC side provides power support to the DC side and the extra DC side power transfer to support to the AC side. Therefore, it is important to analyze the power balance between the operating mode of the AC-DC sides and the switching strategy between the modes. Based on the behavior of DC bus and its energy fluctuation during the change of EVs load and the other DC sources power status and the voltage relation between AC and DC, ILC power control strategy is designed. The control strategy can calculate the power to be exchanged on both sides based on the voltage and current information on both sides, besides controlling the power balance between AC and DC, and satisfying the role of mutual support between AC and DC active power.

### 3.5 Conclusion

In this research work, for PV system, an interleave DC/DC converter is utilized to maximize the power being harnessed from solar profile. In this case, the interleaved converter also provides regulated voltage at the output. For the BSS, a bidirectional interleaved DC/DC converter topology is proposed and implemented to support the bidirectional power flow and to keep the necessary power balance. At the grid side, a rectifier/inverter conversion stage is implemented to keep the DC bus at regulated value and to support

bidirectional power flow between the grid and other components of the hybrid power sources. The main objectives of the power conversion phase are regulating the DC bus at desired value, maintaining the power flow between the connected sources with high efficiency, keeping an overall power quality profile in term of harmonics.

## **Chapter 4: Lithium-ion Battery modelling and SoC estimation**

## 4.1 Introduction

Lithium-ion battery are promising energy storage solution for many applications thanks to their high energy storage capacity, important power density and low self-discharge rate. the BSS has been widely used in the stationary application [166]. The accurate battery measurements give more feasibility for BSS in the stationary applications as in the charging station. within this chapter, based on the dynamic characteristics of the battery, an Equivalent circuit model (ECM) is developed using resistances, capacitance, and voltage source. then, it is used for identifying the battery parameters by implementing an experimental characteristic measurement. In other hand, the battery state of charge SoC represents another important parameter. The SoC displays the current remaining battery capacity. SoC is the ratio of the remaining battery capacity to the rated capacity under a certain discharge rate [167]. The remaining power of the battery can only be expressed indirectly through the SoC value, so accurate estimation of the SoC value is very important. At present, the common methods for estimation of SoC, ampere-hour integration method, open circuit voltage (OCV) method; load voltage method; discharge experiment method; internal resistance measurement method; linear model method, Kalman filter method and neural network method. In this chapter, battery equivalent circuit model is established, and the battery state equation model is Built. Then, using Matlab for simulation, substituting the simulation results and parameters into the extended Kalman filter algorithm for SoC estimation, and then comparing the estimated SoC value with the actual value.

## 4.2 Lithium-ion Battery modelling

Battery modeling is considered an important to understand the battery characteristics such as charge/discharge and SoC estimation. The battery model can be classified into four categories: Ideal, Behavioral, Equivalent circuit and Electrochemical Models. The choice of one of these models is a trade-off between model complexity, accuracy and parameters identification [166]. To identify the main parameters of a battery, a Thevenin circuit model, named dual polarization model (DP) or the 2<sup>nd</sup> order RC model is proposed. Besides, the model-based simulation data and the experimental ones is achieved to estimate the model-based parameters. A Thevenin model is presented in Fig 4.1 to refine the description of polarization characteristics and simulate the concentration polarization and the electrochemical polarization separately. The circuit consists of voltage source  $V_{oc}$ , an ohmic resistance  $R_0$  represents the internal resistance can be used to describe the resistive of battery electrolyte behavior and produce the ohmic voltage drop during current pulse.

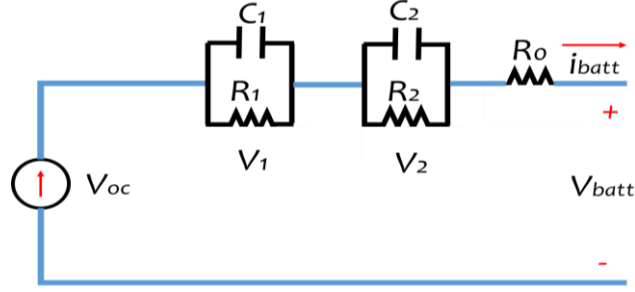


Fig 4.1: Schematic diagram for the DP model.

Two parallel resistive and capacitive branches consist of ( $R_1$  and  $C_1$ ) to represent the electrochemical polarization resistance and capacitance, ( $R_2$  and  $C_2$ ) to represent the concentration polarization resistance and capacitance while  $R_0$  is responsible for the instantaneous voltage drop/rise. The double branches are used to represent the short and long-term transient responses due to the relaxing time effect of the battery, resulting from the diffusion of ions during the charging or discharging process.  $V_1$  and  $V_2$  are the voltages over  $C_1$  and  $C_2$  respectively [167, 168]. This model can accurately capture the cell dynamics and can be easily implemented in a real-time application. The electrical behavior of the DP circuit can be expressed in continuous time by equations (4.1) and (4.2):

$$V_{batt} = V_{oc} - V_1 - V_2 - R_0 i_{batt} \quad (4.1)$$

$$\begin{cases} \dot{V}_1 = \frac{V_1}{R_1 C_1} + \frac{i_{batt}}{C_1} \\ \dot{V}_2 = \frac{V_2}{R_2 C_2} + \frac{i_{batt}}{C_2} \end{cases} \quad (4.2)$$

The discrete time of  $V_1$  and  $V_2$  are given by equations (4.3) and (4.5):

$$V_1(t) = V_1 e^{\frac{-t}{\tau_1}} - R_1 (1 - e^{\frac{-t}{\tau_1}}) i_{batt} \quad (4.3)$$

$$V_2(t) = V_2 e^{\frac{-t}{\tau_2}} - R_2 (1 - e^{\frac{-t}{\tau_2}}) i_{batt} \quad (4.4)$$

$$V_{batt}(t) = V_{oc}(soc(t)) - V_1(t) - V_2(t) - R_0 i_{batt} \quad (4.5)$$

To identify the parameters of the battery model, the battery test bench has been designed and implemented as shown in Fig 4.2. The estimation of the battery model parameters has been carried out based on the battery measurements. The charge/discharge of the battery was performed at room temperature with relatively new and unused cells. The lithium-ion battery was charged in two modes during the experiments: the constant current (CC) mode followed by the constant voltage (CV) mode. During the charging mode, the charging current was CC mode, while the battery voltage gradually increased to the value reached in the CV mode. In CV mode, the battery voltage remained constant. In the discharge mode, the same procedure was performed.

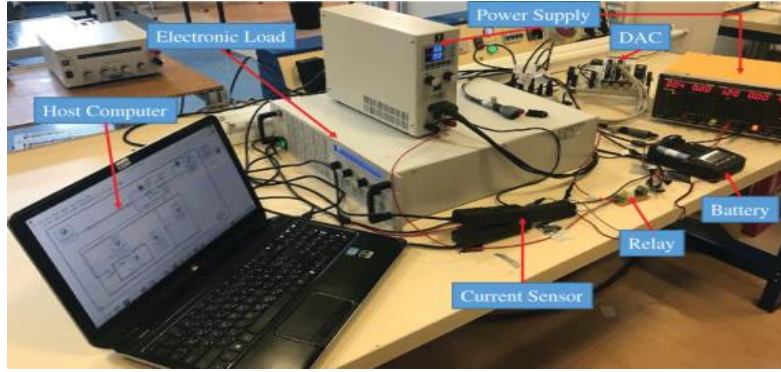


Fig 4.2: Battery test bench.

Fig 4.3 illustrates the battery dynamic behavior. In general, the curve in figure shows the different period characteristic curves. Most notably, the charge and discharge curves of a battery were represented to show the battery voltage as a function of time. The charge/discharge cycles can define the characteristics of a cell such as the voltage levels, the battery life, the number of charge cycles.

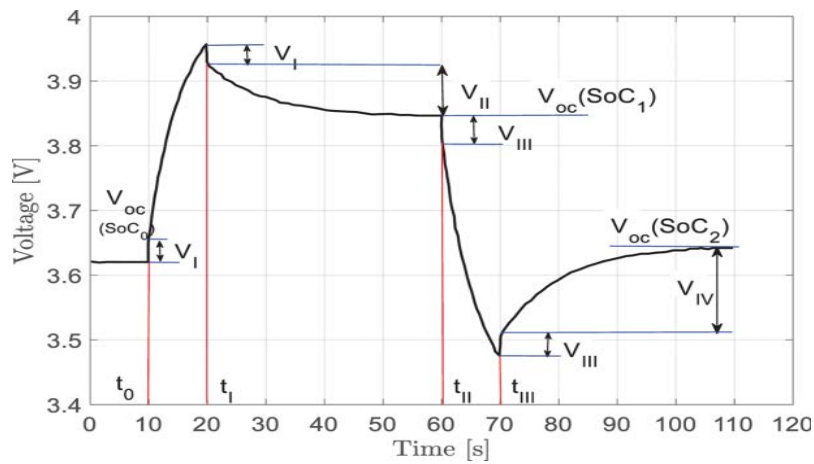


Fig 4.3: Battery voltage during charging and discharging.

The curve charge and discharge can be divided into time periods to understand the charge and discharge behavior of the battery as following:

**Period ( $t_0 - t_I$ ):** when the battery is charged with a CC, the charging current  $I$  is negative, and the battery's output voltage increases due to the internal resistance  $R_0$ . Thereafter, under the control of the  $V_{oc}$ , the battery output voltage continues to increase exponentially as the SoC increasing.

**Period ( $t_{II} - t_{III}$ ):** the battery is discharged with a positive CC, the battery output voltage decreases due to the internal resistance  $R_0$ , then continues to decrease exponentially under  $V_{oc}$  control as the SoC decreases. The Thevenin model output voltage can be expressed during the charge and discharge cycles by equations (3.6) and (3.7).

$$R_0 = \begin{cases} -V_I/I_{cha} \rightarrow \text{charging} \\ -V_{III}/I_{discha} \rightarrow \text{discharging} \end{cases} \quad (4.6)$$

$$\begin{cases} V_{batt\ cha} = V_{oc}(SoC1) - V_1(t_I)e^{\frac{-t}{\tau_1}} - V_2(t_I)e^{\frac{-t}{\tau_2}} \\ V_{batt\ cha} = V_{oc}(SoC2) - V_1(t_{III})e^{\frac{-t}{\tau_1}} - V_2(t_{III})e^{\frac{-t}{\tau_2}} \end{cases} \quad (4.7)$$

The identification of the Thevenin model can be implemented by determining the instantaneous values of ( $SoC1$ ), ( $SoC2$ ),  $V1(tI)$ ,  $V1(tIII)$ ,  $V2(tI)$ ,  $V2(tIII)$ ,  $\tau_1$  and  $\tau_2$  in equations (4.7). An exponential function with two-time constants  $f(t) = A + Be^{-at} + Ce^{-\beta t}$  represents the nonlinear voltages curves, the Matlab<sup>®</sup> fitting function is used for estimating the values of the coefficients A, B, C,  $\alpha$ , and  $\beta$  for to calculating all DP model parameters by applying equations (4.8)- (4.13).

$$\begin{cases} V_{oc}(SoC1) = A \\ V_{oc}(SoC2) = A' \end{cases} \quad (4.8)$$

$$\begin{cases} V_1(t_I) = B; V_2(t_I) = C \\ V_1(t_{III}) = B'; V_2(t_{III}) = C' \end{cases} \quad (4.9)$$

$$\begin{cases} \tau_1 = 1/\beta \\ \tau_2 = 1/\alpha \end{cases} \quad (4.10)$$

$$\begin{cases} R_{1,cha} = \frac{V_1(t_I)}{\langle 1 - e^{\frac{-t_{cha}}{\tau_1}} \rangle I_{cha}} \\ R_{1,disch} = \frac{V_1(t_{III})}{\langle 1 - e^{\frac{-t_{disch}}{\tau_1}} \rangle I_{disch}} \end{cases} \quad (4.11)$$

$$\begin{cases} R_{2,cha} = \frac{V_2(t_I)}{\langle 1 - e^{\frac{-t_{cha}}{\tau_2}} \rangle I_{cha}} \\ R_{1,disch} = \frac{V_2(t_{III})}{\langle 1 - e^{\frac{-t_{disch}}{\tau_2}} \rangle I_{disch}} \end{cases} \quad (4.12)$$

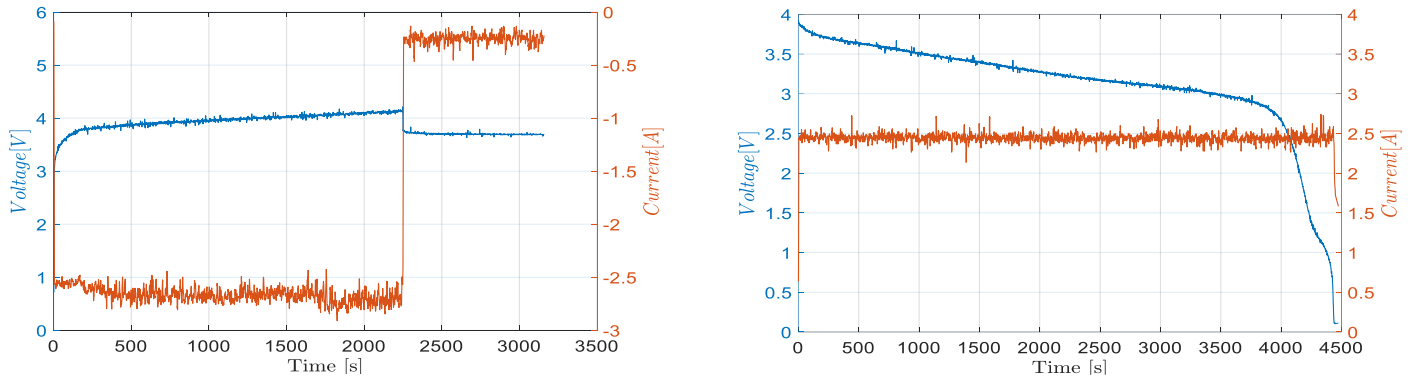
$$\begin{cases} C_1 = \tau_1/R_1 \\ C_2 = \tau_2/R_2 \end{cases} \quad (4.13)$$

The Lithium-ion battery parameters in Table 2, were identified based on the model equations (4.11), (4.12) and (4.13).

Table 4.1: The battery parameters values at charging and discharging.

Parameters	Charging (Ohm)	Discharging (F)
R0	0.157	0.161
R1	0.040	0.038
R2	0.0192	0.0194
C1	262.2	3.8.4
C2	869.7	860.8

Fig 4.5 shows the  $V_{oc}$  of the battery hysteresis characteristic and behavior with full CC/CV charge and discharge, the test was performed to monitor the battery voltage to estimate SoC.



(a) Experimental  $V_{batt}$  curves of the battery /CC charging. (b) Experimental  $V_{batt}$  curves of the battery /CC discharging.

Fig 4.5: Experimental current and voltage profiles of charge/discharge.

Since the OCV of a lithium battery is similar in value to the electromotive force, and there is a corresponding relationship between the SOC value and the electromotive force, the SOC can be estimated by reading the battery's open circuit voltage. In the simulation environment, discharge a lithium battery with a capacity of 2.7Ah and a nominal voltage of 4.2V at a current of nearly 1cycle [168]. After each 5% discharge, when the test stand for specific time in order to completely stabilize the OCV until the SOC value is 0%. The measured relationship between SOC and OCV is shown in Fig 4.6.

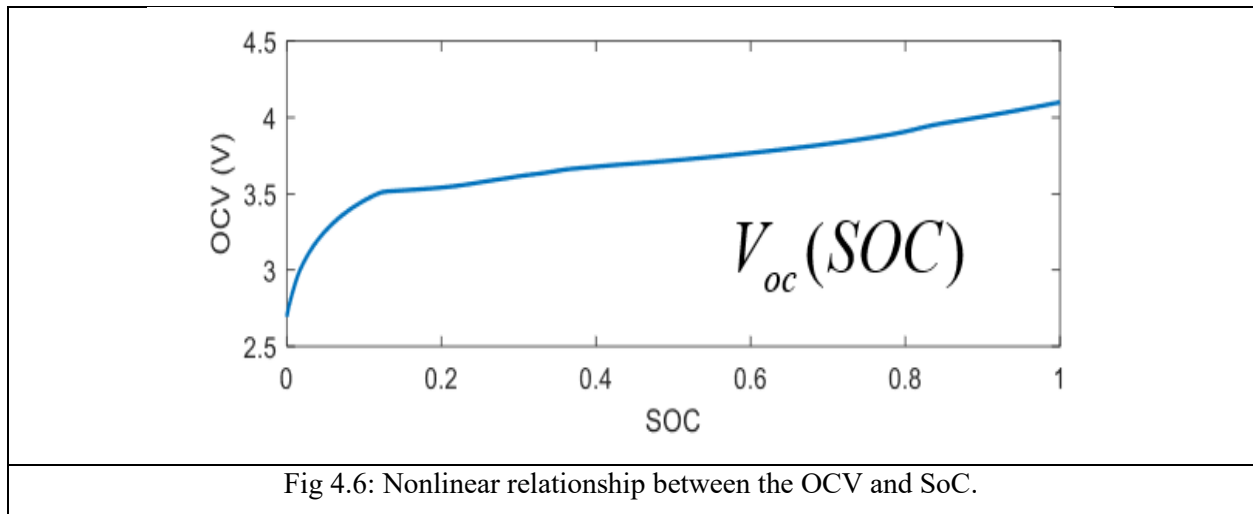


Fig 4.6: Nonlinear relationship between the OCV and SoC.

It can be seen that the corresponding relationship between SoC and OCV at both ends of the SoC value is more obvious, while the change amplitude of OCV in the middle part is not obvious. In the middle part, it is easy to cause SoC estimation errors, and the characteristics of long-term standing of the test to make the

open circuit voltage stable make the open circuit voltage method not an ideal to identifying the battery parameters and SoC estimation. In next section SoC estimation method is proposed.

### 4.3 SoC estimation method for lithium-ion battery

Nowadays, the commonly SoC estimation methods are including the discharge experiment method, the open circuit voltage method, the ampere-hour integration method, the neural network method and the Kalman filter method, etc. During use of the experimental discharge method, the battery pack may have to be disconnected of charging or discharging. While the neural network method requires a large amount of baseline data for training [176-180]. Therefore, this section discusses the Kalman filter (KF) and extended Kalman filter (EKF) methods which are commonly used.

#### 4.3.1 Establish lithium battery equivalent model

The ECM of the lithium-ion battery consists of ohmic internal resistance that conforms to Ohm's law and capacitive polarization internal resistance. The first order Thevenin equivalent model allows more accurate simulation of the dynamic charge and discharge characteristics of the battery. The first order Thevenin equivalent circuit of the lithium battery is established as shown in Fig 4.7.  $E$  is the electromotive force of the lithium battery, which is similar in value to the open circuit voltage;  $R1$  is the ohmic internal resistance, which causes a sudden change in the voltage at the battery terminals during charging and discharging;  $R2$  and  $C1$  are the polarization resistance and the polarization capacitance, respectively, which cause the voltage at the battery terminals during charging and discharging [167, 177]. In order to facilitate the calculations, an ECM in first-order RC is proposed in this section.

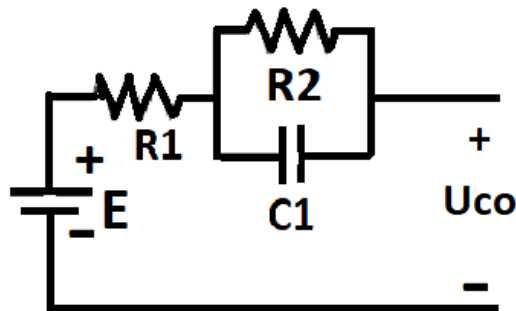


Fig 4.7: The first order Thevenin equivalent model.

#### 4.3.2 Kalman filter algorithm

Kalman filter is used to estimate the state value of a time-discrete system that are described by the linear stochastic equation and obtain the best approximation value of the battery state values in the sense of minimum mean error from the observation value. It uses the estimated value at the previous moment and

the observed value to update the estimation of the state variables, and its insensitivity to the initial value is very suitable for application in SoC estimation [176, 177]. The discrete model in a state equation:

$$x_{t+1} = A_t x_t + B_t U_t + W_t \quad (4.14)$$

Observation equation:

$$Y_t = C_t x_t + D_t U_t + V_t \quad (4.15)$$

A, B, C, and D: are state transition matrix, state quantity control matrix, observation matrix, and observation control matrix, which are all determined by system characteristics;  $X$ ,  $Y$ ,  $U$  are state quantity, observation quantity, and control quantity respectively;  $W_t$  and  $V_t$  are process noise and observation noise respectively, generally Gaussian white noise with a variance of 0 [178]. Generally, the battery current and terminal voltage can be measured. Without considering the charge and discharge rate, the combined with the ampere-hour integration method and the first order Thevenin equivalent circuit, the discrete state equation and observation equation in the SOC estimation are written as:

$$SoC_t = SoC_{t-1} - \frac{I_t \Delta t}{Q_r} \quad (4.16)$$

$$U_{CO. t} = E_t - I_t R_1 - U_{C. t} + V_t \quad (4.17)$$

Where,  $I$ ; is the current flow through the battery, and  $U_C$  is the voltage across the polarizing capacitor. In addition to SOC, take  $U_C$  as another state quantity and calculate  $U_C$  according to the first-order circuit full response equation.

$$U_{C. t} = I_{t-1} R_2 [ U_{C. t} - I_{t-1} R_2 ] e^{\frac{\Delta t}{R_2 C}} \quad (4.18)$$

Add  $U_C$  as the state quantity to the state equation to obtain the Kalman filter calculation formula in SoC estimation:

$$\begin{bmatrix} SoC_t \\ U_{C. t} \end{bmatrix} = \begin{bmatrix} 1 & 0 \\ 0 & \exp(\frac{\Delta t}{R_2 C}) \end{bmatrix} \begin{bmatrix} SoC_{t-1} \\ U_{C. t-1} \end{bmatrix} + \begin{bmatrix} -\frac{\Delta t}{Q_r} \\ R_2 - (1 - \exp(\frac{\Delta t}{R_2 C})) \end{bmatrix} I_{t-1} + \begin{bmatrix} W_{1. t-1} \\ W_{2. t-1} \end{bmatrix} \quad (4.19)$$

$$U_{CO. t} = E_t - I_t R_1 - U_{C. t} + V_t \quad (4.20)$$

Where  $E_t$  is the electromotive force of the battery, and there is a corresponding relationship with the state variable SoC

$$E_t = F (SoC_t) \quad (4.21)$$

It is clear from Fig4.6 that this correspondence is non-linear, as the conventional Kalman filters are only suitable for linear systems, therefore an extended Kalman filter is proposed.

### 4.3.3 Extended Kalman filter to estimate SOC

Extended Kalman Filter for non-linear systems represents an extension of the Kalman Filter. A linearization is performed at each time step to approximate the non-linear system to a linear time-varying system in the EKF. Thereafter the time-varying linear system is then used in a KF, giving an EKF for the non-linear system. In a similar manner to a KF, the EKF utilizes both the measured input and the measured output values to estimate the minimum mean square error of the real state [ 179, 180].

The EKF transforms the nonlinear system into a linear system through linear transformation. For nonlinear systems, the discrete-time state space model is as follows:

$$X_t = f(X_{t-1}, U_{t-1}) + W_{t-1} \quad (4.22)$$

$$Y_t = g(X_t, U_t) + V_t \quad (4.23)$$

Where, equation (4.22) represents the battery dynamics written in state equation, and equation (4.23) represents the battery output. Functions  $f(X_{t-1}, U_{t-1})$  and  $g(X_t, U_t)$  are the state transition function and observation function or measurement function of the nonlinear system, respectively [178].  $X_t$  is the state vector;  $Y_t$  is the observation vector;  $U_t$  is the input vector;  $W_t$  and  $V_t$  are the process and measurement Gaussian white noise, respectively, where the two processes are not related to each other.  $W_t \sim (0, Q_t)$ ,  $V_t \sim (0, R_t)$ ;  $Q_t$  and  $R_t$  are the variance matrix of process noise and measurement noise, respectively.

In each prediction step the transition function observation function of the system are linearized by Taylor series close to around the prior predicted value  $\hat{x}_t$ , and the rest of series with high order are truncated.

By perform Taylor series expansion of nonlinear observation function. Assuming that  $g(X_t, U_t)$  are differentiable at all operating points

$$g(X_t, U_t) \approx g(\hat{X}_t, U_t) + \left. \frac{\partial g(X_t, U_t)}{\partial x_t} \right|_{x_t=\hat{x}_t} (x_t - \hat{x}_t) \quad (4.24)$$

$$C_t = \left. \frac{\partial g(X_t, U_t)}{\partial x_t} \right|_{x_t=\hat{x}_t} \quad \text{And substituting into equation (4.23) can get}$$

$$Y_t = C_t x_t + g(\hat{X}_t, U_t) - C_t \hat{x}_t + V_t \quad (4.25)$$

Among them,  $g(\hat{X}_t, U_t) - C_t \hat{x}_t$  has no functional relationship with  $x_t$ , so it is directly regarded as  $D_t U_t$ ,

Thus, the equation (4.25) is transformed as follows:

$$Y_t = C_t x_t + D_t U_t + V_t \quad (4.26)$$

$$\begin{bmatrix} SoC_t \\ U_{C. t} \end{bmatrix} = \begin{bmatrix} 1 & 0 \\ 0 & \exp(\frac{\Delta_t}{R_2 C}) \end{bmatrix} \begin{bmatrix} SoC_{t-1} \\ U_{C. t-1} \end{bmatrix} + \begin{bmatrix} -\frac{\Delta_t}{Q_r} \\ R_2 - (1 - \exp(\frac{\Delta_t}{R_2 C})) \end{bmatrix} I_{t-1} + \begin{bmatrix} W_{1. t-1} \\ W_{2. t-1} \end{bmatrix} \quad (4.27)$$

$$U_{Co. t} = \left[ \frac{\partial F(SoC_t)}{\partial SoC_t} - 1 \right] \begin{bmatrix} SoC_t \\ U_{C. t} \end{bmatrix} - I_t R_1 + V_t \quad (4.28)$$

The extended Kalman calculation formula and process are as follows:

$$\begin{cases} \hat{x}_t^- = A_{t-1} \hat{x}_{t-1} + B_{t-1} U_{t-1} \\ \hat{P}_t^- = A_{t-1} \hat{P}_{t-1}^+ A_{t-1}^T + Q_t \\ K_t = \hat{P}_t^- C_t^T (C_t \hat{P}_t^- C_t^T + R_t)^{-1} \\ \hat{x}_t = \hat{x}_t^- + K_t (Y_t - C_t \hat{x}_t^- - D_k U_k) \\ P_t = (I - k_t C_t) P_t^- \end{cases} \quad (4.29)$$

In general, the EKF can be worked as follow; firstly, by calculation the priori estimated value  $\hat{x}_t^-$  according to the state quantity at the previous moment, and then estimation the prior estimation error covariance matrix  $\hat{P}_t^-$ . The first two steps are called the time update equation. Then the obtaining the gain coefficient  $K_t$  according to  $\hat{P}_t^-$  and the current time observation matrix  $C_t$ , and then the fourth step where the calculation of the optimal time value according to the prior estimation value of the state quantity and the current time observation value [180]. Finally, the update of the covariance error matrix.

To construct and implement the SoC estimation model based on the Thevenin model and the KF and EKF algorithms, the SoC estimation model in MATLAB is implemented, based on the MATLAB simulation environment, the SoC estimation of lithium-ion batteries is performed by combining the lithium-ion battery model, the EKF algorithm as shown in Fig 4.8.



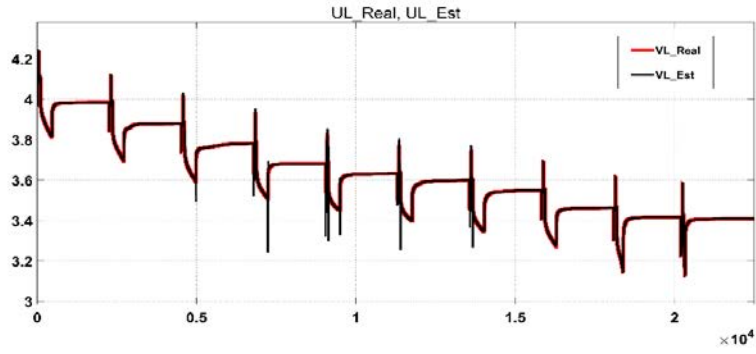


Fig 4.9: The real voltage load and the estimated voltage under UDDS.

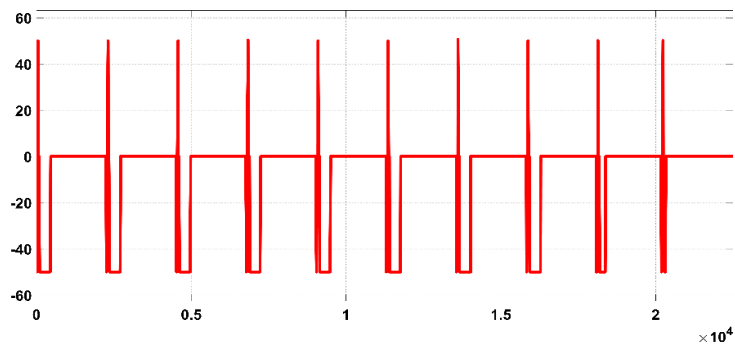
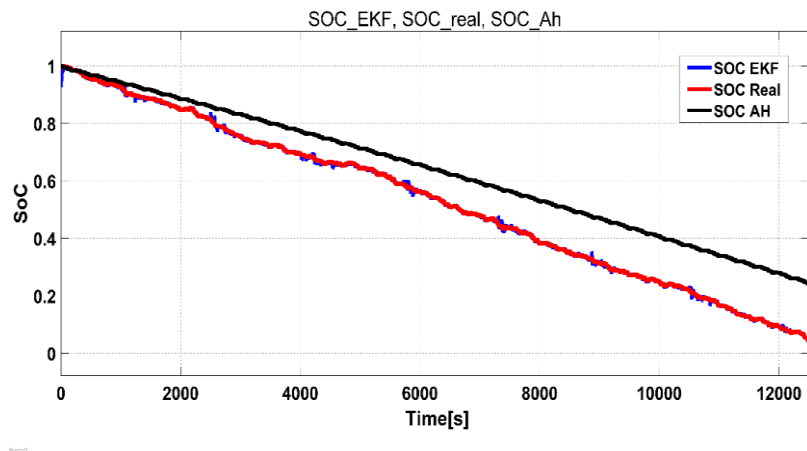


Fig 4.10: battery input current.

The insensitivity of the extended Kalman filter method to the initial value of SoC and the ability to correct SoC errors can be verified through set the input separately. The EKF SoC of the battery is estimated by 90% and 10%. The simulation results are shown in Fig 4.1, where the plots of the EKF estimated value, the SoC real value and SoC Ah value. besides, the Err value.



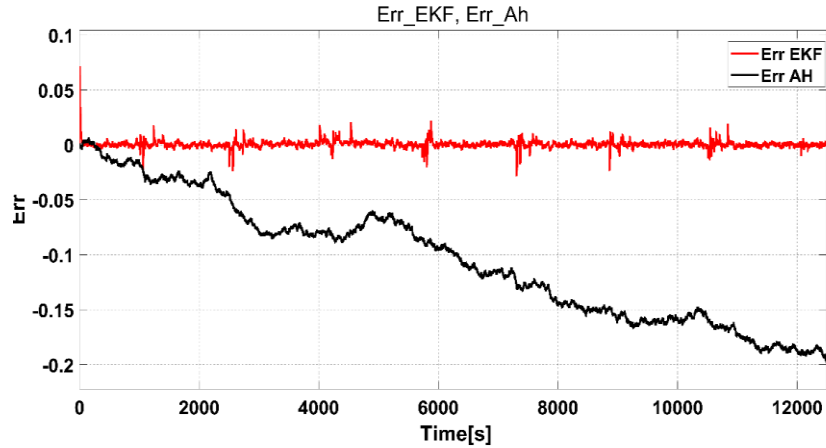


Fig 4.11: EKF SoC estimation 90-20% and SoC estimation Error.

The following conclusions are drawn from the simulation results: when the ampere-hour integration method is used purely, if the initial value is wrong, the initial error will always exist, which greatly reduces the accuracy of SoC estimation; using EKF to estimate SoC is not sensitive to the initial value, EKF The SoC value can be corrected in a short time. Through data analysis, it can be concluded that when the initial SoC differs from the real SoC by 50%, EKF can correct the error to within 5%; after EKF finish error correction, the estimation error fluctuates between -2% and 2% due to the addition of Gaussian noise, and the maximum does not exceed 3%; and as time progresses and the number of iterations increases, the EKF error will become smaller and the estimated SoC value coming closer to the real value.

#### 4.5 Conclusion

The accurate SoC estimation gives high reliability and stability. In applications such where the lithium battery can be used such EV main and charging station as BSS where the SoC play important role for designing the energy management system. In practical applications, many influencing factors, such as temperature, discharge rate, battery aging, etc., on the SoC estimation need to be considered, but for the extended Kalman filter, as long as the model is established reliably, If the parameter identification is accurate, the estimated SoC value can be moved closer to the real value.

**Chapter 5: Energy Management of proposed EVs charging model**

## 5.1 Introduction

A hybrid EV charging station consisting of a PV system, a battery and a main grid is developed in this research work. The on-line management strategy is proposed to maximize the use of renewable energy. To overcome the intermittent nature of solar energy, BSS are incorporated to balance charging demands under various operating conditions. The energy management strategy aims to reduce energy consumption from the main grid [137]. In order indirectly reduce costs, instability risk and pollution. The energy management approach uses meteorological information and load demand statistics to optimize the use of solar and grid energy through charging station [181].

The main attributes of the proposed energy management strategy are to:

1. Maximize the use of renewable energy.
2. Assist intermittent renewable energy using the electrical storage.
3. Use grid energy to compensate for the gap between generation and load demand in the worst-case scenario.
4. Minimize the energy drawn from the grid, especially during peak periods, to minimize costs, pollution and increase the stability of grid operations.

Comprehending these attributes, energy management strategy can be used for generating the reference signals for controllers of power conversion stage to meet the requirements under various operating conditions. Various intermittent conditions with different levels of PV penetration and BSS SoC are considered. The performance of energy management strategy and power conversion stage are studied and validated to ensure the generation- consumption balance considering:

$$P_{PV} \pm P_{Grid} \pm P_{BSS} = P_{EV} \quad (5.1)$$

Where ( $P_{PV}$ ,  $P_{Grid}$ ,  $P_{BSS}$ ,  $P_{EV}$  refer to (PV power, grid power, BSS power and EVs power) respectively. Electrical battery plays the pivotal role; it behaves as a rapid buffer between PV, grid and EVs load. In case of surplus energy from PV, energy can either be stored in BSS or consumed in grid. In case of shortfall of PV generation, the deficit can be provided by either BSS or grid. Since the time response of BSS is rapid, the preference of energy management is to compensate surplus/shortfall of PV through BSS. In this case, grid participates only when battery reaches its limits in terms of SoC or energy. Therefore, including BSS in hybrid EVs charging stations expands the penetration level of both EVs and renewable energy in conventional charging station. Although the inclusion of BSS in hybrid system is important, the overall management becomes difficult due to the different constraints relevant to power conversion/controller stages.

The proposed on-line management strategy considers real-time profile of PV system and battery different SoC levels to examine the control and EMS and the charging of EVs during intermittent conditions. Grid assists the charging process during worse case scenarios only. Energy management strategy considers the grid peak/off-peak hours to provide flow of energy under different conditions. The energy management produces power reference signals for appropriate control of converters connected to grid through the bidirectional ILC. In Fig 5.1 the overall topology operates to maximize the utilization of PV and BSS, while putting less stress on the grid side.

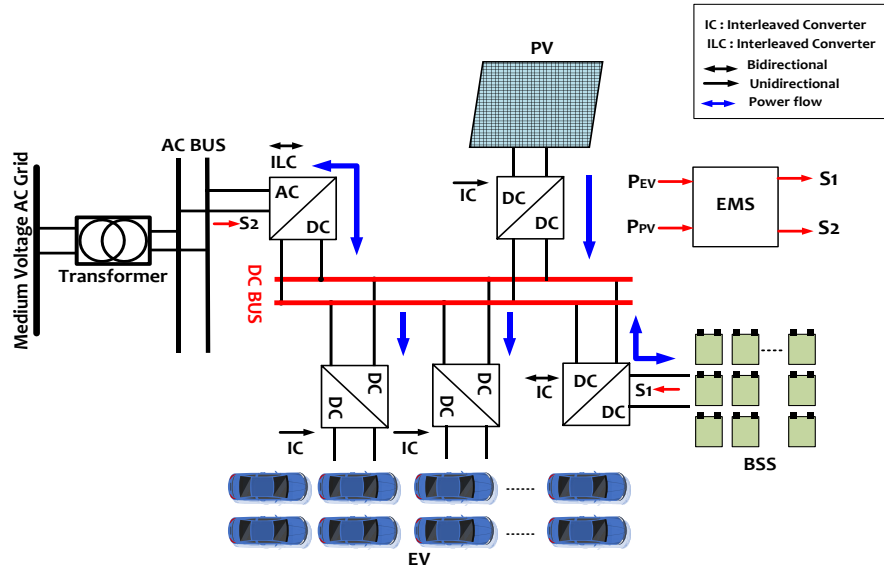


Fig 5. 3: General system structure and EMS of the EV charging station.

## 5.2 General operating modes of charging station

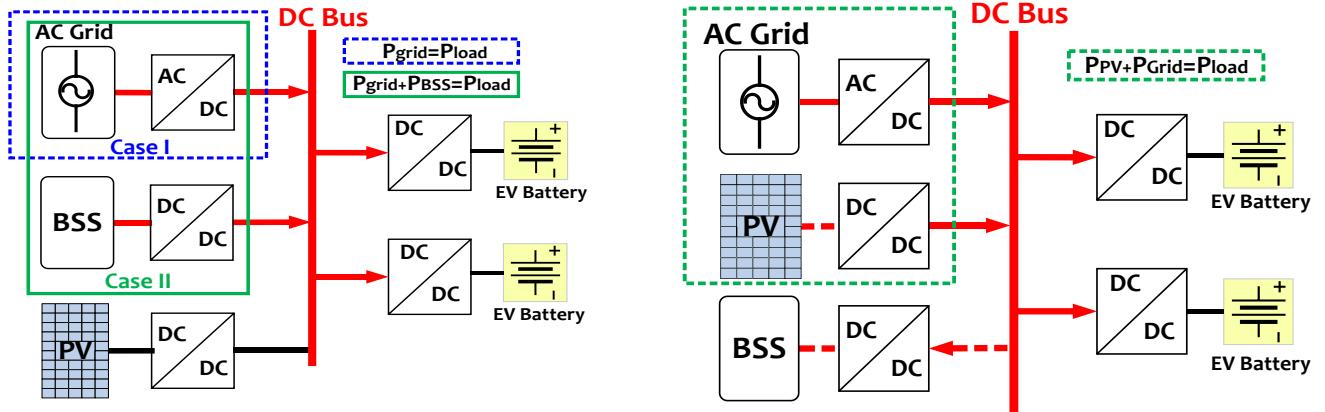
The classification of charging station-operating modes according to the quantity of energy produced by the sources and the direction of the power flow are summarized in Table 5.1.

Table 5. 2: General charging station operating modes.

Mode	Operating Mode	Power Flow	Conditions
1	Case I	On-grid operation	$P_{Grid} = P_{load}$
	Case II	BSS & Occasionally grid support	$P_{BSS} + P_{Grid} = P_{load}$
2	PV and grid-connected	$P_{PV} + P_{Grid} = P_{load}$	$VDC_{ref1} \leq VDC < VDC_{ref2}$
3	PV charging only & Occasionally BSS support	$P_{PV} + P_{BSS} = P_{load}$	$VDC_{ref2} \leq VDC < VDC_{ref3}$
4	Off-grid operation	$P_{PV} = P_{load}$	$VDC-Bus \geq VDC_{ref3}$

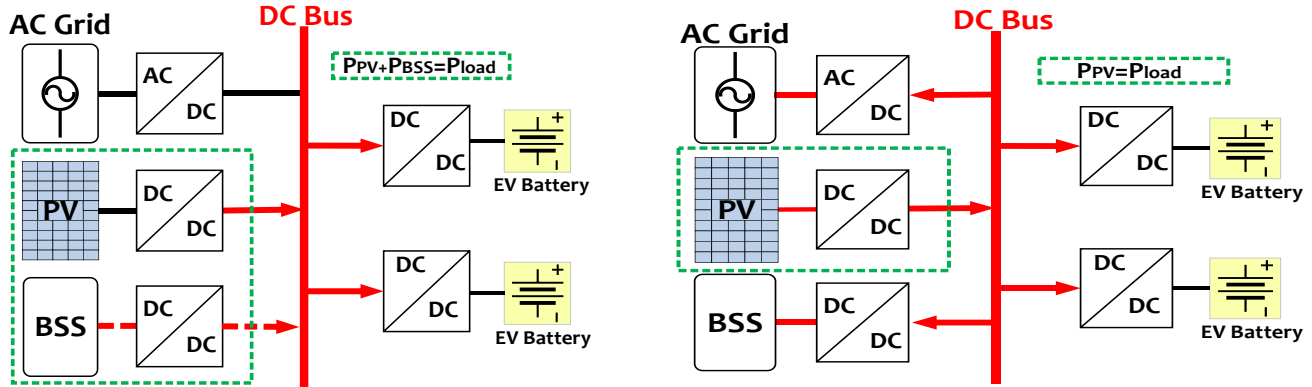
To describe the general operating modes of charging station, a set of parameters ( $IT$ ,  $I_{Tmax}$ ,  $VDC_{ref1}$ ,  $VDC_{ref2}$ ,  $VDC_{ref3}$ ,  $V_{EV}$ , and  $VBH$ ) should be considered;  $IT$  is the distribution transformer load,  $I_{Tmax}$  is the maximum transformer load, and DC bus voltage  $VDC$  designates the voltage on the DC bus. In fact, the selection of

voltage reference values is performed based on the change in the solar irradiance strength by considering the VDC and the equivalent power provided by the PV generator. The three reference voltage levels on the DC bus are  $V_{DC_{ref1}}$ ,  $V_{DC_{ref2}}$ , and  $V_{DC_{ref3}}$ ;  $V_{EV}$  and  $V_{BSS}$  denote the detected battery voltages of the EV and BSS respectively.  $V_{BH}$  refers to the battery voltage pertaining to the SoC cut-off value. When  $V_{EV}$  is equal to  $V_{BH}$ , the EV charging process terminates. The power flow direction for charging stations at different operating modes is shown in Fig 5.2.



Mode 1: Grid rectifier/BSS-based charging scheme.

Mode 2: Grid rectification/PV-based charging scheme.



Mode 3: PV/BSS-based charging scheme.

Mode 4: PV-based charging scheme.

Fig 5. 4: Generic power flow scenarios of charging stations.

**Mode 1-Case I:** the PV system does not generate energy because of the low radiation and inclement weather conditions. In this case, the boost converter is isolated, and the grid provides the power necessary for EV charging. If the DC bus voltage is greater than  $V_{DC_{ref1}}$ , the controller changes to mode 2, in which the buck converter adjusts the output voltage to charge the EV. Because of the off-peak period of the grid, the controller continues to provide electricity via the grid until vehicle charging is completed. On the other hand,

if  $V_{EV}$  exceeds  $V_{BH}$  and the grid supplies power to charge the BSS, then the controller terminates the EV load by deactivating the buck converter.

**Mode 1-Case II:** This mode resembles case I. It is characterized by a rise in the local demand at the distribution transformer. To minimize the stress on the grid, the EV load must be momentarily interrupted through the deactivation of the bi-directional DC/AC device linked to the grid. Because the distribution transformer is derived from the extra-load by charging the EV, this component will constantly provide power to the local loads during the entire charging process. During peak periods, the EV may be recharged through the BSS if the amount of stored energy is sufficient to satisfy the EV recharging requirement. In case of grid re-activation ( $I_T < I_{Tmax}$ ), the EV load will be restored, and the EV will be recharged.

**Mode 2:** the output of the PV system is less than the power necessary to charge the EV. Thus, all the power produced by the PV is sent to the EV along with grid support. The DC link voltage changes according to the irradiation. This DC link variation is detected by the controller to produce voltage that is equivalent to the output of the DC/AC bi-directional converter via the rectification process. In this case, the bi-directional DC/AC converter is separated from the grids. When  $I_T$  is greater than  $I_{Tmax}$ , the charging of EV by the PV system continues; on the other hand, the grid manages the peak load demand.

**Mode 3:** all the power necessary to charge the EV is generated by the PV system for charging the EV. The controller prevents the overload of the EVs by terminating its charge. This mode occurs when the DC link voltage varies between  $V_{DCref2}$  and  $V_{DCref3}$ .

**Mode 4:** The DC link voltage is greater than  $V_{DCref3}$ , and the PV produces excess power. The additional power provided by the PV is transferred into the grid through the bi-directional DC/AC converter. After charging the EVs, all the power produced by the PV source is transmitted into the grid. This procedure resembles the typical operation of PV production systems.

### 5.3 Rule- based Energy management system (REMS) algorithm

Effective energy management has become very essential due to both the energy shortage and high costs [181]. the energy management can increase the system's efficiency thus achieving significant energy savings with substantial economic advantages [182, 184]. The proposed EMS involves rule-based strategies, essentially in the form of "if then" scenarios. The "if" are associated with different possible scenarios and the "then" performs the operating modes. [185]. In these modes, the energy flow between the components of the system can be performed. The energy transaction, i.e. power sales and purchases, can be performed directly using the REMS Controller [186].

In this thesis, rule- based energy management is developed considering hybrid operation of PV with battery to assist charging of EVs either with or without main grid (standalone operation). In the former case, energy management algorithm effectively maximizes the utilization of renewable energy with the supplementary assist of both BSS and grid. In the proposed energy management, the BSS SoC must be confined at the limits  $SoC_{min}$  and  $SoC_{max}$ . Referring to SoC estimation for the battery in chapter 4, the SoC limits are between 90% and 10%.

The algorithm steps are considered to maximize the utilization of renewable to ensure lesser stress on grid side through:

1. The algorithm checks the presence of EV load, available PV power BSS energy state.
2. BSS either provide the charging process or behave as load itself, depending on the SoC of battery and condition of PV energy.
3. Grid play the role to either mitigate the deficit for charging EV load and BSS charging by extra power from grid to achieve (valley filing).
4. The algorithm is especially sensitive to peak load times of grid and in that scenario effectively utilize the BSS in preference either to take extra energy from PV or to supplement PV in case of deficiency.

Table 5.2 presents a summary of the simulation data is used by the REMS. In addition, as an assumption, to prevent overcharging, the BSS SoC battery set at 90% as SoC max. On the other hand, the SOC level should not be lower than 20% as SOC min [61,62].

Table 5.2: parameter and Abbreviation used in the energy management strategy.

Parameter	Abbreviation	Value
EV charging price	Chrg_Pr	0.17 €
Grid electricity price	GE_Pr	Variable
Photovoltaic supply EVs	PV2EV	
Battery storage supply EVs	BSS2EVs	
Grid supply EVs	G2EV	
PV power	PV_pr	
Charging price	Chrg_Pr	
EV_Dmd	EV demand	

To increase charger utilization and charge EVs in time, an hour is set to reach  $SOC_{max}$ . Consequently, based on EV demand, the charging level can be controlled by REMS, where the DC charger is 750V and 63A. Besides, a constant charge price is applied at a fixed value €, cents/kWh. However, this is lower than the grid electricity price at parity and below the parity conditions. In general, the grid electricity prices are proportional to the grid load.

### **Mode1: PV to EV**

In this scenario, the energy is transferred from PV to EV within this operating mode. To decrease the reliance on the main grid, priority is given to the use of PV power. The energy is bought from the PV at PV\_Pr and delivered to the EV at a fixed charging price. Depending on scenarios, the amount of power supplied from PV to EV can be varied.

In case 1: if PV power is available to supply the EV demand, and it can work in stand-alone mode or off grid. Therefore, the PV2EV is equal to the full power needed by the EV.

$$PV2EV = EV\ demand \times \Delta t \quad (5.2)$$

In case 2: if PV power is less EV\_demand, 100% of PV energy is used to recharge the EVs.

$$PV2EV = PV\ power \times \Delta t \quad (5.3)$$

The residual EV demand is supplied under mode 2 and/or 3.

### **Mode 2: BSS to EV**

Mode 2 is switched into operation if the PV system cannot completely cover the EV demand, simultaneously overloading at the grid, the energy supplied will be varied based on two different scenarios.

In case 1, when the gap between EV demand and PV power is lower than the available BSS power, then the power required to charge the EVs is supplied by the BSS.

$$BSS2EV = (EV\ demand - PV\ power) \times \Delta t \quad (5.4)$$

In case 2, if the gap is greater than available BSS power, then all energy of BSS is utilized for the charging. To ensure that charging process is not interrupted, the remaining amount of power is provided by the grid. Accordingly, the energy supplied by the BSS for charging the EV as:

$$BSS2EV = available\ BSS\ power \times \Delta t \quad (5.5)$$

Where the available power of the BSS represents the maximum power (kW) that the BSS can provide without interruption over the time step  $\Delta t$  until its SOC decreases to the lower limit  $SOC_{min}$ . It is given as:

$$available\ BSS\ power = \frac{((SoC(t) - SoC(min)) \times N_{batt} \times C_{batt})}{\Delta t} \quad (5.6)$$

In both scenarios, BSS power is bought from BSS\_Pr and sold to Chrg\_Pr. In the case of the insufficient PV power, this mode works as a back-up system.

### **Mode 3: grid to EV**

Under Mode 3, power is bought from utility grid at  $GE\_Pr$  and is sold to EV at  $Chrg\_Pr$ . There are two possible scenarios where this mode works as well. In case 1, if both PV and BSS are not capable of supplying  $EV\_demand$  while the grid is overloaded, then the deficit is provided from the grid.

$$G2EV = (EV\ demand - (PV\ power + available\ BSS\ power)) \times \Delta t \quad (5.7)$$

In case 2,  $PV\_power$  is lower than  $EV\_demand$  when the grid is in the off-peak mode. In this situation, there is no power use from BSS for charging EVs and power deficit is supplied from the grid to use the potential of a low  $GE\_Pr$ . This is process known as the Valley filling. Energy consumed from the grid to charge EVs equals to the difference between the EVs *demand* and PV *power*.

$$G2EV = (EV\ demand - PV\ power) \times \Delta t \quad (5.8)$$

### **Mode 4: PV to BSS**

In case  $PV\_power > EV\_demand$  and  $SOC < SOC_{max}$ , the mode 4 is switched on. Here, the purchase and sale prices of energy are equal. Nevertheless, there is a difference in the energy amount provided from PV to BSS. In case 1, in case the difference between  $PV\_power$  and  $EV\_demand$  is greater than the Required  $BSS\_power$ , the total demand of BSS is supplied by the excess PV power

$$PV2BSS = Required\ BSS\ power \times \Delta t \quad (5.9)$$

The required BSS power represents the power (kW) needed to increase the SOC from the initial to the high  $SOC_{max}$  values during the time step  $\Delta t$ . It can be given as:

$$Required\ BSS\ power = \frac{(SoC(max) - SoC(t)) \times N_{batt} \times C_{batt}}{\Delta t} \quad (5.10)$$

In case 2, there is small difference between  $PV\_power$  and  $EV\_demand$  than Required  $BSS\_power$ . All the excess of  $PV\_power$  is transmitted to BSS. Therefore, it is possible to describe this scenario as:

$$PV2BSS = (PV\ power - EV\ demand) \times \Delta t \quad (5.11)$$

Mode 4 reduces the reliance on the main grid through energy savings at the BSS. Stored energy can be used at insufficient  $PV\_power$  and at the grid peak load.

### **Mode 5: PV to grid**

In this mode, if  $PV\_power$  is higher than the sum of  $EV\_demand$  and Required  $BSS\_power$ , then the PV2G is activated. Therefore, the energy transfer amount is depending on the BSS SOC. In case 1, if  $SOC < SOC_{max}$ , the BSS is charged from the excess  $PV\_power$ . Residual power is exported to the power grid.

$$PV2G = (PV\ power - (EV\ demand + Required\ BSS\ power)) \times \Delta t \quad (5.12)$$

In case 2, the BSS SOC<sub>max</sub> at max limit. Thus, all excess PV power is transferred to the main grid.

$$PV2G = (PV\ power - EV\ demand) \times \Delta t \quad (5.13)$$

In both scenarios, the power is sold from a PV to grid based PV\_Pr system. To supply the utility company a financial benefits, the power price is lower than the current GE\_Pr . This mode of operation is accomplished by a two-step conversion: by the DC-DC converter and the bi-directional inverter [143]. this operation is essential to compensate for the economic losses resulting from the continuous daytime charging at a fixed cost.

### **Mode 6: grid to BSS / valley-filling**

The mode G2BSS is operated if the main grid at is not at peak load period at the same time PV power is insufficient to charge BSS (SOC to SOC<sub>max</sub>). Recharging the batteries at no load period can achieve valley-filling. However, depending on two scenarios, power transfer amount can be varied. In case 1, if there is an excess of PV power, then the BSS is primarily charged by the PV; the residual Required BSS power can be imported from the main grid.

$$G2BSS = (Required\ BSS\ power - (PV\ power - EV\ demand )) \times \Delta t \quad (5.14)$$

In case2, if there is no excess PV power, the required BSS power is imported from the main grid.

$$G2BSS = (Required\ BSS\ power) \times \Delta t \quad (5.15)$$

Under this mode the power is imported from the grid under the GE\_Pr. The low tariff is used to compensate for the economic losses of the system. Mode 6 is operated by using a bi-directional converter and a bi-directional inverter at grid side.

### **5.3.1 Charging system operating scenarios**

The proposed charging system operations are classified in 3 basic scenarios, where they can be divided based on EVs demand and PV power as:

1. EVs demand higher than PV power (Over-load).
2. EVs demand less than or equal PV power (Under-load).
3. EVs demand is zero, PV power available (No load).

Over and under-load scenarios are made to ensure continuous charging at a fixed charging price. To offset the economic losses of the system, no load and operation is occurred under specific conditions defined.

### ***5.3.2 EVs demand higher than PV power***

In case PV produces power, the charging process begins directly by using mode 1 (PV2EV). Due to the overload situation, in which EV demand > PV power, the PV power cannot meet the EV demand value; the difference can be addressed by BSS or the grid. The G2EV mode is activated if the grid is in off-peak hours. Simultaneously, the SoC is verified; if the SoC < SoC<sub>max</sub>, then the BSS can also be charged from the grid (G2BSS), mode 6 under GE\_Pr. Hence, either the EV or the BSS use the valley-filling option with benefit from GE\_Pr low. Alternatively, in case the grid at peak load and the available power of BSS is greater than or equal to EV demand, the EV demand is supplied by BSS (BSS2EV) under mode 2. Nevertheless, if available power of BSS < residual EV demand, the grid supports BSS to supply the EVS demand (G2EV) under mode 3. In the worst scenario, assuming that PV and BSS are insufficient, the residual of EV demand will be supplied by the grid (Gd2EV) under mode 3. The power is supplied to the EVs at low charging price, regardless of the source. Fig 5. 3 shows the flowchart of the charging system operational under the over-load situation.

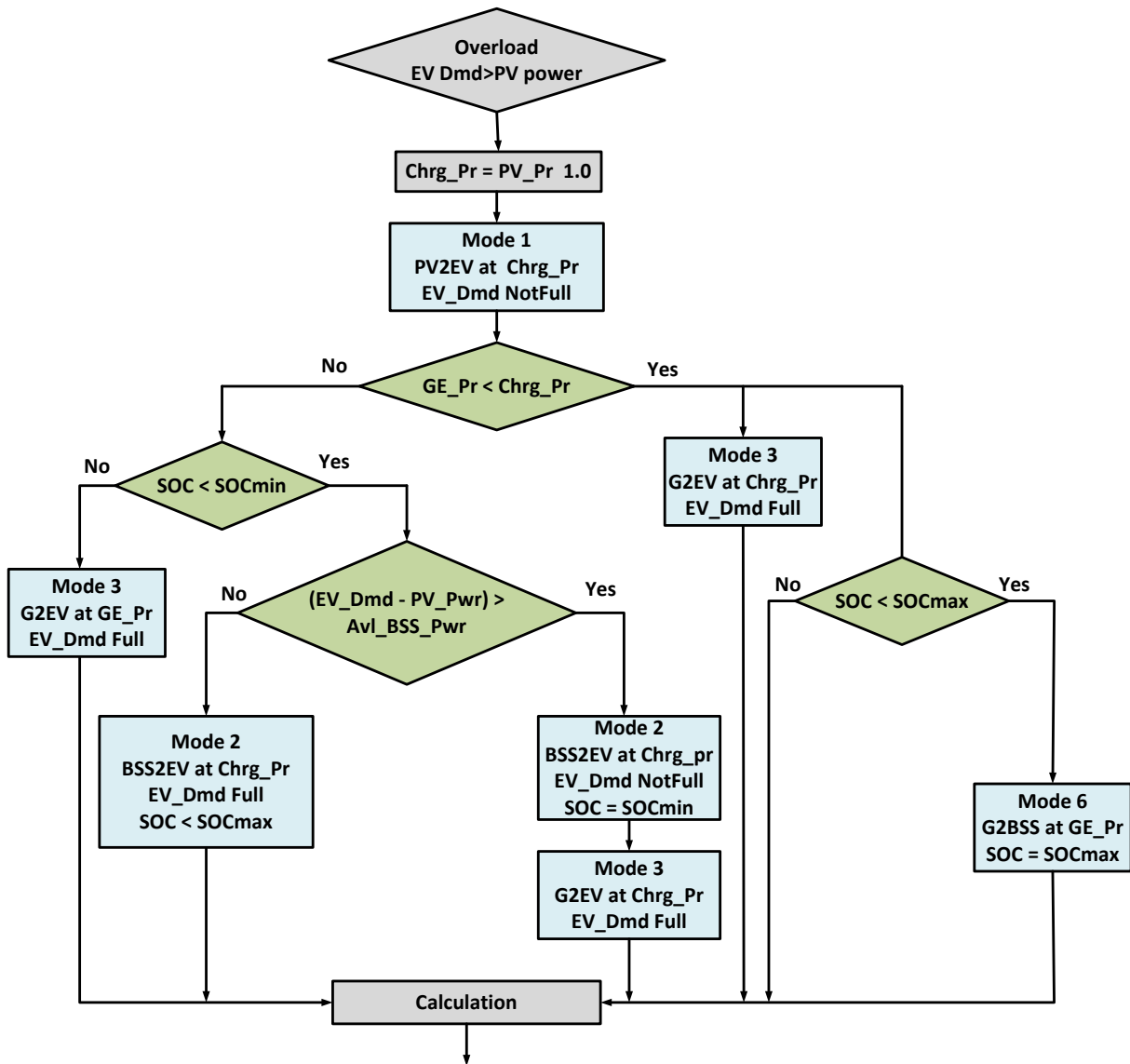


Fig 5.3: Operation at overload situation.

### 5.3.3 EVs demand less than or equal PV power

The operation during the underload scenario is shown in Fig. 5.4. Here, the produced  $PV\_Pwr \geq EV\_Dmd$ ; therefore, the excess  $PV\_Pwr$  can be supplied to the BSS so that the SoC is increased. Otherwise, the surplus  $PV\_Pwr$  can be supplied to the grid to gain financial. Surplus  $PV\_Pwr$  has priority to charge the BSS (PV2BSS) under mode 4. If, however,  $BSS\_Pwr > \text{exceeds } PV\_Pwr$ , the residual demand is fulfilled by a valley-filling process under mode 6 (G2BSS). However, if  $PV\_Pwr > BSS\_Pwr$ , the residual power is sold to the grid (PV2G) under mode 5.

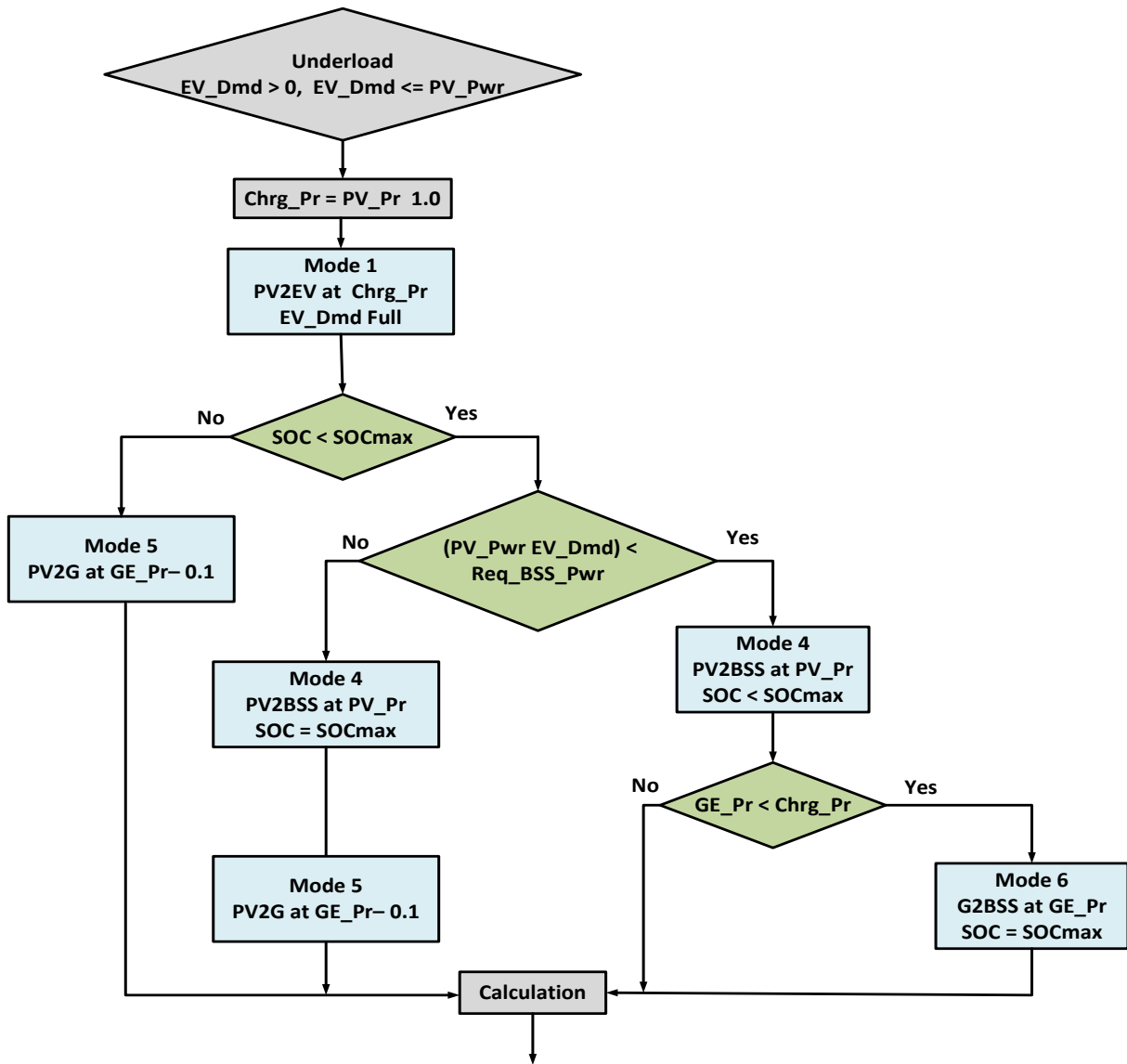


Fig 5.4: Operation at underload situation.

### 5.3.4 EVs demand is zero, PV power available

In case of no load, it is possible for the PV\_Pwr total to 1) charge the BSS and/or 2) supply the grid. The SOC of the BSS is verified first; if the SOC is below the SoCmax, the PV\_Pwr is charged the BSS (PV2BSS) under mode 4. However, if the PV\_Pwr is higher than the BSS\_Pwr, the surplus power is sold to the grid (PV2G) under mode 4, as shown in Fig 5.5 if BSS\_Pwr > PV\_Pwr, the BSS can obtain the residual power

from the grid (G2BSS) via a valley - filling (Mode 6). However, if the BSS at SOCmax, all PV\_Pwr is sold to the grid (PV2G).

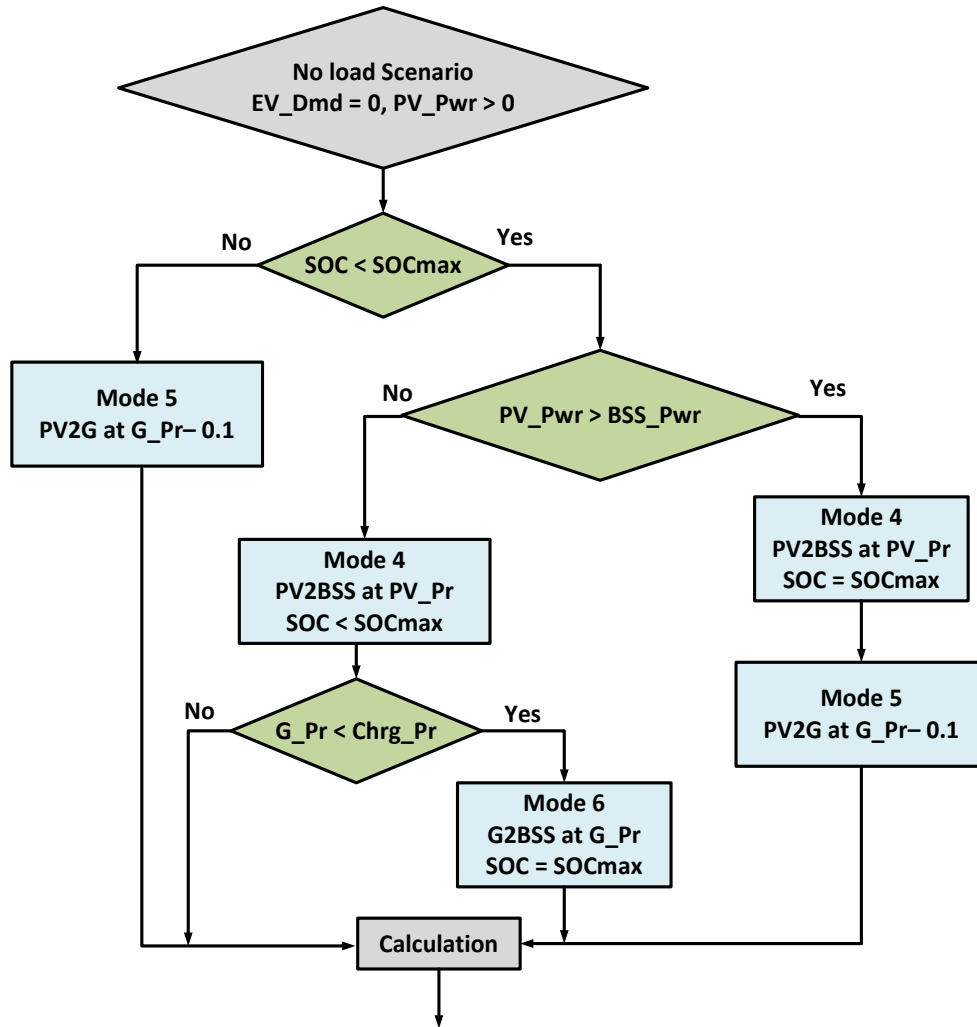


Fig 5.5: Operation at underload situation.

## 5.4 Results and discussion

The EVs charging system modeling is simulated in MATLAB. The aim of the simulation is to test the capabilities of the REMS algorithm to deliver an uninterrupted charging process with a constant or lower price at different operating conditions. Typically, these tests are performed for an uninterrupted charging at a constant charging price:

- 1) Under different weather conditions (normal and abnormal days).
- 2) With different levels of BSS SoC.

3) The variable price of electricity at grid as shown in Fig 5.6

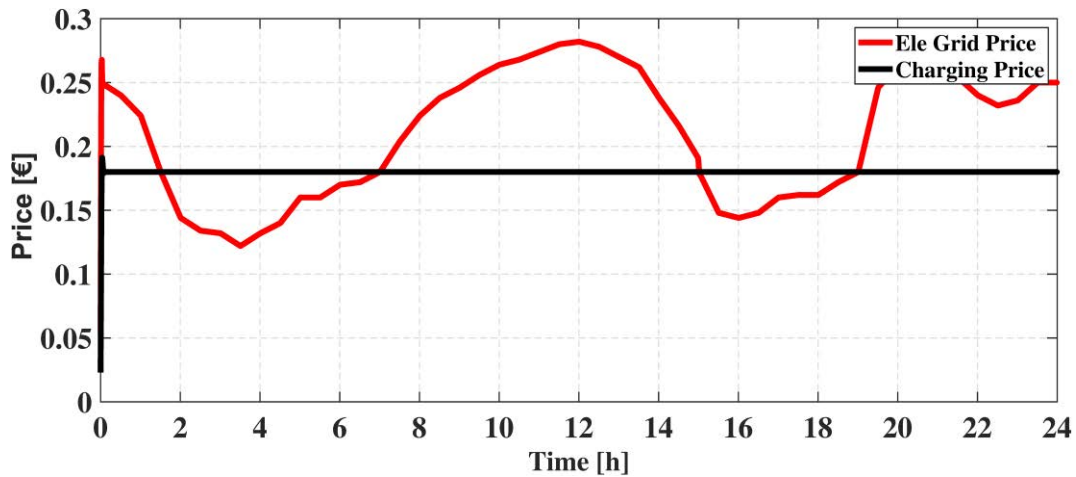


Fig5.6: Electricity grid price and EV charging price.

The charging price (Chrg\_Pr) is set to a constant value of 0.18 euro/kWh according to [187]. This value is lower than the average grid electricity price at parity and below the parity conditions. As the grid electricity prices are directly proportional to its load, the off-peak conditions are defined on the basis of the grid electricity price.

In Fig5.6 the grid electricity price is lower than the charging price at periods (1.30 a.m.) to (7:00 a.m.) and in the period (15:00 p.m.) to (19:00 p.m.) these periods represent the off peak of the grid side.

#### 5.4.1 Charging EVs load Clear Day Profile

Fig 5.7 shows the EV load profile under the condition that the PV power is high, the increase in PV power is regular, indicating that the irradiation is not affected by a sudden change in the weather. During the morning (before 9:00 a.m.) and evening (after 18:00 p.m.), the irradiation is low, and the PV power is insufficient to charge all EVs. In this situation, the charging of EVs is fulfilled by activating additional modes, namely BSS2EVs and G2EVs. Prioritization of energy sources with the comparison of the GE price and the charging price is done by the proposed EMS according to the following order: PV2EVs, BSS2EVs, and G2EVs. Priority is given to the use of PV energy first.

The battery is used if the PV power is insufficient to fulfill EV charging. If the joint contribution of the two sources is still insufficient, grid power is used to maintain the continuous load. This sequence can be clearly seen in Fig 5.7 A, from 8:00 a.m. to 18:00 p.m. under "Uninterruptible load using PV, BSS, and grid at high and low grid electricity prices. The transition from the PV2EVs BSS2EVs to the G2EV and PV2EV operating mode is determined by grid electricity price and started at 15:00p.m. to 19:00 p.m. Hence, the BSS and EV load is charged outside of the grid peak hours, with the load is supplied by the grid under low price of

electricity to ensure uninterrupted charging. In the mode of EVs load more than the PV power the charging system was tested under different BSS SoC levels, if the SoC levels is on the middle level or high level the charging system will be operated under the charging price and grid price completely as shown in Fig 5.7 A and Fig 5.7 B, if the SoC at low level the charging system will use the grid power beside the PV power to fill full the EVs load As shown in Fig5.7 C.

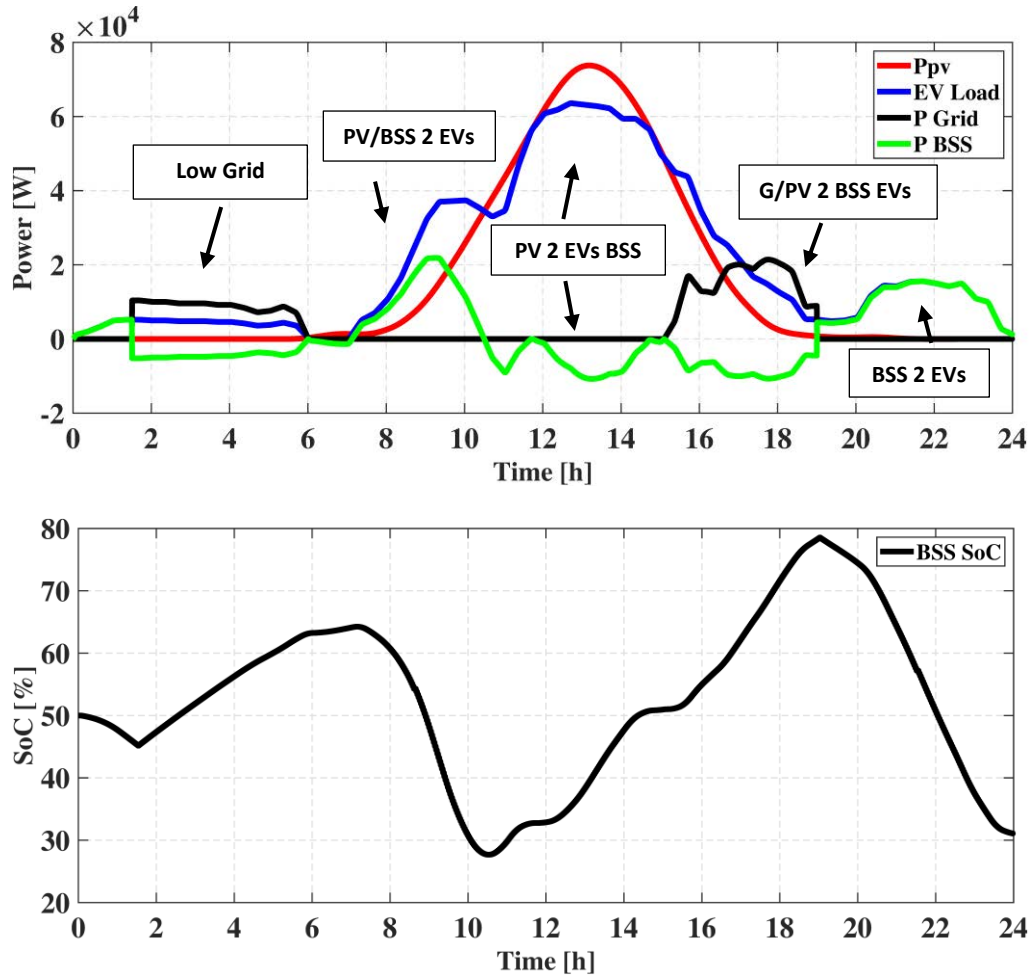


Fig 5.7 A: Power flow of charging system components and BSS SoC at 50 %.

With the same PV profile, simulation of REMS based PV charging system with same of EVs load profile and different BSS SoC is establish. In this context, Fig 5.7 B explains the power profiles of the overall system components to meet the EVs load requirement. Since BSS SoC is 85%, thus the demand gap is provided by BSS besides PV and grid in case low electricity price. In this case, extra energy is absorbed by BSS or grid in case of SoC high to keep the power balance. Not only it decreases the operational cost of electricity production by grid side but also reduce the charging cost. In general, the proposed REMS provide power balance between connected sources and EVs load.

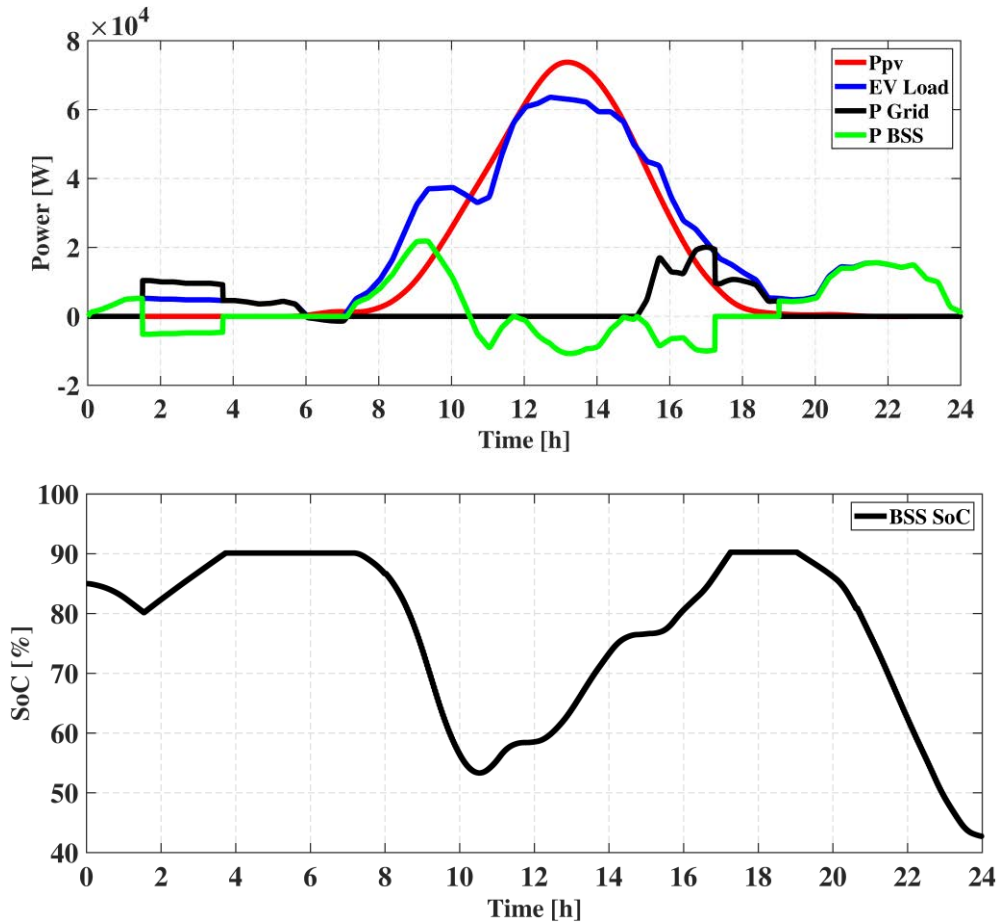


Fig 4.7 B: Power flow of charging system components and BSS SoC 85 % on clear day.

The results of REMS can be seen in the resilience of the charging price. This is shown in Fig 5.7 B " charging at constant or lower prices at off peak grid ". During the time of the day, the charging price is kept constant as desired, 0.18 euro/kWh. This is regardless of the type of power source used and the variation in the electricity price at the grid. In addition, Fig 5.7 B shows that EV charging is uninterrupted despite the simultaneous use of all three energy sources. In addition, the system minimizes the load on the grid. During peak periods, grid power becomes a last option.

The system and REMS are tested under BSS SoC is 25% as shown In Fig 5.7 C. Since the SoC of battery is low, the BSS charged by the extra power from PV to keep the power balance and maximize the local utilization of excessive PV energy meanwhile, it charges from the grid at low price. In case of energy gap between sources and load, the deficiency in power demand is provided by grid since the BSS SoC is low. The SoC of battery shown in Fig 5.7 C which illustrates the incrementally rising SoC of BSS since it only absorbs extra energy from PV and grid at no peak period and discharge under the desirable SoC level.

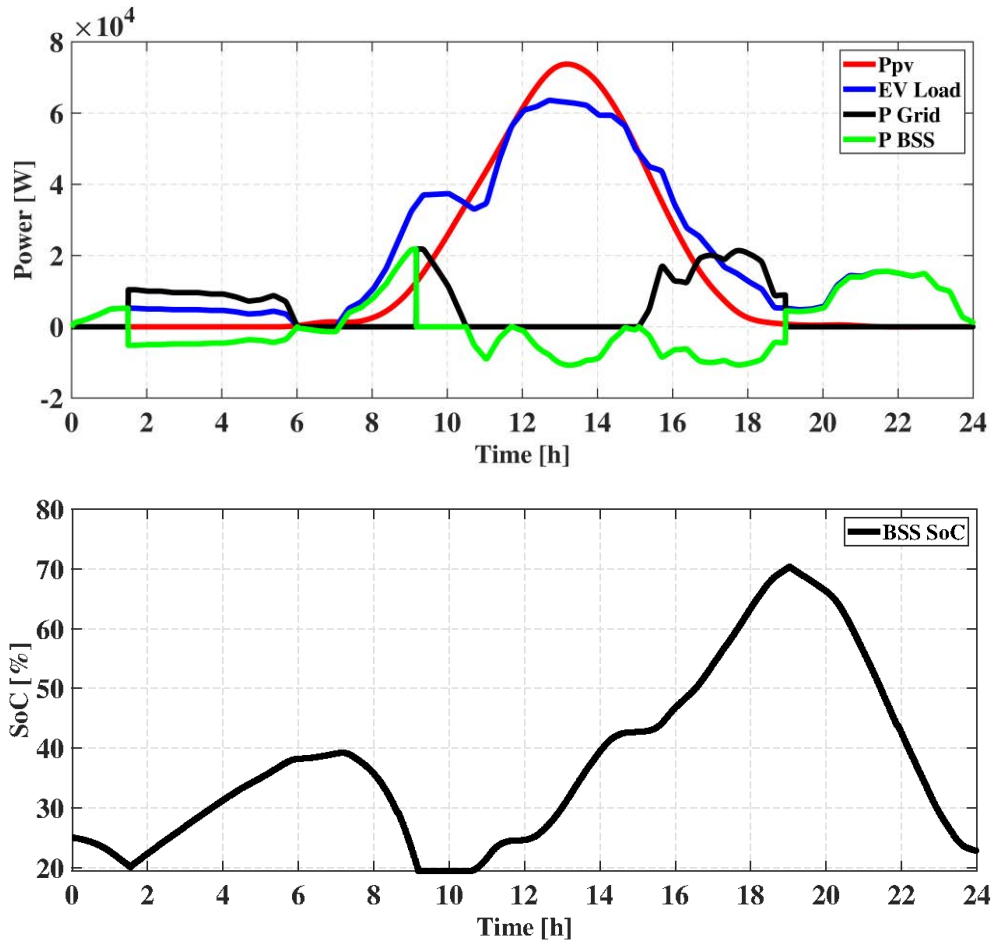


Fig. 5.7C: Power flow of charging system components and BSS SoC 25 % on clear day.

The REMS enable the charging system to export energy to grid at the peak load period as shown in Fig 5.8, this condition can be achieved under the PV2G at low load levels and high and after charging BSS to desirable level.

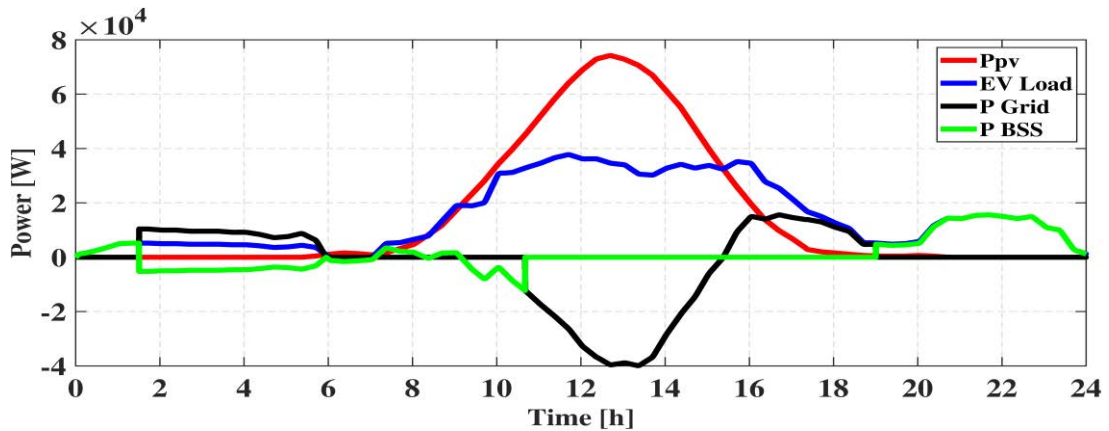


Fig5.8: PV energy to grid in case of SoC high and low EVs load.

### 5.4.2 Charging EVs on Cloudy Day Profile

The one-day charging operation with abnormal weather conditions, i.e., intermittent solar irradiation, where the intermittency is reflected by the fluctuating of PV power as shown in Fig 5.9 (A, B and C). However, it is obvious that EV's demand is fulfilled without any interruption, despite these fluctuations. In addition, Fig 4.9 A, shows that charging is done with the desired constant price and low grid price during off-peak periods, independent of continuous grid electricity price variations.

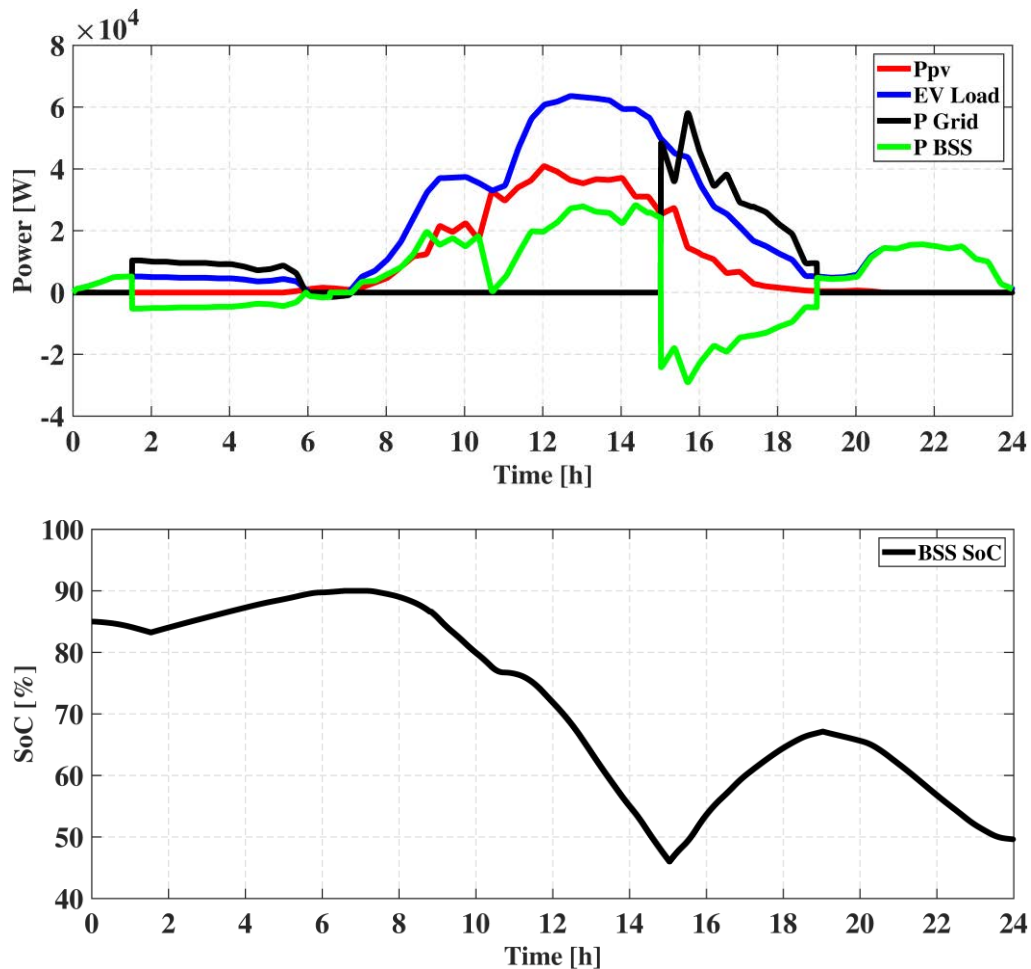


Fig. 5.9 A: power flow and BSS SoC 85 % on cloudy day.

Fig 5.9 A show that from 1:00 am to 7:00 am and from 15:00 pm to 19:00 pm the valley is covered by BSS2Grid (filling). It shows that the "Valley-filling" can take place whenever off-peak period, regardless of the time of day. It should be noted that, although the BSS has reached the first level of 20% low SOC during the hours of 15:00 pm to 19:00 pm, EVs are charged by grid power and the BSS due to the lower grid electricity price. The Valley-filling operation capitalizes on the low grid price, while charging BSS energy for the next use, especially during peak grid periods. This means that, outside peak periods, the use of grid energy for EV charging takes priority over BSS if the SoC is at max limit.

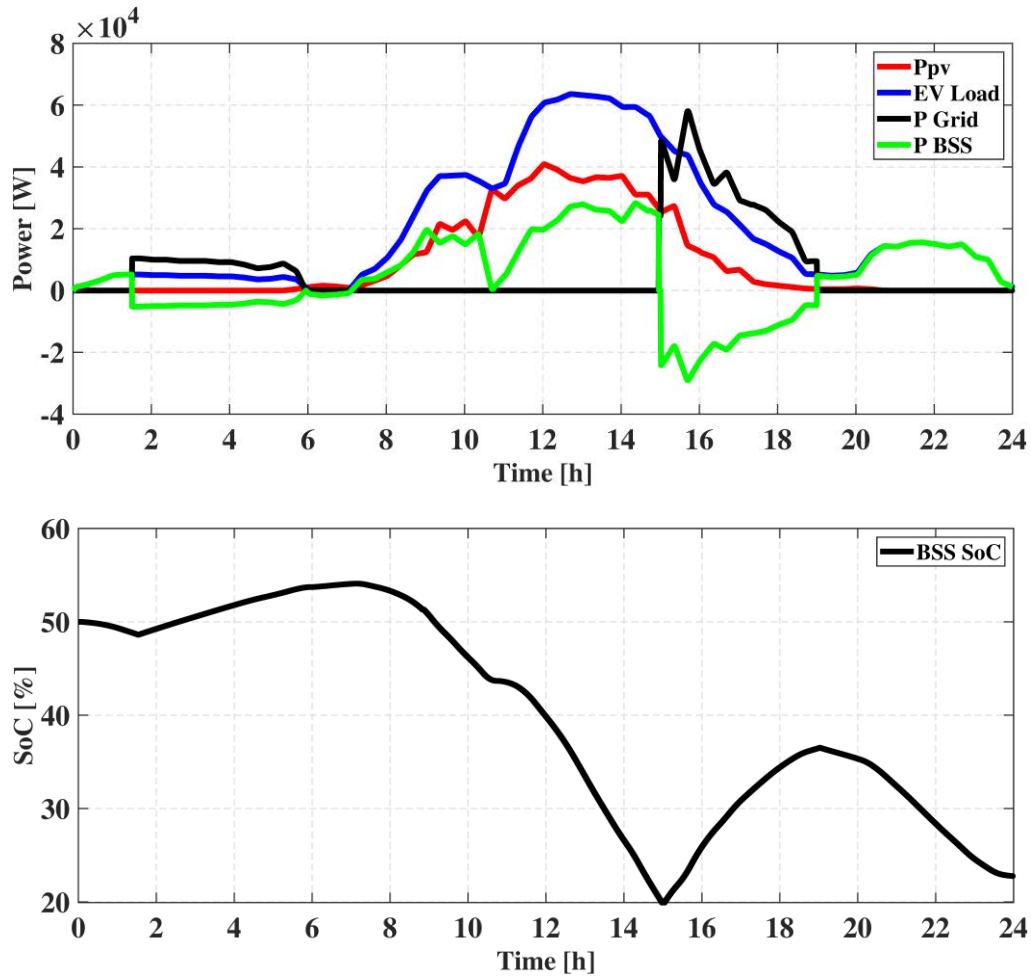


Fig 5.9 B: power flow and BSS SoC 50 % on cloudy day.

The results in Fig 5.9 B, show that both systems (EV and BSS) are benefitting from the low price of the grid during off-peak network hours. It is important to note that the operation of valley-filling by EV while maintaining an uninterruptible load is a feature of the proposed REMS.

The performance evaluation of the proposed management strategy is extended by considering a cloudy profile here. PV power in this case is highly intermittent and not sufficient to meet the EVs load profile. Here the initial SoC of BSS is 25% for the extended cloudy profile. Since the SoC of BSS is very low to surplus power for the intermittent operation is provided by grid. The BSS for the whole operation participates with the available energy. However, the SoC levels are adjusted to be at 90% and 20% within REMS, within this condition on cloudy day when the level SoC is low, REMS re-adjust the SoC low level at 10% in order to fulfill the EVs load from the BSS and PV as much as possible and to reduce the grid reliance in Fig 5.9 C.

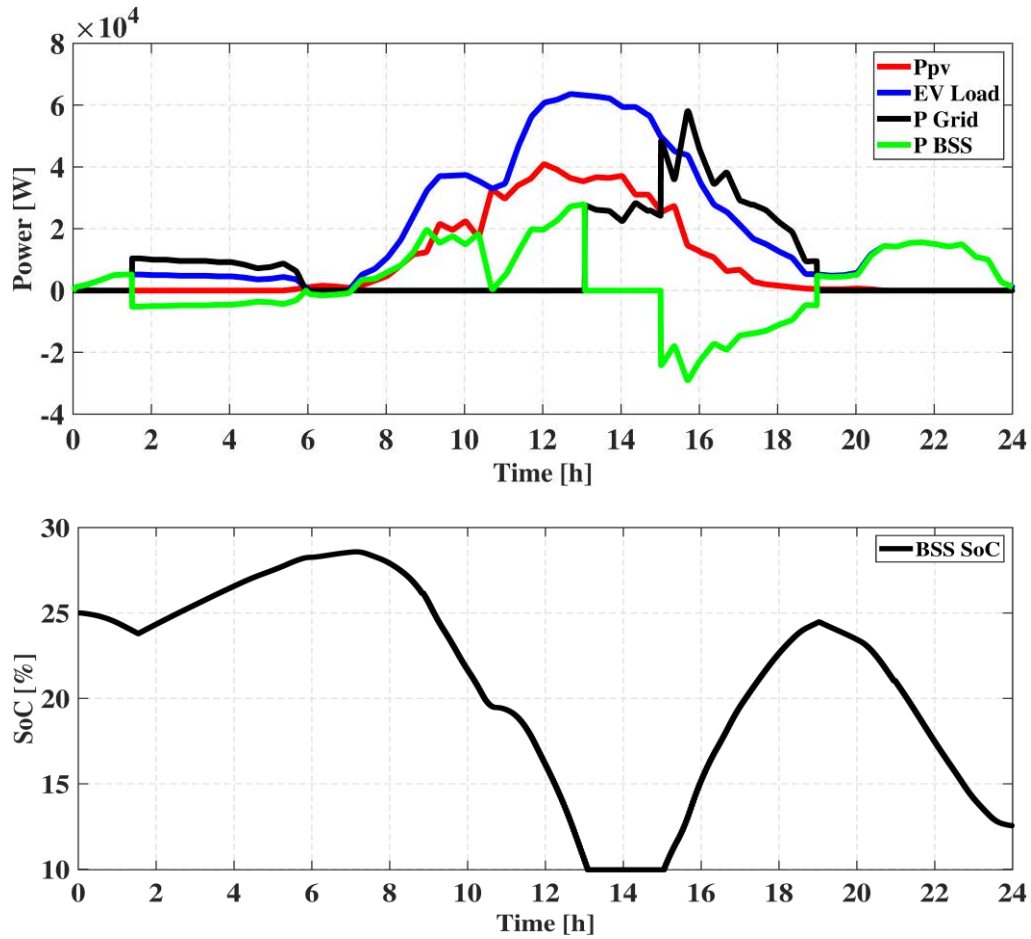


Fig 5.9 C: power flow and BSS SoC 25 % on cloudy day.

### 5.5 A Comparison of the PV BSS grid-based REMS with grid charging

The PV BSS grid-based charging system with REMS is compared with the charging system using grid only. Here, the grid power is calculated for the same EV load and assuming that there is no PV and BSS, beside applying different grid electricity price for different days. Moreover, the BSS SoC is assumed in high level and PV irradiation is high as shown in Fig 5.10 (A, B, C and D). The average charging prices per day with the same EV load are set at the same levels in all cases.

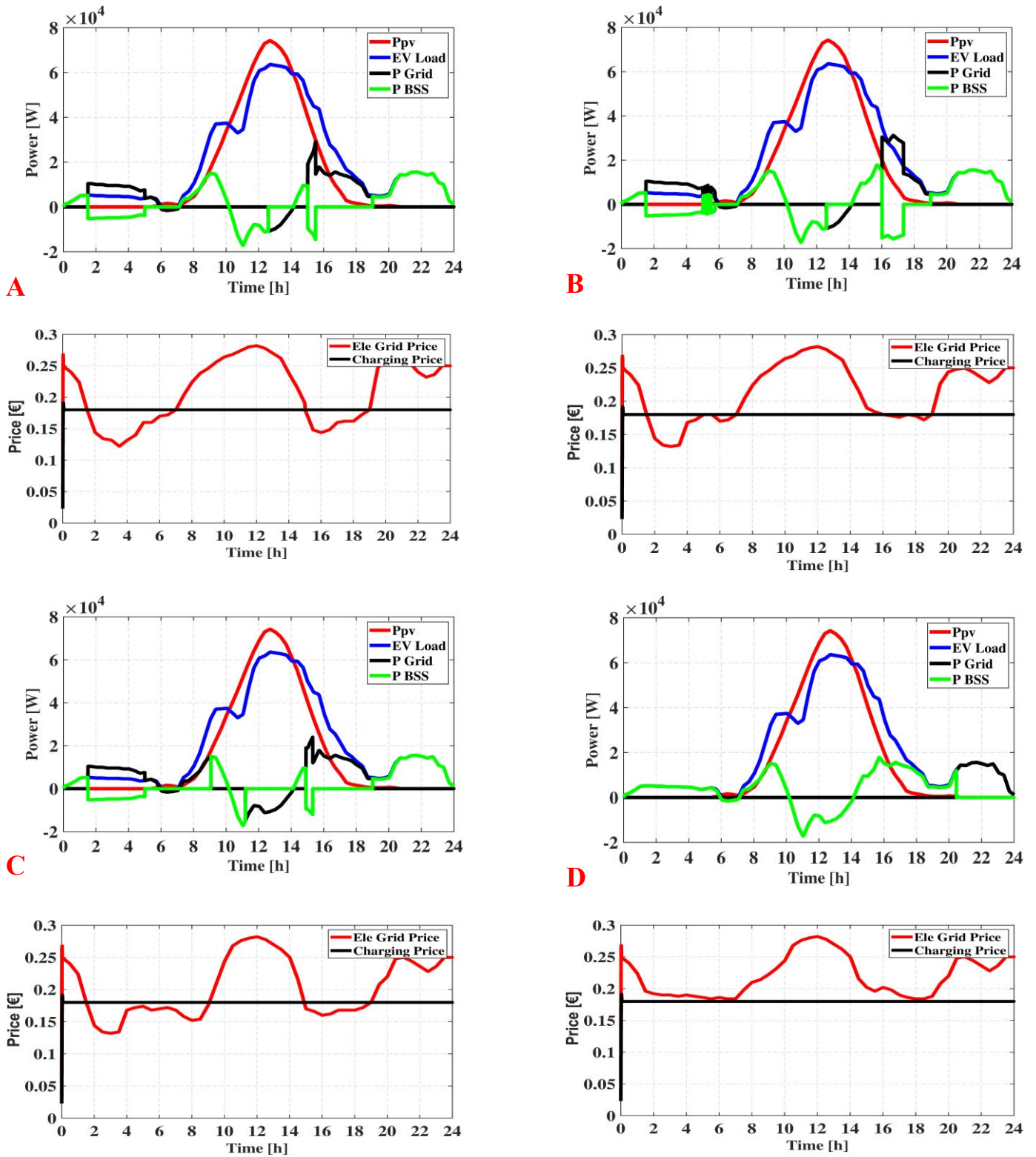


Fig 5.10: Different charging scenarios considering different grid electricity price.

with considering (Gd2EV and Gd2 BSS) which represent the amount of energy purchased from the grid at time t to charge the EV and the BSS. Similarly, the selling price is the sum of the energy sold to grid from PV under the grid electricity price. The energy price under REMS and grid only can be calculated from Matlab directly under the proposed prices. From the results in Table 5.3, the REMS is clearly shown to be about 12.1-12.5 % less than the grid-based charge only for the 24-hour scenario.

Table 5.3: Price comparison of REMS-based PV BSS grid charging and the grid charging.

Profile	Average charging price (€)		Reduction in charging price using REMS (%)
	REMS charging	Grid Charging	
A	55.3	67.4	12.1
B	56.2	68.6	12.4
C	53.6	66.1	12.5
D	55.5	67.8	12.3

## **Conclusion and Discussion**

## **General economic value considerations, Recommendations and Future research directions**

Although the impacts of a large number of EVs and their charging facilities on the safety of electricity grids have been investigated by several studies reported in literature, relatively few have assessed the economic value of electricity grid operation and EV load schedule. In this context, the studies many literature have proposed and implemented a real-time advanced EMS to optimize the micro-grid performance including the EV load; their objectives were to minimize energy costs and carbon dioxide and pollutant emissions while maximizing the capacity of the available RES. It is concluded that charging stations can also perform a function in peak-load shaving and valley-filling. The economic value of the foregoing is mainly reflected in the following aspects.

- i. A reasonable EV charge planning achieves valley-filling and peak-clipping. That is, by smoothing the load curve, it becomes possible to reduce the cost of electric generation and delay the investment on a new charging facility set that depends on the grid as power source to reduce the peak load.
- ii. The electrical energy stored in a large number of EV batteries may be used for frequency and voltage regulation by investing on discharge facilities and improving the reliability of the power system.
- iii. The efficient management of charging and discharging of a large number of EVs and the coordination of intermittent renewable energy sources can improve the capacity of the electrical system to accommodate these power supplies and thereby improve the cost-effectiveness of system operation. In other words, although the electricity grid has a limited capacity to accept intermittent renewable energy sources, the widespread use of EVs contributes to increase the power system capacity.

Some studies published in literature have considered the first two aforementioned aspects; however, no systematic research has ever been conducted on the third, although a few studies have this problem. So far, there is no rigorous analytical tool to assess the economic value of different EV distributions and grid penetration rates for different combinations of intermittent renewable energy sources. The economic value is mainly the potential savings on the operating and investment costs of the electricity grid. A comprehensive mathematical model is required to assess the economic value and study the appropriate load and management strategies to maximize the economic value of EVs and their facilities in power system planning and operation. Moreover, in the analysis of the impact of EVs on the economics of power system operation and planning, it is important to take into consideration the specific characteristics of the electricity distribution system being studied, i.e., the associated electricity market model and regulatory policies. In the context of the electricity market, the impact of EVs on the economics of the electricity grid is particularly remarkable. In addition, the value of EVs in terms of greenhouse gas emission reduction is also an important aspect that has to be examined; to a large extent, this depends on the combination of the types of electricity production for

EV charging. This combination generally exhibits a typical variation pattern throughout the day. Research can be conducted on the following three levels.

A. Integration of EVs based on home charging and commercial facility charging; emphasis is placed on the economic value of charging and discharging EVs in a typical home at several commercial CPs or at specialized battery recharge/replacement stations.

B. Widespread penetration of EVs at specific locations in the distribution grid; tools have been developed to assess the economic impact of power systems on a large number of EVs at specific locations in the distribution system when they are connected at the substation level. The research should consider two cases, private use and commercial use, because these two situations are considerably different.

C. System-level search; the focus should be on the impact of numerous EVs on the electricity sales market as a whole and on the retail distribution market after extensive access to the electricity grid. Three scenarios can be studied for each level: (i) absence of EV charging and discharging management; (ii) optimized EV charging and discharging management; (iii) optimized EV charging and discharging management in a smart grid framework and use of renewable energies.

### **Future research directions**

Concerning EV charging models, it is necessary to introduce more diversity in order to introduce further variability into the model assumptions. For instance, if several magnitudes of charging power, charging locations, and battery capacities are modelled by the same work, then such will provide a more accurate model that reflects the different requirements of various EVs. Moreover, few articles report on the modelling of the charging and integration of EVs in urban areas. Future research on V2G and management of charging and discharging can aid in identifying a compromise between the requisites of vehicle owners and power grid stability.

The high penetration of PV and EVs in the electricity market requires more research. Further studies on the response of vehicle owners to the requirements of grid operators should be implemented; benchmarking research, which evaluates both the produced power costs and charging costs, must be explored.

### **Conclusion**

The PV energy and electric vehicles are essential elements in minimizing both CO<sub>2</sub> emissions and fossil fuels consumption. Even though electric vehicles are more economical and environmentally friendly than gasoline cars, the increased penetration of electric vehicles is restricted mainly due to several reasons. Out of these reasons, the charging scheduling of electric vehicles and efficient design of dedicated charging facility are the most noticeable ones. If the charging facility solely relies on central grid to meet the electric

vehicles load, there will be unwanted overloading of the distribution system due to this new load. This would result in extensive stress on main grid, which may occur during peak load hours increasing the operational cost and incremental the greenhouse gasses. In this context, designing a dedicated charging station can enable lesser dependency on the main grid together with efficient scheduling of electric vehicles load.

In this research work, a dedicated renewable assisted charging station is proposed, simulated and validated under different weather and load profiles. The PV, BSS and EVs load are connected through a common DC bus. Furthermore, the main grid is connected to the common DC bus via a rectifier/inverter stage. The benefits of using common DC bus is the overall reduction in power conversion steps. In the context of power conversion, to enhance the efficiency of conversion, while providing a reliable and consistent power supply, interleave converters are utilized individually for PV, BSS and EVs load. In case of PV system, interleave boost converter with maximum power point tracking is utilized. For BSS a bidirectional interleave converter is suggested and analyzed. Hence, the interleave converter provides several benefits, such as low ripples output, less stress on converter components and lesser losses in passive elements resulting in higher conversion efficiency. It also provides intrinsic redundancy, which is the capability to tolerate a faulty condition.

The overall performance of the hybrid charging system together with interleave conversion stage under various intermittent conditions depends on efficient design of coordinated control mechanism and the respective energy management strategy. The overall control mechanism consists of various decentralized controllers. There is an interlinking converter for rectifier/inverter of the main grid. For the interleave converters of battery storage and electric vehicles charger, a traditional PI controller is used. For the PV system, a PO algorithm-based controller is used for interleave boost converter to extract maximum power from the PV. A centralized energy management strategy is developed to generate the reference signals for individual controllers, so that maximum preference is given to maximization of local PV utilization. The energy management strategy also ensures lesser dependency on the grid to reduce the operational cost along with greenhouse effect. The BSS plays a vital role in energy management as it behaves like a rapid buffer either to absorb surplus power from PV or to meet the deficiency at EVs load side.

The performance of the proposed centralized energy management strategy together with interleave conversion stages is studied and validated with different real-time scenarios. These scenarios consist of different weather profiles covering the 24h horizon and various intermittent EVs loading conditions. The modeling of the whole system and the corresponding simulations are performed in Matlab/Simulink environment. In order to examine the performance of proposed strategy, different real-time PV profiles covering sunny, partially sunny and cloudy conditions are considered and simulated with different levels of SoC of BSS. During all the scenarios, it is recorded, analyzed and concluded that energy balance between

sources and the EVs load retains. Moreover, the system retains a consistent regulated voltage at DC bus due to the proposed energy management and control architecture.

The energy management strategy provides adequate generation-load balance and the suggested controllers provide a rapid and stable response under variable operating conditions.

The future perspectives relevant to this research work are highlighted as:

- i. Location and V2G Technology: The selection of the charging station site is critical in distribution grid planning. The partial load demand can be offset to some extent by considering the V2G technology, taking advantage of the discharge characteristics of EVs, and adopting the marginal access mode; consequently, the foregoing can change the direct supply load space prediction of the charging station. The location of the substation should also be considered in relation to future developments in the city.
- ii. Optimal Sizing and Capacity: The capacity of EV charging facilities should be fully considered in the design of the EV charging station. The total capacity of the charging station should be able to satisfy the EV load; accordingly, overloading is avoided.
- iii. Reliability and power density: To increase the reliability of the power supplied to areas where the density of EV charging facilities is relatively large, the reserve of spare capacity can be appropriately increased. This improves the overall system reliability apart from unifying the layout of charging facilities and achieving a reasonable load distribution.
- iv. Mass integration of EVs: If a large number of EVs are connected to the grid, the power supply behavior will vary; consequently, this may change the power flow in the distribution grid. The uncertainty in the EV load density will introduce considerable problems to the location, capacity, and planning of EV charging stations.

### List of Publications

1. **ELTOUMI, Fouad**, BADJI, Adberrezak, BECHERIF, Mohamed, *et al.* Experimental Identification using Equivalent Circuit Model for Lithium-Ion Battery. *International Journal of Emerging Electric Power Systems*, 2018, vol. 19, no 3.
2. BADJI, Abderrezak. ABDESLAM, Djaffar Ould. BECHERIF, Mohamed, **ELTOUMI, Fouad**, *et al.* Analyze and evaluate of energy management system for fuel cell electric vehicle based on frequency splitting. *Mathematics and Computers in Simulation*, 2020, vol. 167, p. 65-77.
3. **ELTOUMI, Fouad**. M., BECHERIF, Mohamed. RAMADAN SAAD, Haitham, *et al.* The key issues of electric vehicle charging via hybrid power sources: Techno-economic viability, analysis, and recommendations. *Renewable and Sustainable Energy Reviews*, 2020, p. 110534.

4. IQBAL, Mehroze, BENMOUNA, Amel, **ELTOUMI, Fouad**, et al. Cooperative operation of parallel connected boost converters for low voltage-high power applications: an experimental approach. Energy Procedia, 2019, vol. 162, p. 349-358.

**4. F. Eltoumi**, M. Becherif, H. S. Ramadan prediction of electricity demand due to plug-in electric vehicles connected to the grid, International Conference on Alternative Fuels Future and Challenges, Istanbul , Turkey.

## Reference

1. Barone, G., et al., *Building to vehicle to building concept toward a novel zero energy paradigm: Modelling and case studies*. Renewable and Sustainable Energy Reviews, 2019. **101**: p. 625-648.
2. Sujitha, N. and S. Krithiga, *RES based EV battery charging system: A review*. Renewable and Sustainable Energy Reviews, 2017. **75**: p. 978-988.
3. Hansen, K., B.V. Mathiesen, and I.R. Skov, *Full energy system transition towards 100% renewable energy in Germany in 2050*. Renewable and Sustainable Energy Reviews, 2019. **102**: p. 1-13.
4. Rhys-Tyler, G.A., W. Legassick, and M.C. Bell, *The significance of vehicle emissions standards for levels of exhaust pollution from light vehicles in an urban area*. Atmospheric Environment, 2011. **45**(19): p. 3286-3293.
5. Grande, L.S.A., I. Yahyaoui, and S.A. Gómez, *Energetic, economic and environmental viability of off-grid PV-BESS for charging electric vehicles: Case study of Spain*. Sustainable Cities and Society, 2018. **37**: p. 519-529.
6. Alghoul, M.A., et al., *The role of existing infrastructure of fuel stations in deploying solar charging systems, electric vehicles and solar energy: A preliminary analysis*. Technological Forecasting and Social Change, 2018. **137**: p. 317-326.
8. Anoune, K., et al., *Sizing methods and optimization techniques for PV-wind based hybrid renewable energy system: A review*. Renewable and Sustainable Energy Reviews, 2018. **93**: p. 652-673.
9. Antonanzas, J., et al., *Review of photovoltaic power forecasting*. Solar Energy, 2016. **136**: p. 78-111.
10. Ashique, R.H., et al., *Integrated photovoltaic-grid dc fast charging system for electric vehicle: A review of the architecture and control*. Renewable and Sustainable Energy Reviews, 2017. **69**: p. 1243-1257.
11. Hernandez, J.C. and F.S. Sutil, *Electric Vehicle Charging Stations Fedded by Renewable: PV and Train Regenerative Braking*. IEEE Latin America Transactions, 2016. **14**(7): p. 3262-3269.
12. Hoarau, Q. and Y. Perez, *Interactions between electric mobility and photovoltaic generation: A review*. Renewable and Sustainable Energy Reviews, 2018. **94**: p. 510-522.
13. Han, X., et al., *Economic evaluation of a PV combined energy storage charging station based on cost estimation of second-use batteries*. Energy, 2018. **165**: p. 326-339.
14. Hill, C.A., et al., *Battery Energy Storage for Enabling Integration of Distributed Solar Power Generation*. IEEE Transactions on Smart Grid, 2012. **3**(2): p. 850-857.
15. George, V., et al. *A Novel Web-Based Real Time Communication System for PHEV Fast Charging Stations*.
16. Goli, P. and W. Shireen, *PV powered smart charging station for PHEVs*. Renewable Energy, 2014. **66**: p. 280-287.
17. Hung, D.Q., Z.Y. Dong, and H. Trinh, *Determining the size of PHEV charging stations powered by commercial grid-integrated PV systems considering reactive power support*. Applied Energy, 2016. **183**: p. 160-169.
18. Riboldi, C.E.D., *Energy-optimal off-design power management for hybrid-electric aircraft*. Aerospace Science and Technology, 2019: p. 105507-105507.
19. Shi, R., S. Semsar, and P.W. Lehn, *Constant Current Fast Charging of Electric Vehicles via a DC Grid Using a Dual-Inverter Drive*. IEEE Transactions on Industrial Electronics, 2017.
20. Zhang, J., et al., *Design scheme for fast charging station for electric vehicles with distributed photovoltaic power generation*. Global Energy Interconnection, 2019. **2**(2): p. 150-159.
21. Jia, L., Y. Zhu, and Y. Wang. *Architecture design for new AC-DC hybrid micro-grid*. Institute of Electrical and Electronics Engineers Inc.
22. Rahman, M.S., et al. *EV charging in a commercial hybrid AC/DC microgrid: Configuration, control and impact analysis*. Institute of Electrical and Electronics Engineers Inc.
23. Hansen, M. and B. Hauge, *Scripting, control, and privacy in domestic smart grid technologies: Insights from a Danish pilot study*. Energy Research & Social Science, 2017. **25**: p. 112-123.

24. Capasso, C. and O. Veneri, *Experimental study of a DC charging station for full electric and plug in hybrid vehicles*. Applied Energy, 2015. **152**: p. 131-142.
25. Guichi, A., et al., *Energy management and performance evaluation of grid connected PV-battery hybrid system with inherent control scheme*. Sustainable Cities and Society, 2018. **41**: p. 490-504.
26. Mesarić, P. and S. Krajcar, *Home demand side management integrated with electric vehicles and renewable energy sources*. Energy and Buildings, 2015. **108**: p. 1-9.
27. Ouai, A., et al., *Control and energy management of a large scale grid-connected PV system for power quality improvement*. Solar Energy, 2018. **171**: p. 893-906.
28. Medora, N.K., *7 - Electric and Plug-in Hybrid Electric Vehicles and Smart Grids*, B.W.B.T.T.P.G. D'Andrade, Editor. 2017, Academic Press. p. 197-231.
29. Tan, Z., Q. Tan, and M. Rong, *Analysis on the financing status of PV industry in China and the ways of improvement*. Renewable and Sustainable Energy Reviews, 2018. **93**: p. 409-420.
30. Chen, W., et al., *Environmental impact assessment of monocrystalline silicon solar photovoltaic cell production: a case study in China*. Journal of Cleaner Production, 2016. **112**: p. 1025-1032.
31. Jin, C., J. Tang, and P. Ghosh, *Optimizing electric vehicle charging with energy storage in the electricity market*. IEEE Transactions on Smart Grid, 2013. **4**(1): p. 311-320.
32. Li, Y., W. Gao, and Y. Ruan, *Performance investigation of grid-connected residential PV-battery system focusing on enhancing self-consumption and peak shaving in Kyushu, Japan*. Renewable Energy, 2018. **127**: p. 514-523.
33. Kobayashi, H., et al. *Method for preventing islanding phenomenon on utility grid with a number of small scale PV systems*. IEEE.
34. Li, S., et al., *Optimization for a Grid-connected Hybrid PV-wind-retired HEV Battery Microgrid System*. Energy Procedia, 2017. **105**: p. 1634-1643.
35. Lunz, B. and D.U. Sauer, *Electric road vehicle battery charging systems and infrastructure*. Advances in Battery Technologies for Electric Vehicles, 2015: p. 445-467.
36. Ahmad, A., et al., *A Review of the Electric Vehicle Charging Techniques, Standards, Progression and Evolution of EV Technologies in Germany*. Smart Science, 2018. **6**(1): p. 36-53.
37. Hoofman, N., et al., *A review of the European passenger car regulations – Real driving emissions vs local air quality*. Renewable and Sustainable Energy Reviews, 2018. **86**: p. 1-21.
38. Martínez-Lao, J., et al., *Electric vehicles in Spain: An overview of charging systems*. Renewable and Sustainable Energy Reviews, 2017. **77**: p. 970-983.
39. Foley, A.M., I.J. Winning, and B.P. O Gallachoir. *State-of-the-art in electric vehicle charging infrastructure*. IEEE.
40. Khan, W., F. Ahmad, and M.S. Alam, *Fast EV charging station integration with grid ensuring optimal and quality power exchange*. Engineering Science and Technology, an International Journal, 2018.
41. Falvo, M.C., et al. *EV charging stations and modes: International standards*. in *2014 International Symposium on Power Electronics, Electrical Drives, Automation and Motion*. 2014. IEEE.
42. Francfort, J., *Electric vehicle charging levels and requirements overview*. Clean Cities December, 2010.
43. Yilmaz, M. and P.T. Krein, *Review of battery charger topologies, charging power levels, and infrastructure for plug-in electric and hybrid vehicles*. IEEE transactions on Power Electronics, 2012. **28**(5): p. 2151-2169.
44. Moses, P.S., et al. *Power quality of smart grids with plug-in electric vehicles considering battery charging profile*. in *2010 IEEE PES Innovative Smart Grid Technologies Conference Europe (ISGT Europe)*. 2010. IEEE.
45. Kisacikoglu, M.C., M. Kesler, and L.M. Tolbert, *Single-phase on-board bidirectional PEV charger for V2G reactive power operation*. IEEE Transactions on Smart Grid, 2014. **6**(2): p. 767-775.
46. Taghizadeh, S., M. Hossain, and J. Lu. *Bidirectional isolated vehicle to grid (V2G) system: An optimized implementation and approach*. in *2015 IEEE PES Asia-Pacific Power and Energy Engineering Conference (APPEEC)*. 2015. IEEE.

47. Longo, M., et al. *Recharge stations: A review*. in *2016 Eleventh International Conference on Ecological Vehicles and Renewable Energies (EVER)*. 2016. IEEE.
48. Amoroso, F.A., *Managing charging of electric vehicles in electricity transmission and distribution networks*. Eco-Friendly Innovation in Electricity Transmission and Distribution Networks, 2015: p. 363-376.
49. Arunkumari, T. and V. Indragandhi, *An overview of high voltage conversion ratio DC-DC converter configurations used in DC micro-grid architectures*. Renewable and Sustainable Energy Reviews, 2017. **77**: p. 670-687.
50. Benysek, G. and M. Jarnut, *Electric vehicle charging infrastructure in Poland*. Renewable and Sustainable Energy Reviews, 2012. **16**(1): p. 320-328.
51. Fathabadi, H., *Novel grid-connected solar/wind powered electric vehicle charging station with vehicle-to-grid technology*. Energy, 2017. **132**: p. 1-11.
52. Ghenai, C., et al., *Grid-tied and stand-alone hybrid solar power system for desalination plant*. Desalination, 2018. **435**: p. 172-180.
53. Abdulla, K., et al. *Optimal operation of energy storage systems considering forecasts and battery degradation*. Institute of Electrical and Electronics Engineers (IEEE).
54. Kusakana, K., *Optimal energy management of a residential grid-interactive Wind Energy Conversion System with battery storage*. Energy Procedia, 2019. **158**: p. 6195-6200.
55. Zeng, J., W. Qiao, and L. Qu, *An Isolated Three-Port Bidirectional DC-DC Converter for Photovoltaic Systems With Energy Storage*. IEEE Transactions on Industry Applications, 2015. **51**(4): p. 3493-3503.
56. Novoa, L. and J. Brouwer, *Dynamics of an integrated solar photovoltaic and battery storage nanogrid for electric vehicle charging*. Journal of Power Sources, 2018. **399**: p. 166-178.
57. Aluisio, B., et al., *Optimal operation planning of V2G-equipped Microgrid in the presence of EV aggregator*. Electric Power Systems Research, 2017. **152**: p. 295-305.
58. Eldeeb, H.H., S. Faddel, and O.A. Mohammed, *Multi-Objective Optimization Technique for the Operation of Grid tied PV Powered EV Charging Station*. Electric Power Systems Research, 2018. **164**: p. 201-211.
59. Ferro, G., et al., *An optimization model for electrical vehicles scheduling in a smart grid*. Sustainable Energy, Grids and Networks, 2018. **14**: p. 62-70.
60. Bhatti, A.R., et al., *Electric vehicles charging using photovoltaic: Status and technological review*. Renewable and Sustainable Energy Reviews, 2016. **54**: p. 34-47.
61. Coffinan, M., P. Bernstein, and S. Wee, *Integrating electric vehicles and residential solar PV*. Transport Policy, 2017. **53**: p. 30-38.
62. Figueiredo, R., P. Nunes, and M.C. Brito, *The feasibility of solar parking lots for electric vehicles*. Energy, 2017. **140**: p. 1182-1197.
63. Islam, M.S. and N. Mithulananthan, *PV based EV charging at universities using supplied historical PV output ramp*. Renewable Energy, 2018. **118**: p. 306-327.
64. Jadhav, S., et al. *Bidirectional DC-DC converter in Solar PV System for Battery Charging Application*. IEEE.
65. Liu, C., et al., *Opportunities and challenges of vehicle-to-home, vehicle-to-vehicle, and vehicle-to-grid technologies*. Proceedings of the IEEE, 2013. **101**(11): p. 2409-2427.
66. Ghenai, C., T. Salameh, and A. Merabet, *Technico-economic analysis of off grid solar PV/Fuel cell energy system for residential community in desert region*. International Journal of Hydrogen Energy, 2018.
67. Bayati, M., et al., *A novel control strategy for Reflex-based electric vehicle charging station with grid support functionality*. Journal of Energy Storage, 2017. **12**: p. 108-120.
68. Zhou, T., et al. *Power flow control in different time scales for a wind/hydrogen/super-capacitors based active hybrid power system*. in *2008 13th International Power Electronics and Motion Control Conference*. 2008. IEEE.
69. Series, I., *Microgrids and active distribution networks*. The institution of Engineering and Technology, 2009.
70. Gonzalez, A., *Integration of photovoltaic sources and battery based storage systems—A DC analysis and distributed maximum power point tracking solution*. 2019.

71. Tran, V.T., et al., *An Efficient Energy Management Approach for a Solar-Powered EV Battery Charging Facility to Support Distribution Grids*. IEEE Transactions on Industry Applications, 2019. **55**(6): p. 6517-6526.
72. Gassab, S., et al., *Power management and coordinated control of standalone active PV generator for isolated agriculture area-case study in the South of Algeria*. Journal of Renewable and Sustainable Energy, 2019. **11**(1): p. 015305.
73. Talebi, P. and M. Hejri, *Distributed Control of a Grid-connected PV-battery System for Constant Power Generation*. Journal of Energy Management and Technology, 2019. **3**(3): p. 14-29.
74. Koskela, J., A. Rautiainen, and P. Järventausta, *Using electrical energy storage in residential buildings—Sizing of battery and photovoltaic panels based on electricity cost optimization*. Applied energy, 2019. **239**: p. 1175-1189.
75. Talavera, D., et al., *A new approach to sizing the photovoltaic generator in self-consumption systems based on cost-competitiveness, maximizing direct self-consumption*. Renewable energy, 2019. **130**: p. 1021-1035.
76. Torreglosa, J.P., et al., *Decentralized energy management strategy based on predictive controllers for a medium voltage direct current photovoltaic electric vehicle charging station*. Energy Conversion and Management, 2016. **108**: p. 1-13.
77. Mohamed, A., et al., *Real-time energy management algorithm for plug-in hybrid electric vehicle charging parks involving sustainable energy*. IEEE Transactions on Sustainable Energy, 2014. **5**(2): p. 577-586.
78. Ye, B., et al., *Feasibility Study of a Solar-Powered Electric Vehicle Charging Station Model*. Energies, 2015. **8**(11): p. 13265-13283.
79. Chukwu, U.C. and S.M. Mahajan, *V2G parking lot with PV rooftop for capacity enhancement of a distribution system*. IEEE Transactions on Sustainable Energy, 2013. **5**(1): p. 119-127.
80. Chandra Mouli, G.R., P. Bauer, and M. Zeman, *System design for a solar powered electric vehicle charging station for workplaces*. Applied Energy, 2016. **168**: p. 434-443.
81. Fazelpour, F., et al., *Intelligent optimization to integrate a plug-in hybrid electric vehicle smart parking lot with renewable energy resources and enhance grid characteristics*. Energy Conversion and Management, 2014. **77**: p. 250-261.
82. Calise, F., et al., *A novel paradigm for a sustainable mobility based on electric vehicles, photovoltaic panels and electric energy storage systems: Case studies for Naples and Salerno (Italy)*. Renewable and Sustainable Energy Reviews, 2019. **111**: p. 97-114.
83. Bracco, S., et al., *Electric Vehicles and Storage Systems Integrated within a Sustainable Urban District Fed by Solar Energy*. Journal of Advanced Transportation, 2019. **2019**.
84. Vermaak, H.J. and K. Kusakana, *Design of a photovoltaic-wind charging station for small electric Tuk-tuk in DR Congo*. Renewable energy, 2014. **67**: p. 40-45.
85. Li, X., L.A.C. Lopes, and S.S. Williamson. *On the suitability of plug-in hybrid electric vehicle (PHEV) charging infrastructures based on wind and solar energy*. IEEE.
86. Lee, S., et al. *Classification of charging systems according to the intelligence and roles of the charging equipment*. in *2013 International Conference on ICT Convergence (ICTC)*. 2013. IEEE.
87. Kumar, V.A. and M. Arounassalame. *PV-FC hybrid system with multilevel boost converter fed multilevel inverter with enhanced performance*. IEEE.
88. Rasinab, Z. and M.F. Rahmana. *Grid-connected quasi-Z-source PV inverter for electricvehicle charging station*. IEEE Computer Society.
89. Stein, G. and T.M. Letcher, *15 - Integration of PV Generated Electricity into National Grids*, T.M. Letcher and V.M.B.T.A.C.G.t.S.E.S. Fthenakis, Editors. 2018, Academic Press. p. 321-332.
90. Zheng, Y., et al., *Integrating plug-in electric vehicles into power grids: A comprehensive review on power interaction mode, scheduling methodology and mathematical foundation*. Renewable and Sustainable Energy Reviews, 2019. **112**: p. 424-439.
91. Chen, Z., et al., *Integrated mode and key issues of renewable energy sources and electric vehicles' charging and discharging facilities in microgrid*. 2013.

92. Tabrizi, M., G. Radman, and A. Tamersi. *Micro grid voltage profile improvement using micro grid voltage controller*. in *2012 Proceedings of IEEE Southeastcon*. 2012. IEEE.
93. Wang, R., P. Wang, and G. Xiao, *Two-stage mechanism for massive electric vehicle charging involving renewable energy*. IEEE Transactions on Vehicular Technology, 2016. **65**(6): p. 4159-4171.
94. Mouli, G.C., P. Bauer, and M. Zeman. *Comparison of system architecture and converter topology for a solar powered electric vehicle charging station*. in *2015 9th International Conference on Power Electronics and ECCE Asia (ICPE-ECCE Asia)*. 2015. IEEE.
95. ZHU, K., D. JIANG, and P. HU, *Study on a new type of DC distribution network containing electric vehicle charge station*. Power system technology, 2012. **36**(10): p. 35-41.
96. Locment, F. and M. Sechilariu, *Modeling and simulation of DC microgrids for electric vehicle charging stations*. Energies, 2015. **8**(5): p. 4335-4356.
97. Dragičević, T., et al., *DC microgrids—Part I: A review of control strategies and stabilization techniques*. IEEE Transactions on power electronics, 2015. **31**(7): p. 4876-4891.
98. Guerrero, J.M., et al., *Hierarchical control of droop-controlled AC and DC microgrids—A general approach toward standardization*. IEEE Transactions on industrial electronics, 2010. **58**(1): p. 158-172.
99. Kandil, S.M., et al., *A combined resource allocation framework for PEVs charging stations, renewable energy resources and distributed energy storage systems*. Energy, 2018. **143**: p. 961-972.
100. Hu, J., et al., *A coordinated control of hybrid ac/dc microgrids with PV-wind-battery under variable generation and load conditions*. International Journal of Electrical Power & Energy Systems, 2019. **104**: p. 583-592.
101. Aryani, D., J.-S. Kim, and H. Song, *Interlink Converter with Linear Quadratic Regulator Based Current Control for Hybrid AC/DC Microgrid*. Energies, 2017. **10**(11): p. 1799-1799.
102. Amirkhan, S., et al., *A robust control technique for stable operation of a DC/AC hybrid microgrid under parameters and loads variations*. International Journal of Electrical Power & Energy Systems, 2020. **117**: p. 105659-105659.
103. Hanna, R., et al., *Energy dispatch schedule optimization for demand charge reduction using a photovoltaic-battery storage system with solar forecasting*. Solar Energy, 2014. **103**: p. 269-287.
104. Wen, L., et al., *Design and application of microgrid operation control system based on IEC 61850*. Journal of Modern Power Systems and Clean Energy, 2014. **2**(3): p. 256-263.
105. Rahman, M.S., M.J. Hossain, and J. Lu, *Coordinated control of three-phase AC and DC type EV-ESSs for efficient hybrid microgrid operations*. Energy Conversion and Management, 2016. **122**: p. 488-503.
106. Goli, P. and W. Shireen, *Control and Management of PV Integrated Charging Facilities for PEVs*. 2015. p. 23-53.
107. Richardson, P., D. Flynn, and A. Keane, *Local versus centralized charging strategies for electric vehicles in low voltage distribution systems*. IEEE Transactions on Smart Grid, 2012. **3**(2): p. 1020-1028.
108. Pathak, P.K. and A.K. Yadav, *Design of battery charging circuit through intelligent MPPT using SPV system*. Solar Energy, 2019. **178**: p. 79-89.
109. Yona, A., *Energy management systems for DERs*. Integration of Distributed Energy Resources in Power Systems, 2016: p. 132-156.
110. Gamboa, G., et al. *Control strategy of a multi-port, grid connected, direct-DC PV charging station for plug-in electric vehicles*. in *2010 IEEE Energy Conversion Congress and Exposition*. 2010. IEEE.
111. Tayab, U.B., et al., *A review of droop control techniques for microgrid*. Renewable and Sustainable Energy Reviews, 2017. **76**: p. 717-727.
112. Bidram, A. and A. Davoudi, *Hierarchical structure of microgrids control system*. IEEE Transactions on Smart Grid, 2012. **3**(4): p. 1963-1976.
113. Nehrir, M., et al., *A review of hybrid renewable/alternative energy systems for electric power generation: Configurations, control, and applications*. IEEE Transactions on Sustainable Energy, 2011. **2**(4): p. 392-403.
114. Schonberger, J., R. Duke, and S.D. Round, *DC-bus signaling: A distributed control strategy for a hybrid renewable nanogrid*. 2006.

115. Tsikalakis, A.G. and N.D. Hatziargyriou. *Centralized control for optimizing microgrids operation*. in *2011 IEEE power and energy society general meeting*. 2011. IEEE.
116. Zhang, J., et al. *Control strategy of interlinking converter in hybrid AC/DC microgrid*. in *2013 International Conference on Renewable Energy Research and Applications (ICRERA)*. 2013. IEEE.
117. Hu, J., et al., *A model predictive control strategy of PV-Battery microgrid under variable power generations and load conditions*. *Applied Energy*, 2018. **221**: p. 195-203.
118. Ramachandran, B., S.K. Srivastava, and D.A. Cartes, *Intelligent power management in micro grids with EV penetration*. *Expert Systems with Applications*, 2013. **40**(16): p. 6631-6640.
119. Tabrizi, M.A., G. Radman, and A. Tamersi. *Micro grid voltage profile improvement using micro grid voltage controller*.
120. Shi, W., et al., *Real-Time Energy Management in Microgrids*. *IEEE Transactions on Smart Grid*, 2017. **8**(1): p. 228-238.
121. Tégani, I., et al., *Optimal Sizing Design and Energy Management of Stand-alone Photovoltaic/Wind Generator Systems*. *Energy Procedia*, 2014. **50**: p. 163-170.
122. Qi, X., et al. *An on-line energy management strategy for plug-in hybrid electric vehicles using an Estimation Distribution Algorithm*. Institute of Electrical and Electronics Engineers Inc.
123. Rydh, C.J. and B.A. Sandén, *Energy analysis of batteries in photovoltaic systems. Part II: Energy return factors and overall battery efficiencies*. *Energy Conversion and Management*, 2005. **46**(11-12): p. 1980-2000.
124. Haddadian, G., et al., *Optimal scheduling of distributed battery storage for enhancing the security and the economics of electric power systems with emission constraints*. *Electric Power Systems Research*, 2015. **124**: p. 152-159.
125. Chiang, S.J., K.T. Chang, and C.Y. Yen, *Residential photovoltaic energy storage system*. *IEEE Transactions on Industrial Electronics*, 1998. **45**(3): p. 385-394.
126. Bhatti, A.R., Z. Salam, and R.H. Ashique, *Electric Vehicle Charging Using Photovoltaic based Microgrid for Remote Islands*. *Energy Procedia*, 2016. **103**: p. 213-218.
127. Ma, Z., D.S. Callaway, and I.A. Hiskens, *Decentralized charging control of large populations of plug-in electric vehicles*. *IEEE Transactions on Control Systems Technology*, 2011. **21**(1): p. 67-78.
128. Davis, B.M. and T.H. Bradley, *The efficacy of electric vehicle time-of-use rates in guiding plug-in hybrid electric vehicle charging behavior*. *IEEE Transactions on Smart Grid*, 2012. **3**(4): p. 1679-1686.
129. Leonori, S., et al. *Optimization of a microgrid energy management system based on a fuzzy logic controller*. in *IECON 2016-42nd Annual Conference of the IEEE Industrial Electronics Society*. 2016. IEEE.
130. Franco, J.F., M.J. Rider, and R. Romero, *A mixed-integer linear programming model for the electric vehicle charging coordination problem in unbalanced electrical distribution systems*. *IEEE Transactions on Smart Grid*, 2015. **6**(5): p. 2200-2210.
131. Delfanti, M., D. Falabretti, and M. Merlo, *Energy storage for PV power plant dispatching*. *Renewable Energy*, 2015. **80**: p. 61-72.
132. Ding, H., et al. *Coordinated control strategy of energy storage system with electric vehicle charging station*.
133. Xiao, G., et al. *Review of the impact of electric vehicles participating in frequency regulation on power grid*. in *2013 Chinese automation congress*. 2013. IEEE.
134. Almeida, P.R., et al. *Automatic generation control operation with electric vehicles*. in *2010 IREP Symposium Bulk Power System Dynamics and Control-VIII (IREP)*. 2010. IEEE.
135. Galus, M.D. and G. Andersson. *Balancing renewable energy source with vehicle to grid services from a large fleet of plug-in hybrid electric vehicles controlled in a metropolitan area distribution network*. in *CIGRE International Symposium*. 2011.
136. Liu, L., et al., *A review on electric vehicles interacting with renewable energy in smart grid*. *Renewable and Sustainable Energy Reviews*, 2015. **51**: p. 648-661.
137. Gu, W., et al., *Demand response and economic dispatch of power systems considering large-scale plug-in hybrid electric vehicles/electric vehicles (PHEVs/EVs): A review*. *Energies*, 2013. **6**(9): p. 4394-4417.

138. Vandoorn, T.L., et al., *Microgrids: Hierarchical control and an overview of the control and reserve management strategies*. IEEE industrial electronics magazine, 2013. **7**(4): p. 42-55.
139. Kang, Q., et al., *Centralized charging strategy and scheduling algorithm for electric vehicles under a battery swapping scenario*. IEEE Transactions on Intelligent Transportation Systems, 2015. **17**(3): p. 659-669.
140. Bessa, R.J. and M.A. Matos, *Economic and technical management of an aggregation agent for electric vehicles: a literature survey*. European transactions on electrical power, 2012. **22**(3): p. 334-350.
141. Marinelli, M., et al., *Validating a centralized approach to primary frequency control with series-produced electric vehicles*. Journal of Energy Storage, 2016. **7**: p. 63-73.
142. Wu, C., H. Mohsenian-Rad, and J. Huang, *Vehicle-to-aggregator interaction game*. IEEE Transactions on Smart Grid, 2011. **3**(1): p. 434-442.
143. Xu, Z., et al., *Coordination of PEVs charging across multiple aggregators*. Applied energy, 2014. **136**: p. 582-589.
144. Gan, L., U. Topcu, and S.H. Low, *Optimal decentralized protocol for electric vehicle charging*. IEEE Transactions on Power Systems, 2012. **28**(2): p. 940-951.
145. Xydas, E., C. Marmaras, and L.M. Cipcigan, *A multi-agent based scheduling algorithm for adaptive electric vehicles charging*. Applied energy, 2016. **177**: p. 354-365.
146. Elsayed, A.T., A.A. Mohamed, and O.A. Mohammed, *DC microgrids and distribution systems: An overview*. Electric Power Systems Research, 2015. **119**: p. 407-417.
147. Hamilton, C., et al. *System architecture of a modular direct-DC PV charging station for plug-in electric vehicles*. in *IECON 2010-36th Annual Conference on IEEE Industrial Electronics Society*. 2010. IEEE.
148. Wong, N. and M. Kazerani. *A review of bidirectional on-board charger topologies for plugin vehicles*. in *2012 25th IEEE Canadian Conference on Electrical and Computer Engineering (CCECE)*. 2012. IEEE.
149. Kutkut, N.H. and K.W. Klontz. *Design considerations for power converters supplying the SAE J-1773 electric vehicle inductive coupler*. in *Proceedings of APEC 97-Applied Power Electronics Conference*. 1997. IEEE.
150. Gow, J.A., *Modelling, simulation and control of photovoltaic converter systems*. 1998, © JA Gow.
151. Anisha Bhimanapati, L., et al., *Investigations and Analysis of PV - Battery based Micro grid Energy Management System*. Materials Today: Proceedings, 2018. **5**(11): p. 22931-22942.
152. Na, L. and Z. De-min. *Research on MPPT control based on combined algorithm of perturbation observation*. IEEE.
153. Jiang, P., W. Zhang, and Z. Jin. *Photovoltaic array MPPT based on improved perturbation observation method*. IEEE.
154. Reshma Gopi, R. and S. Sreejith, *Converter topologies in photovoltaic applications – A review*. Renewable and Sustainable Energy Reviews, 2018. **94**: p. 1-14.
155. Amir, A., et al., *Comparative analysis of high voltage gain DC-DC converter topologies for photovoltaic systems*. Renewable Energy, 2019. **136**: p. 1147-1163.
156. Cheong, S.V., S.H. Chung, and A. Ioinovici, *Duty-Cycle Control Boosts DC-DC Converters*. IEEE Circuits and Devices Magazine, 1993. **9**(2): p. 36-37.
157. Badji, A., et al., *Analyze and evaluate of energy management system for fuel cell electric vehicle based on frequency splitting*. Mathematics and Computers in Simulation, 2019. **167**: p. 65-77.
158. Boyar, A. and E. Kabalci. *Comparison of a Two-Phase Interleaved Boost Converter and Flyback Converter*.
159. Chou, T.-H., et al. *An interleaved high gain boost converter for high power PV system applications*. IEEE.
160. Gules, R., L.L. Pfitscher, and L.C. Franco. *An interleaved boost DC-DC converter with large conversion ratio*. in *2003 IEEE International Symposium on Industrial Electronics (Cat. No. 03TH8692)*. 2003. IEEE.
161. Ishii, T. and Y. Mizutani, *Variable frequency switching of synchronized interleaved switching converters*. 1999, Google Patents.
162. Lee, H.-S., et al., *Reduction of input voltage/current ripples of boost half-bridge DC-DC converter for photovoltaic micro-inverter*. Solar Energy, 2019. **188**: p. 1084-1101.

163. Lee, W., B.-M. Han, and H. Cha. *Battery ripple current reduction in a three-phase interleaved dc-dc converter for 5kW battery charger*. in *2011 IEEE Energy Conversion Congress and Exposition*. 2011. IEEE.
164. Meesrisuk, W., N. Sarasiri, and A. Jangwanitlert. *Ripple current reduction using interleaving technique for three-level ZVZCS DC-DC converter*. IEEE.
165. Newlin, D.J.S., R. Ramalakshmi, and S. Rajasekaran. *A performance comparison of interleaved boost converter and conventional boost converter for renewable energy application*. in *2013 International Conference on Green High Performance Computing (ICGHPC)*. 2013. IEEE.
166. Eltoumi, F., et al., *Experimental Identification using Equivalent Circuit Model for Lithium-Ion Battery*. *International Journal of Emerging Electric Power Systems*, 2018. **19**(3).
167. Subburaj, A.S. and S.B. Bayne. *Analysis of dual polarization battery model for grid applications*. in *2014 IEEE 36th International Telecommunications Energy Conference (INTELEC)*. 2014. IEEE.
168. Zhao, X., et al., *State of charge estimation based on a new dual-polarization-resistance model for electric vehicles*. *Energy*, 2017. **135**: p. 40-52.
169. Wang, Y.-F., et al., *Interleaved high-conversion-ratio bidirectional dc-dc converter for distributed energy-storage systems—circuit generation, analysis, and design*. *IEEE Transactions on Power Electronics*, 2015. **31**(8): p. 5547-5561.
170. Wei, X., K. Tsang, and W. Chan, *DC/DC buck converter using internal model control*. *Electric Power Components and Systems*, 2009. **37**(3): p. 320-330.
171. Tarakanath, K., S. Patwardhan, and V. Agarwal. *Internal model control of dc-dc boost converter exhibiting non-minimum phase behavior*. in *2014 IEEE International Conference on Power Electronics, Drives and Energy Systems (PEDES)*. 2014. IEEE.
172. Adi, F.S., H. Song, and J.-S. Kim, *Interlink Converter Controller Design based on System Identification of DC Sub-Grid Model in Hybrid AC/DC Microgrid*. *IFAC-PapersOnLine*, 2019. **52**(4): p. 45-50.
173. Gao, Z., H. Zhao, and J. Wang, *Bidirectional droop control of AC/DC hybrid microgrid interlinking converter*. *DEStech Transactions on Environment, Energy and Earth Sciences*, 2018(icner).
174. Sajid, A., et al. *Control of Interlinking Bidirectional Converter in AC/DC Hybrid Microgrid Operating in Stand-Alone Mode*. in *2019 IEEE Milan PowerTech*. 2019. IEEE.
175. Zhang, L., et al. *Interlinking modular multilevel converter of hybrid AC-DC distribution system with integrated battery energy storage*. in *2015 IEEE Energy Conversion Congress and Exposition (ECCE)*. 2015. IEEE.
176. Di Domenico, D., Fiengo, G., & Stefanopoulou, A. (2008, September). Lithium-ion battery state of charge estimation with a Kalman filter based on an electrochemical model. In *2008 IEEE International Conference on Control Applications* (pp. 702-707). Ieee.
177. Xiong, R., He, H., Sun, F., & Zhao, K. (2012). Evaluation on state of charge estimation of batteries with adaptive extended Kalman filter by experiment approach. *IEEE Transactions on Vehicular Technology*, **62**(1), 108-117.
178. Chen, Z., Qiu, S., Masrur, M. A., & Murphey, Y. L. (2011, July). Battery state of charge estimation based on a combined model of Extended Kalman Filter and neural networks. In *The 2011 International Joint Conference on Neural Networks* (pp. 2156-2163). IEEE.
179. Luo, Y., Qi, P., Kan, Y., Huang, J., Huang, H., Luo, J., ... & Zhao, S. (2020). State of charge estimation method based on the extended Kalman filter algorithm with consideration of time-varying battery parameters. *International Journal of Energy Research*, **44**(13), 10538-10550.
180. Chen, C., Xiong, R., Yang, R., Shen, W., & Sun, F. (2019). State-of-charge estimation of lithium-ion battery using an improved neural network model and extended Kalman filter. *Journal of Cleaner Production*, **234**, 1153-1164.
181. Wang, Y., Sun, Z., & Chen, Z. (2019). Development of energy management system based on a rule-based power distribution strategy for hybrid power sources. *Energy*, **175**, 1055-1066.
182. Xia, M., Chen, M., & Chen, Q. Rule-based energy buffer strategy of energy router considering efficiency optimization. *International Journal of Electrical Power & Energy Systems*, **125**, 106378.

183. Hofman, T., Steinbuch, M., Van Druten, R., & Serrarens, A. (2007). Rule-based energy management strategies for hybrid vehicles. *International Journal of Electric and Hybrid Vehicles*, 1(1), 71-94.
184. Bhatti, A. R., & Salam, Z. (2018). A rule-based energy management scheme for uninterrupted electric vehicles charging at constant price using photovoltaic-grid system. *Renewable energy*, 125, 384-400.
185. Nebey, A. H. (2020). Energy management system for grid-connected solar photovoltaic with battery using MATLAB simulation tool. *Cogent Engineering*, 7(1), 1827702.
186. Eltoumi, F. M., Becherif, M., Djerdir, A., & Ramadan, H. S. (2020). The key issues of electric vehicle charging via hybrid power sources: Techno-economic viability, analysis, and recommendations. *Renewable and Sustainable Energy Reviews*, 110534.
187. <https://www.comparethemarket.com/car-insurance/content/cost-of-charging-an-electric-car-globally>

## Abendex

### Large scale of EVs aggregation -Optimal Charging

$E_0$	Intercept electricity price model $10^{-4}$ C\$/kWh
$E_1$	Slope electricity price model $1.2 * 10^{-4}$ C\$/kWh
$S$	Set of the EVs
$x_{m i}$	Charging power
$f_{m i}$	EV $m$ is connected to the grid at interval $i$
$z_i$	Total load in the interval $i$
$L_i^B$	Base load
$\tau$	Length of an interval, 1 hour
$B_m^{cap}$	Battery capacity
$\beta$	$5 \times 10^{-4}$ C\$/kWh <sup>2</sup>
$\eta$	$10^{-3}$ C\$/kWh <sup>2</sup>
$\psi^A \psi^F$	quadratic convex functions
EVs number	200

A global intelligent charging/discharging scheduling of EVs is proposed to reduce to the air pollution and operational cost. The overall cost for the charging and discharging of EVs is optimized and reduced using optimization scheme. Depending on the power demand, EVs charge when the power demand is low. Likewise, the EVs discharging is performed when the load is comparatively low. By taking into consideration the charging times and charging periods in advance, the strategy globally minimizes the charging cost of EVs. In addition, the mathematical model of batteries life time reduction is also incorporated in the overall model. In this model the set of EVs is divided in two parts: One part only includes the charging of EVs while second part includes both charging and discharging of EVs. The cost and associated constraints are given in equations (1)-(6).

$$F_C = \sum_{i \in N} \left( \left( E_0 z_i + \frac{E_1}{2} z_i^2 \right) - \left( E_0 L_i^B + \frac{E_1}{2} (L_i^B)^2 \right) \right) \quad (1)$$

Minimize  $x, F_C$  subjected to

$$z_i = y_i + L_i^B = \sum_{m \in S} x_{m i} f_{m i} + L_i^B, \quad i \in N \quad (2)$$

$$0 \leq x_{m i} \leq P_{max}, \quad \forall m \in S_{cha}, \quad i \in N \quad (3)$$

$$-P_{max} \leq x_{m i} \leq P_{max}, \quad \forall m \in S_{cha,discha}, \quad i \in N \quad (4)$$

$$0 \leq B_m^{ini} + \sum_{m \in q_i} \tau x_{m k} f_{m k} \leq B_m^{cap}, \quad m \in S, \quad i \in N \quad (5)$$

$$B_m^{ini} + \sum_{m \in q_i} \tau x_{m k} f_{m k} \geq \gamma B_m^{cap}, \quad \forall m \in S \quad (6)$$

The battery life time reduction is also added in the objective function as given in equations (7-8). The overall objective function is then to reduce the charging cost of EVs alongside reducing the life time reduction of batteries.

$$\psi = \sum_{m \in S} (\psi_m^A + \psi_m^F) = \sum_{m \in S} \left( \sum_{i \in N} \beta x_{mi}^2 + \sum_{i=2}^N \eta (x_{mi} - x_{m(i-1)})^2 \right) \quad (7)$$

$$F_C \text{ batt life reduction} = \sum_{i \in N} \left( \left( E_0 z_i + \frac{E_1}{2} z_i^2 \right) - \left( E_0 L_i^B + \frac{E_1}{2} (L_i^B)^2 \right) \right) \quad (8)$$

$$+ \sum_{m \in S} \left( \sum_{i \in N} \beta x_{mi}^2 + \sum_{i=2}^N \eta (x_{mi} - x_{m(i-1)})^2 \right)$$

The proposed global optimal allocation scheme is compared to equal allocation scheme and global allocation scheme. The considered time horizon is 24 hours. The total charging load is given in Fig.1.

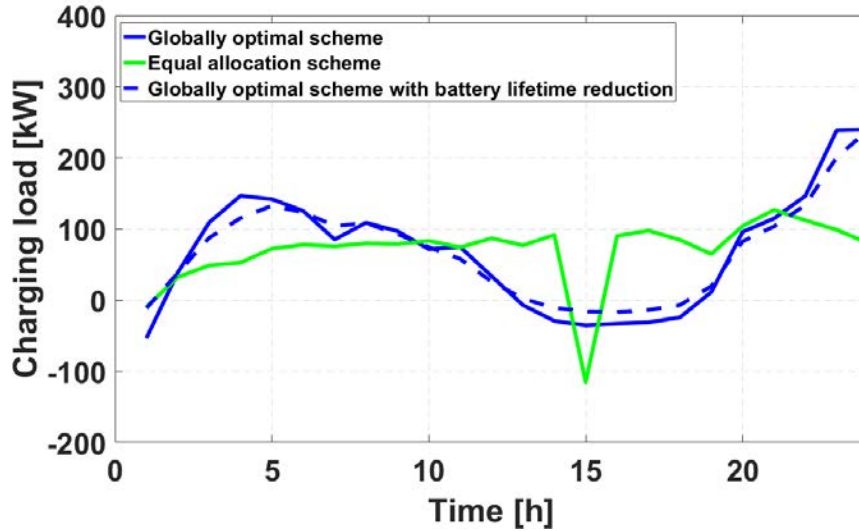


Fig.1: Change in charging capacity in each interval.

In comparison to Fig. 1, the total load including the charging load and domestic load is displayed in Fig. 2.

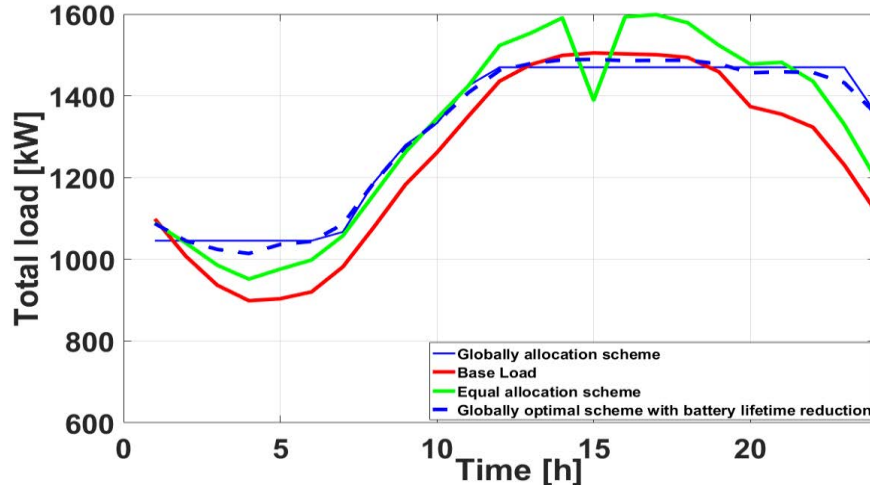


Fig .2: The total load variation.

Using the global optimal allocation scheme, the charging power and energy of one randomly selected EV are given in Fig. 3 and 4.

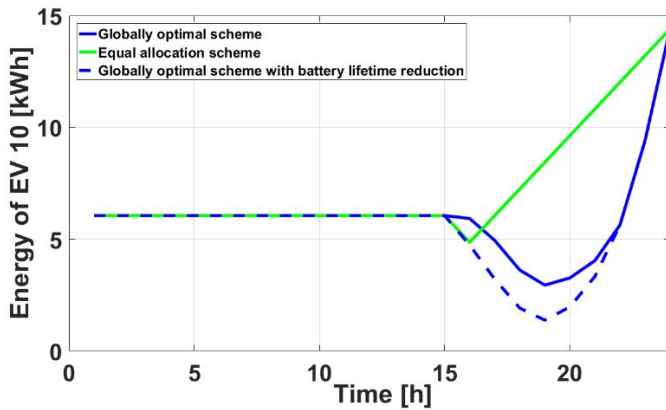


Fig .3: Energy of EV 10 variation.

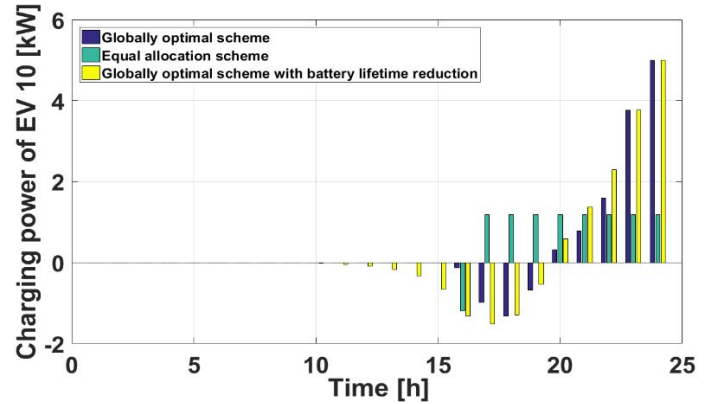


Fig .4: The change in charging power of EV 10.

The proposed global optimal scheme with battery life reduction provides lower optimization cost compared to the similar schemes such as equal allocation scheme and global allocation scheme.

The comparison of the operational cost is presented in Fig. 5

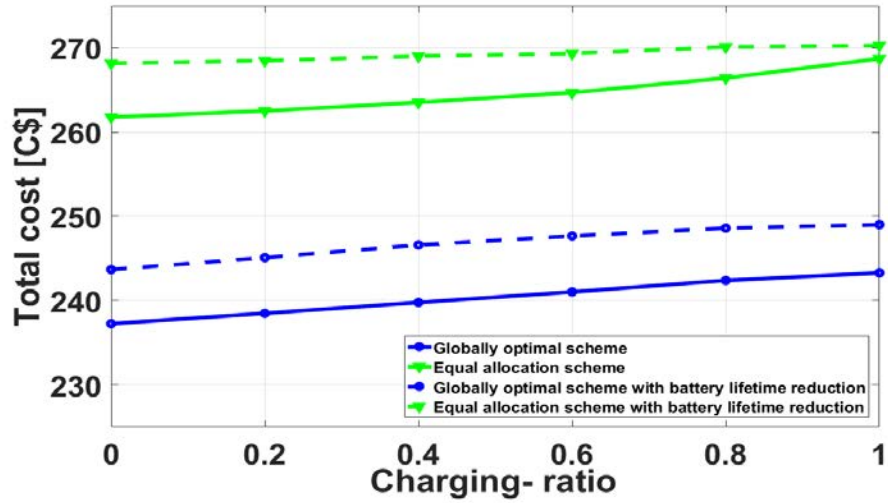


Fig.5: Total cost changes with different charging ratio.

In brief and conclusion, the global optimal allocation scheme with battery life reduction is superior to sub optimal allocation schemes and schemes without battery life reduction. It is evident from fig. 5. The reduction of approximately 9 percent is recorded comparing to equal allocation scheme.

**Title : Charging Station for Electric Vehicles Using Hybrid Sources**

**Keywords :** EV charging station, power conversion stages, battery modelling, energy management system.

**Abstract:** Higher penetration of electric vehicles (EVs) and plug-in hybrid electric vehicles requires efficient design of charging stations to supply appropriate charging rates. This would trigger stress on conventional grid, thus increasing the cost of charging. Therefore, the use of on-site renewable sources such as photo-voltaic (PV) energy alongside to the conventional grid can increase the performance of charging station. In this thesis, PV source is used in conjunction with grid to supply EV load. The PV is known for its intermittent nature that is highly dependent on geographical and weather conditions. An efficient bidirectional power conversion stage is introduced for BSS in the form of interleaved buck-boost converter to ensure the safe operation of BSS and reduce the losses during conversion stage. This topology enables reducing the current ripples and therefore, increasing the power quality. To extract the maximum power from PV system under intermittent weather conditions, MPPT is used alongside with interleaved boost converter to ensure the continuity of power from PV source. Similarly, for vehicles charger stage, to meet the dynamic power demands of EVs; while, keeping the balance between available generation amounts, interleaved converter is proposed combined to sub-management strategy. To operate the system under desirable conditions, an on-line energy management strategy is proposed. This real-time strategy works in hierarchical manner, initializing from maximized utilization of PV source, then using BSS to supplement power and utilizing grid during intermittent conditions affecting PVs. The management strategy ensures reliable operation of system, while maximizing the PV utilization, meeting the EVs demand and maximizing the life of the BSS.

**Titre: station de recharge pour véhicules électriques utilisant des sources hybrides**

**Mots clés :** station de charge de véhicule électrique, étages de conversion de puissance, modélisation de la batterie, système de gestion de l'énergie.

**Résumé :** Une plus grande utilisation des véhicules électriques (VE) et hybrides rechargeables exige une conception efficace des stations de recharge pour fournir des taux de charge appropriés. Le raccordement d'une station sur le réseau électrique conventionnel provoquerait des perturbations, ce qui augmenterait le coût de la recharge. Par conséquent, dans ce scénario, l'utilisation de sources renouvelables sur site telles que l'énergie photovoltaïque (PV) en appui au réseau conventionnel peut augmenter les performances de la station de recharge. Dans cette thèse, une source PV est utilisée conjointement avec le réseau pour compléter la charge des VE. Le PV est connu pour sa nature intermittente qui dépend fortement des conditions géographiques et météorologiques. Un étage de conversion de puissance bidirectionnel efficace est introduit pour le BSS sous la forme d'un convertisseur buck-boost entrelacé pour assurer le fonctionnement du BSS et réduire les pertes pendant la phase de conversion. Cette topologie a des caractéristiques qui permettent d'améliorer les ondulations du courant et par conséquent, d'augmenter considérablement la qualité de l'énergie. De même, pour l'étage de charge des véhicules, afin de répondre aux demandes dynamiques de puissance des VE; tout en maintenant l'équilibre entre les quantités de production disponibles, un convertisseur d'entrelacement est proposé en complément de la stratégie de sous-gestion. En particulier, cette étape de conversion et de gestion porte sur la faible utilisation du réseau notamment lors de pointes de puissance. Pour exploiter l'ensemble du système dans des conditions souhaitables, une stratégie de gestion de l'énergie en ligne est proposée. Cette stratégie en temps réel fonctionne de manière hiérarchique, en s'initialisant à partir d'une utilisation maximale de la source PV, puis en utilisant le BSS pour compléter l'alimentation et en utilisant le réseau en cas de conditions intermittentes ou lorsque la quantité de PV est faible. La stratégie de gestion assure un fonctionnement fiable du système, tout en maximisant l'utilisation du PV, en répondant à la demande des VE et en maximisant la durée de vie du BSS. Dans cette thèse, un système de charge hybride basé sur le PV, le BSS et le réseau conventionnel est proposé pour répondre aux besoins de charge des VE.